Generation of a neonatal sepsis model in humanized mice

DISSERTATION ZUR ERLANGUNG DES DOKTORGRADES
DER NATURWISSENSCHAFTEN (DR. RER. NAT.)
DER FAKULTÄT FÜR BIOLOGIE UND VORKLINISCHE MEDIZIN
DER UNIVERSITÄT REGENSBURG

vorgelegt von

Wolfgang Ernst

aus

Trostberg

im Jahr 2012

Das Promotionsgesuch wurde eingereicht am: 03.09.12

Die Arbeit wurde angeleitet von: Frau Prof. Dr. Daniela N. Männel

Unterschrift:

TABLE OF CONTENTS

ZUSAMMENFASSUNG

Streptococcus agalactiae (Streptokokkus der Serogruppe B (GBS)) ist ein grampositives Bakterium und in gesunden Erwachsenen als harmloser Kommensale in der gastrointestinalen und vaginalen Flora zu finden. In Neonaten jedoch ist dieser Keim einer der Hauptverursacher von Pneumonie, Atemversagen, Bakteriämie, Sepsis und Meningitis. Im Rahmen dieser Dissertation konnte ein neues Tiermodell für GBS-induzierte Sepsis in einer Maus mit einem humanen Immunsystem (humanisierte Maus), generiert werden. Dadurch, dass das Immunsystem von humanisierten Mäusen Defizite vergleichbar der von humanen Neugeborenen aufweist, ist die humanisierte Maus ein geeignetes Infektionsmodell für humane Neugeborene. Dieses neue Tiermodell wurde verwendet um die Effekte zweier Medikamente, die routinemäßig in der Klinik eingesetzt werden, auf GBS-Sepsis zu untersuchen: Betamethason (Lungenreifung) und Indomethazin (Wehenhemmer). Obwohl beide Medikamente vielfach Anwendung in der Perinatalmedizin finden, ist wenig über ihre Wirkung auf das neonatale Immunsystem und den Krankheitsverlauf bekannt. Anfänglich (24h nach der Infektion) führte Betamethason zu keinen ausgeprägten Veränderungen der untersuchten Zytokinspiegel oder Leukozytenpopulationen, jedoch induzierte das Medikament eine Verringerung der systemischen Bakterienlast in infizierten Tieren. Nach 3 Tagen führten sowohl Betamethason als auch Indomethazin zu einer Abnahme von T und B Zellen in der Milz, einer Zunahme von B Zellen im Knochenmark (BM) und einem Rückgang myeloider Zellen im BM. Diese Veränderungen gingen mit einem Anstieg der systemischen Bakterienlast einher. Der Anstieg der systemischen Bakterienlast und die Veränderungen der Leukozytenpopulationen im BM nach Indomethazingabe waren nicht ausgeprägt, jedoch führte dieses Medikament zu einem Anstieg von Interleukin-8 im Serum infizierter Tiere. Beide Medikamente führten zu keinen deutlichen Veränderungen in den untersuchten Leukozytenpopulationen oder der Bakterienbeseitigung nach länger anhaltender Infektion (7 Tage). Diese Studie zeigt, dass beide Medikamente Einfluss auf humane Immunzellen während einer Infektion *in vivo* ausüben. Aufgrund der Tatsache, dass die Behandlung zu einer Erhöhung der Bakterienlast führt, was zum Auftreten oder zur Zunahme von Organschäden führen kann, sollten beide Medikamente in Kombination mit Antibiotika verabreicht werden, um die Bakterienlast zu senken.

ABSTRACT

Streptococcus agalactiae (group B streptococcus (GBS)) is a gram-positive bacterium and a harmless commensal in the gastrointestinal and vaginal flora of healthy adults. In neonates however, GBS is a leading cause for pneumonia, respiratory failure, bacteremia, sepsis and meningitis. In this study, a new animal model for GBS-induced sepsis is introduced, a mouse featuring a human immune system (humanized mouse). The immune system of humanized mice and human neonates exhibit similar deficiencies, making the animals a well suited infection model for human newborn infants. This novel animal model was used to analyze the effect of two drugs routinely used in the clinic: Betamethasone, for fetal lung maturation and Indomethacin to prevent labor. Although both drugs are frequently utilized in the perinatal care, little is known about their effect on the neonatal immune system and on disease progression in GBS-induced sepsis. Initially (1 day post infection) Betamethasone treatment did not induce marked changes in cytokine levels and leukocyte populations, but resulted in a systemic reduction of live bacteria in infected animals. After 3 days, both Betamethasone and Indomethacin led to a reduction of T and B cells in the spleen, an increase in B cells in the bone marrow (BM) and a decrease in myeloid cells in the BM. These changes in leukocyte populations were accompanied by a systemic increase of live bacteria. While the systemic increase in live GBS and the changes in leukocyte populations in the BM after Indomethacin treatment were not pronounced, the drug led to increased interleukin-8 levels in the serum of infected animals. Both drugs did not induce prominent changes in the analyzed leukocyte populations and in bacterial clearance after prolonged infection (7 days). This study shows that both drugs exerted influences on human immune cells *in vivo* during an ongoing bacterial infection. Since treatment also increases the bacterial load, which can induce or increase organ damage, both drugs should be given in combination with antibiotics to reduce the bacterial burden.

1 INTRODUCTION

1.1 STREPTOCOCCUS AGALACTIAE

1.1.1 BACKGROUND AND DISEASE

Streptococcus agalactiae (group B streptococcus (GBS)) is a leading cause of invasive neonatal infection (Anthony 1977; Tissi et al. 1990; Shet & Ferreri 2004; Maisey et al. 2009). It is a chain-forming, gram-positive coccus that is characterized as catalase-negative, oxidase-negative, hippurate hydrolysis-negative but CAMP-factor positive. In the early 1930s Rebecca Lancefield established a grouping system for hemolytic streptococci based on their hemolytic reaction on blood agar. *Streptococcus pneumoniae* displays alpha hemolysis, characterized by greenish zones surrounding the colonies. The color stems from methemoglobin, which is oxidized hemoglobin. Beta hemolysis lyses the blood cells completely, therefore the hemolysis rings, characteristic for colonies of GBS, are clear. Lancefield also classified GBS into serotypes (Ia, Ib and II-VIII) based on precipitin reactions in animal models using rabbits and mice (Lancefield & Hare 1935; Larsen & Sever 2008). Although the causality between streptococcal infection and puerperal sepsis was discovered by Louis Pasteur in 1879 (Pasteur 1879), GBS was acknowledged to be a harmless commensal bacterium, whereas group A streptococcus has been considered to be the major pathogen, responsible for puerperal sepsis until 1938. Then, GBS had first been recognized as a clinically relevant pathogen by Fry, who described 7 cases of GBS-induced puerperal fever. Three of them had been fatal (Fry 1938). Hood and his colleagues associated GBS colonization with increased risk of perinatal infection in 1961 (Hood et al. 1961). During the 1970s and 1980s, GBS emerged as a significant neonatal pathogen in the USA and Western Europe (Shet & Ferrieri 2004). Studies by Gladstone et al. showed that in the 1980s approximately 50% of all cases of early onset sepsis in neonates were caused by GBS (Gladstone et al. 1990). Before the introduction of the intrapartum antibiotic prophylaxis by the Center of Disease Control (CDC) in the late 1990s and the revised guidelines by the CDC in 2002, 2 of 1000 births displayed early onset disease (EOD) with invasive GBS infection and sepsis. The prophylactic treatment implemented by the CDC includes universal screening of pregnant women for GBS colonization between 35

and 37 weeks of gestation. Subsequently all women carrying GBS are treated with intravenous antibiotics. This led to a decline of EOD from 2 per 1000 to 0.5 per 1000 births (Revised CDC Guidelines 2002; Larson & Sever 2008; Rajagopal 2010). Although the intrapartum antibiotic prophylaxis significantly reduces the incidences of EOD, it does not have a beneficial effect on the number of late onset diseases (LOD), GBS related stillbirth or prematurity. Another major problem is the emergence of antibiotic-resistant strains. Since GBS is sensitive to penicillin, chemoprophylaxis is usually intravenous treatment with Penicillin G. If the women have an allergy to penicillin, they are treated with Clindamycin or Erythromycin. However, 15-30% of GBS strains are resistant to Clindamycin and Erythromycin. Furthermore Penicillin-resistant strains have also emerged recently (Shet & Ferrieri 2004; Larson & Sever 2008; Rajagopal 2010).

Despite intrapartum chemoprophylaxis, GBS still is the most frequent bacteria in term infants (Stoll et al. 2011) and invasive GBS infection of neonates still remains a leading cause of sepsis, bacteremia, pneumonia and meningitis (Schuchat et al. 2001; Moore et al. 2003; Henneke & Berner 2006, Maisey et al. 2009; Tazi et al. 2012).

There is a classification of GBS infections depending on the time point of disease manifestation. When the infection presents in infants between the first few hours of life and 7 days, it is defined as EOD. Usually EOD manifests within the first 24 h after birth. More than 80% of infants suffering from EOD display respiratory distress. Most infants present with pneumonia, respiratory failure, bacteremia and sepsis. EOD also presents with vascular thrombosis and parenchymal hemorrhage, but despite high amounts of GBS in the brain, no leptomeningeal inflammation occurs. Between 5 and 10% develop meningitis. EOD has a mortality rate of 10-15%. The predominant GBS serotypes, responsible for 78-87% of EOD are Ia, III and V (Cowgill et al. 2003; Shet & Ferrieri 2004; Maisey et al. 2009). Since maternal colonization with GBS is a prerequisite for development of EOD (Rajagopal 2010), the most common route for EOD is the transfer of GBS from the mother to the child *in utero*. Here, bacteria from an ascending vaginal GBS infection contaminate the amniotic fluid. This generally happens after rupture of the amniotic membranes. When the fetus aspirates amniotic fluid, GBS are inhaled and reach the lungs where they damage pulmonary epithelial cells. This not only leads to pneumonia and respiratory distress, which are very common for EOD, but also to an intravascular uptake of GBS. When the fetus is unable to rapidly eliminate the bacteria in the bloodstream, bacteremia followed by severe sepsis occurs (Spellerberg 2000). Studies have shown that GBS is able to

cross intact chorioamniotic membranes. The subsequent infection and events often result in stillbirth or even death of the neonate shortly after birth (Galask et al. 1984). Another route for GBS infection is the vertical transmission from mother to child during the passage through the birth canal.

LOD is defined by an onset of disease 7-90 days after birth, with a median onset of one month. Serotype III is the predominant GBS serotype in LOD (50%), followed by Ia (27%) and V (14%). Although the pathogenesis of LOD is not fully understood yet, it is generally acknowledged that horizontal as well as vertical transmission is possible. GBS infection can be acquired from contact with infected infants, health care workers, close contact with the mother and breast feeding. LOD is usually characterized by bacteremia which can quickly progress to meningitis (40-60%) or sepsis. There are also reports that GBS infection can lead to osteoarthritis. The presentation with respiratory distress or pneumonia is rather uncommon due to a different route of infection compared to EOD. Although the mortality rate of LOD is quite low (2-6%), 20% of the neonates surviving GBS meningitis suffer from permanent neurological sequelae. These include seizures, cortical blindness, mental retardation and sensorineural hearing loss. Interestingly enough, the pathophysiology of GBS meningitis differs depending on the time of onset. In contrast to EOD, LOD usually presents with diffuse purulent arachnoiditis (Berman & Baker 1966; Quirante et al. 1974; Shet & Ferrieri 2004; Maisey et al. 2009).

1.1.2 Virulence factors of GBS that facilitate uptake of pathogen

In healthy adults, GBS is a commensal of the human intestinal microflora and also part of the vaginal microbiota in approximately 25% of healthy women without causing any symptoms, let alone a serious infectious disease (Campell et al. 2000, Rajagopal 2009; Tazi et al. 2011). However, under certain circumstances, e.g. in neonates or immune compromised adults, GBS has the ability to cross barriers (e.g. lung and placenta epithelium and blood brain barrier), invade host tissue, elude the immune system and cause a severe invasive bacterial infection. To accomplish this task, GBS expresses a myriad of soluble and surface-bound virulence factors, enabling the pathogen to interact with host cells and avoid clearance by the immune system (Maisey et al. 2009; Rajagopal 2009).

For bacteria to cause disease, they must overcome various barriers. Most of the mechanisms for barrier-crossing involve initial binding to host cells. Studies showed that GBS is able to adhere to human epithelial cells through low avidity interactions of lipoteichoic acid (LTA), which is part of the GBS cell wall. Also, high affinity interactions help strengthen the bond between the host cell and the pathogen. Those are mediated by bacterial surface proteins which mostly bind to components of the extracellular matrix of the host cells. The strength of these interactions is increased under low pH conditions, typical for vaginal mucosa (Maisey et al. 2009). GBS-binding to laminin is mediated by the laminin binding adhesin (Lmb) (Spellerberg et al. 1999). FbsA binds the bacterial surface to fibrinogen (Schubert et al. 2004) and Srr1 attaches to keratin 4 (Samen et al. 2007). Among other functions in immune evasion, the cell surface protein ScpB attaches to fibronectin as well as to integrins (Cheng et al. 2002; Brown et al. 2005). General adherence to host cells is further facilitated by the surface proteins LrrG, BibA and the two pilus proteins PilA and PilC (Seepersaud et al. 2005; Dramsi et al. 2006; Santi et al. 2007).

Four strategies are commonly acknowledged for bacteria to overcome barriers like the blood brain barrier (BBB). The first one is the transcellular pathway, usually including receptor mediated uptake and cytoskeletal modulation. The second option is the paracellular pathway, which includes transient or permanent opening of tight junctions between the host cells. A third route for bacteria to cross barriers is the destruction of the cells that compose the barrier through cytotoxic effects. Another way of circumventing barriers is the so called “Trojan Horse Strategy”. Here, the bacteria facilitate their own uptake by a leukocyte and cross the barrier inside an infiltrating immune cell (Tazi et al. 2012). GBS is thought to use all of these pathways, and expresses a variety of virulence factors to accomplish this task.

In order to overcome barriers using the transcellular pathway, GBS secrets toxins and expresses invasins, which are surface-bound virulence factors that promote bacterial entry into host cells. Entry into host cells (mostly epithelial cells) is not only a possibility to cross barriers, it is also a survival niche for GBS, where the pathogens are protected from immune surveillance. GBS secretes hyaluronate lyase, a protease that cleaves hyaluronan, thereby degrading a chief component of the extracellular matrix. High concentrations of hyaluronan are found in lung and placenta but also in other tissues. Hyaluronate lyase is thought to facilitate the spread of GBS during an infection since studies determined that GBS found in neonates with bacteremia display high concentrations of this enzyme compared to GBS that colonize neonates asymptomatically (Rajagopal 2009). An important protein for epithelial cell invasion is

the surface associated alpha C protein (ACP). ACP enables host cell invasion through interaction with glycosaminoglycan (Baron et al. 2004). ACP also possesses a second mechanism for entering host cells, by binding to $\alpha_1\beta_1$- integrins on the host cell surface (Bolduc 2007). For the uptake of bacteria by the host cell, the cytoskeleton needs to be rearranged. Therefore GBS directly activates Rho GTPases (RhoA, Rac1 and CDC42), which regulate intracellular actin polymerization. GBS can activate focal adhesion kinase (FAK) and paxillin, but also the phosphoinosiotide-3 kinase (PI3K) pathway. Thus GBS actively induces host cell cytoskeleton rearrangement, which in turn leads to the internalization of the bacteria (Fettucciari et al. 2011).

Although the exact mechanism or virulence factors for GBS to be able to use the paracellular pathway are not discovered yet, Soriani and colleagues found that GBS can induce transient opening of junctions (Soriani et al. 2008).

It is evident from the extensive lung endothelial as well as epithelial damage in severe EOD, that destruction of host cells to compromise their barrier function is an important mechanism for entry of GBS into the bloodstream (Nizet et al. 1996; Gibson et al. 1999). The pore-forming toxin primarily responsible for the lysis of host cells is β-haemolysin/cytolysin (β-H/C). Interestingly enough, this toxin promotes lung epithelial cell invasion as well as the release of interleukin (IL)-8 even at subcytolytic doses, suggesting an additional alternative mechanism for entry besides cell lysis (Doran et al. 2002). Furthermore, β-H/C promotes liver failure, impairs cardiac function, and contributes to neurological sequelae by inducing inflammatory responses (Rajagopal 2009). Dipalmitoylphosphatidylcholine (DPPC), part of the lung surfactant, counters not only the cytolytic but also the pro-inflammatory as well as the pro-invasive effects of β-H/C (Nizet et al. 1996). This might help explain why premature neonates, which lack sufficient surfactant production, have an increased risk for EOD.

Another cytolytic protein released by GBS is CAMP factor. Studies have shown that CAMP factor forms pores by oligomerization in host cell membranes, leading to their lysis (Lang & Palmer 2003). Since CAMP factor is not affected by the presence of DPPC, this virulence factor might play an important role for GBS pathogenesis in term neonates with normal surfactant production and presence (Rajagopal 2009).

GBS further expresses a surface-bound glycolytic enzyme called glyceraldehyde-3-phosphate dehydrogenase (GAPDH). This enzyme facilitates not only the binding of host plasminogen to the GBS surface, it also activates this pro-enzyme to acquire

plasmin. Plasmin is a highly tissue-destructive, broad spectrum serine protease, capable of breaking down the extracellular matrix (ECM). Not only does surface-associated plasmin enable GBS to overcome barriers, it is also thought to protect the bacteria from the host immune system since the foreign pathogen is covered with host protein from the ECM and might therefore be regarded as 'self' (Kinnby et al. 2008; Maisey et al. 2009).

Studies have shown that upon phagocytosis GBS is able to survive inside of macrophages for up to 48 h (Cornacchione et al. 1998). GBS also possesses the ability to avoid antimicrobial responses of macrophages and even induce cytoskeleton degradation and apoptosis after invading those host cells (Fettucciari et al. 2011). This suggests that GBS can cross barriers inside of leukocytes, kill their host cells subsequently and colonize tissue protected by cellular barriers like the brain.

1.1.3 VIRULENCE FACTORS OF GBS FOR IMMUNE EVASION

GBS not only expresses virulence factors that facilitate its invasion of various tissues and the host in general, it also expresses various proteins for immune evasion. These factors either reduce or even prevent recognition or help neutralizing host defense mechanisms of the innate immune system, which in turn increases the survival of GBS.

The complement system is a crucial component of the innate immune system. It is essential for opsonization of pathogens, which drastically increases the detection and phagocytosis by macrophages and neutrophils and enables lysis of bacteria through formation of a membrane attack complex. Furthermore, it also induces chemotaxis in phagocytes (Abbas et al. 2007; Maisey et al. 2009). In order to elude recognition and destruction, GBS has developed several strategies to avoid opsonization with complement.

An important factor for GBS virulence is the thick layer of sialic acid-rich capsular polysaccharide (CPS). The CPS defines the serotype (Ia, Ib, II-VII and the recently discovered IX) of GBS since each strain has a different arrangement of monosaccharides (glucose, galactose, N-acetylglucosamine and sialic acid), resulting in serotype specific epitopes. The arrangement of monosaccharides differs from strain to strain, however they share the terminal sialic acid, N-acetylneuraminic

acid (Lewis et al. 2007; Maisey et al. 2009). This terminal sialic acid prevents the deposition of C3, thereby blocking the alternative pathway of the complement system (Edwards et al. 1982). The thick polysaccharide capsule also prolongs the survival of GBS upon phagocytosis (Charland et al. 1996).

Not only does GBS prevent C3 deposition, the pathogen also expresses additional proteins that synergistically work together to inhibit complement activity. The surface-bound protein BibA not only facilitates adhesion of GBS to host cells, it further binds to human C4b binding protein (C4BP), which is a regulator of the classic and the lecithin pathway of the complement system. C4BP increases decay of C3-convertases and helps degrade C3b and C4b, thereby inhibiting complement activity (Santi et al. 2007; Zadura et al. 2009). With the help of the GBS β-protein, the bacteria also bind another regulator of complement activity, complement factor H (CFH) (Hellwage et al. 2004). CFH accelerates the degradation and inhibits new formation of C3-convertases. Furthermore it facilitates cleavage of C3b (Alexander & Quigg 2007). As described above, GBS recruits host proteins to thwart complement activity. However it also expresses own enzymes that affect the complement system, like the C5a peptidase ScpB. This enzyme cleaves human C5a, which is not only an anaphylatoxin but also an important chemoattractant for neutrophils. Thus ScpB reduces recruitment of neutrophils (Takahashi et al. 1995).

Also important for fighting off bacterial infections are cationic antimicrobial peptides (AMP) like defensins and cathelicidins, which also belong to the innate immune system (Hancock & Diamond 2000). AMPs are positively charged and therefore have an electrostatic affinity for the negatively charged LTAs in the cell wall of gram positive bacteria. Once bound to the surface of pathogens, AMPs form membrane pores that disrupt membrane integrity which kills the pathogens. By incorporation of positively charged D-alanine residues into the LTAs, GBS reduces the negative surface charge and therefore its affinity for AMPs (Poiart et al. 2001; Gallo & Nizet 2003). The surface bound penicillin-binding protein PBP1a and the pilus backbone protein PilB also increase the resistance of GBS to AMPs (Hamilton et al. 2006; Maisey et al. 2008).

GBS expresses a number of virulence factors preventing opsonization by complement and subsequent phagocytosis by neutrophils and macrophages. However, if the pathogen is taken up by a phagocyte, it is still able to avoid being killed and degraded by the leukocyte.

The antioxidative carotenoid pigment produced by GBS neutralizes hydrogen peroxide (H_2O_2), hypochlorite (ClO^-), superoxide anions (O_2^-), and singlet oxygen ($^1O_2$). A study by Liu and colleagues implies that this carotenoid enables the bacteria to survive oxidative bursts from phagocytes of premature or septic neonates, which display a diminished oxidative burst function (Liu et al. 2004).

Another protein, providing resistance to reactive oxygen species (ROS), is the superoxide dismutase SodA. This enzyme transforms $2\ O_2^- + 2\ H^+$ into $O_2 + H_2O_2$, which is subsequently metabolized by other enzymes (Poyart et al. 2001).

Due to 100-fold higher oxygen metabolite scavenger glutathione and 10-fold higher glutathione reductase concentrations, the catalase negative GBS resists 10x higher H_2O_2 concentrations than catalase-positive Staphylococcus aureus (Wilson & Weaver 1985). Catalase converts $2\ H_2O_2$ to O_2 and $2\ H_2O$.

1.2 NEONATAL IMMUNE SYSTEM

In the western world, the mortality in the first 60 years of life is highest in the very first year. There, most deaths occur at the very beginning in the first 3 days of life. Interestingly enough, this is the same time when severe bacterial infections and sepsis are most frequent (1-10 per 1000 neonates) (Berner 2005). As mentioned above, before implementing intrapartum antibiotic prophylaxis, almost 50% of early onset sepsis within 72 h after birth were caused by GBS (Gladstone et al. 1990). Severe invasive GBS infections almost exclusively occur in neonates, elderly, or immunocompromised individuals (Maisey et al. 2009), whereas colonized healthy adults typically show no symptoms of infection or disease (Rajagopal 2010).

This raises the obvious question if the immaturity of the neonatal immune system plays a prominent role in the susceptibility of neonates to GBS induced sepsis, especially since the risk of developing an invasive GBS infection increases with immaturity of the child. GBS-associated disease develops in 0.5-1% of term neonates in contrast to 15-20% of preterm neonates from colonized mothers. If the prematurity is very pronounced, below 28 weeks of gestation, the risk of developing an invasive GBS infection increases up to 100% (Schuchat 2001; Berner 2005).

The importance of the immaturity and the deficiencies of the neonatal immune system for the susceptibility to GBS infection was demonstrated in animal studies of

mice. Mancuso and colleagues showed that in neonatal mice, subcutaneous injection of 30 GBS resulted in the death of 60% of the animals. In adult mice the lethal dose for 60% of the infected animals was $5x10^7$ GBS, which represents a more than 10^6-fold higher dose (Mancuso et al. 2004).

The immune system is composed of two branches, the innate immunity and the adaptive immunity. The innate immunity contains the following components: physical (epithelial) as well as chemical (antimicrobial factors e.g. lysozyme) barriers, blood proteins (complement factors, defensins …), cellular components like phagocytes (neutrophils, macrophages) and natural killer cells, as well as regulatory proteins called cytokines which regulate the innate immune response and help activate the adaptive immune response. The innate immunity reacts very rapidly to pathogens (within hours) and contains the infection by killing invading pathogens and preventing systemic dissemination. It further activates the adaptive immune system, consisting of cellular (B and T cells) and humoral (antibodies, cytokines) components. The response of the adaptive branch of the immune system is slower (within days) but also more specific (high diversity of B and T cell receptors) and also possesses an immunological memory, resulting in a faster, more specific and stronger immune response after repeated exposure to the same pathogen (Abbas et al. 2005).

Although the neonatal immune system is able to mount successful immune responses in term as well as preterm infants, it exhibits several limitations and deficiencies in both the innate as well as in the adaptive branch compared to the mature adult immune system.

1.2.1 T CELLS

The fetal immune system develops without contact to pathogens or foreign antigens since the amniotic cavity resembles a sterile environment. Under normal circumstances, the first contact with microbes occurs inside the birth canal during birth (Berner 2005). Therefore, 97% of neonatal T cells feature a naïve phenotype ($CD45RA^+$). In addition to the naivety, which is the presumed reason for a markedly diminished expression of IL-4 and interferon-γ (IFNγ) upon activation, neonatal T cells display several defects (Schelonka & Infante 1998; Chalmers et al. 1998). Activated neonatal T cells produce lower amounts of IL-2 and IL-6 (Watson et al. 1991; Chalmers et al. 1998) and don't fully obtain the adult phenotype since they

express less CD25 (activation marker) but keep expressing CD38 (immaturity marker) (Hassan & Reen 1997). The lower production of IL-2 could be the reason for their diminished activation-induced proliferation upon stimulation *in vitro,* compared to adult T cells (Gasparoni et al. 2003). Considering the reduced cytokine production, it is not surprising that D'Arena and colleagues discovered the markedly decreased ability of neonatal T cells for executing Th1 or Th2 responses (D'Arena et al. 1999). The reduction in IFN-γ production is more pronounced than the reduction in IL-4 production. This could explain why the immune response of neonates is skewed towards Th-2 (Vigano et al. 1999; Adkins et al. 2003; Adkins et al. 2004).

Furthermore, neonatal T cells express lower amounts of CD40 ligand (CD40L), which is an essential ligand for B cell activation and immunoglobulin (Ig) class switching (Schelonka & Infante 1998; Polin et al. 2004).

1.2.2 B CELLS

In neonates the humoral immune response is delayed in onset, has a shorter duration and releases lower amounts of Ig, which have lower average affinity and heterogeneity. It also contains lower amounts of IgG2, which is the prominent IgG subclass induced in response to bacterial capsular polysaccharides (Sanders et al. 1995; Adkins et al. 2004).

Similar to the neonatal T cell population, the naïve phenotype ($CD5^+$) composes the majority of the neonatal B cells. They produce primarily IgM and only low amounts of IgG and IgA upon stimulation, which accounts for the reduced affinity of neonatal antibodies. The overall amount of Ig produced by neonatal B cells is also markedly lower compared to adult B cells (Schelonka & Infante 1998; Splawski et al. 1991).

Furthermore, these immature B cells show a distinctly lower upregulation of major histocompatibility complex (MHC) class II and co-stimulatory factors (e.g. CD86) upon activation (Marshall-Clarke et al. 2000). The expression of CD21 (complement receptor 2) is also diminished. This likely results in weaker activation after binding of antigen/C3d to CD21/CD19/CD81 B cell co-receptor complex. The decreased amount of C3 in neonatal blood exacerbates this deficiency. The reduced expressions of the chemokine receptor 7 (CCR7) and the cell adhesion molecule CD62L (L-selectin) are probably the cause of homing defects in neonatal B cells (Tasker & Marshall-Clarke 2003). Furthermore B cells from neonates not only

express lower amounts of the cytokine receptors for IL-4 and IL-5 and the IL-2 receptor γ chain (IL-2RG) compared to their adult counterparts, they also display a decreased upregulation of IL-2RG upon stimulation with IL-2 and IL-4 (Zola et al. 1995; Saito et al. 1996). Since IL-4, IL-5 and the IL-2RG play a prominent role in growth, maturation, class switching, and antibody secretion (Beagley et al. 1988; Mandler et al. 1993; Recher et al. 2011), the phenotype of the neonatal B cell surface molecules correlates very well with the reduced antibody response in neonates compared to adults. But not only the surface phenotype is different, also intracellular signaling varies. Crosslinking of surface Ig with CD21 leads to intracellular increase of Ca^{2+} and enhanced antibody production in adult B cells. In neonatal B cells the same treatment has no effect on intracellular Ca^{2+} levels or Ig production (Landers et al. 2005).

Neonates produce markedly lower amounts of IgG2 compared to adults. This antibody subclass is produced in response to T cell-independent type 2 (TI-2) antigens (bacterial polysaccharides with high molecular weight) (Adkins et al. 2004; Saunders et al. 2005). A major B cell subset that responds to TI-2 antigens and subsequently produces IgG2 is the marginal-zone B cell (Martin et al. 2001). Neonates only exhibit few marginal-zone B cells. These cells start to develop at the age of 1-2 years and their emergence coincides with the production of specific antibodies against polysaccharides (Timens et al. 1989; Rijkers et al. 1998; Adkins et al. 2004).

The deteriorated antibody response of neonates is not only based on deficient neonatal B cells. Structural defects as well as shortcomings in other neonatal leukocytes (T cells, macrophages, dendritic cells …) contribute to the reduced antibody response (Landers et al. 2005).

For the activation of B cells and subsequent antibody production by T cell-dependent (TD) antigens, lymphoid follicles, follicular-dendritic-cell networks and germinal centers are essential. Animal studies on neonatal mice have shown that these structures do not exist at birth. This probably also contributes to the diminished antibody response of neonates (Adkins et al. 2004).

Infant susceptibility to GBS is most pronounced in the first 3 months of life. This coincides well with lower levels of IgM, diminished antibody responses (especially against capsular polysaccharide antigens) and low levels of the specific antibodies IgG and IgA. The lack of antibody responses against capsular polysaccharides is even exacerbated in GBS infection, since the GBS capsular polysaccharide mimics

the human Lewis antigen and therefore has low immunogenicity (Kasper et al. 1979). Also, the V_H gene repertoire utilized for the variable chain of the B cell receptor is more constrained and the terminal deoxynucleotidyl transferase, which provides junctional diversity in the hypervariable CDR3 region adds fewer nucleotides (adults: 8 between V_H and D_H and 6 between D_H and J_H – neonates: 3 and 2). (Zemlin et al. 2001; Bauer et al. 2002; Berner 2005).

Although there is a transplacental IgG transfer from the mother, this mechanism only partially compensates for the lack of neonatal IgG production. And since the IgG transfer occurs mainly in the last trimester, preterm neonates not only possess an even more immature immune system, but also lack the protection by maternal IgG (Chirico 2005). Furthermore, infants from mothers without GBS-specific IgG are at a disadvantage when being infected with GBS.

1.2.3 MONOCYTES/MACROPHAGES

Although studies of neonatal (cord blood) human monocytes exist, the results are incoherent and often contradicting. Studies that analyzed the cytokine production (IL-1, IL-6, IFN-γ, tumor necrosis factor (TNF)) of cord blood monocytes for example vary in their results, describing lower, equal or even elevated expression compared to adult monocytes upon stimulation. These conflicting results most likely stem from the cell population used for the experiment (whole blood, mononuclear cells (MNC), monocytes/macrophages) and also which agent was used for stimulation (LPS, phytohemagglutinin, bacteria) (Landers et al. 2005). Studies describe equal deficiencies in neonatal T cells, B cells, and neutrophils for humans and mice. Due to the inhomogeneous results from human studies, the findings of mouse experiments will be described in the following paragraph.

Phenotypically, neonatal murine splenic macrophages are mature, since they express similar or even higher amounts of the macrophage marker molecules Mac-1, F4/80, MHC class II, and SR-A (Chelvarajan et al. 2004). Chelvarajan and colleagues showed that neonatal macrophages express lower amounts of Toll-like receptor (TLR)-2, TLR-4 and CD14, responsible for activation of macrophages by the ligands peptidoglycan or LPS, respectively (Aderem & Ulevitch 2000; Chelvarajan et al. 2004). They also showed that upon activation with LPS (also bacteria and peptidoglycan), neonatal macrophages expressed markedly lower amounts of TNF,

IL-1β, IL-6 and IL-12 compared to stimulated adult cells. However, the neonatal macrophages produced significantly more IL-10 (Chelvarajan et al. 2004). As experiments with cells from IL-10 knockout mice have shown, the increased IL-10 expression by stimulated neonatal macrophages is mostly responsible for the low production of the pro-inflammatory cytokines IL-1β and IL-6. This probably is a contributing factor for the Th2 bias of the neonatal immune system, and the susceptibility to bacterial infections. This cytokine profile also seems to be, at least partially, responsible for the unresponsiveness of neonatal B cells to TI antigens, since substitution of IL-1β and IL-6 or anti-IL-10 antibodies enhances neonatal response to TI antigens (high molecular weight polysaccharide) (Chelvarajan et al. 1998; Chelvarajan et al. 2004; Landers et al. 2005).

In summary, the cytokine profile of neonatal macrophages upon activation with bacterial antigens is most likely partially responsible for the Th2 shift of the neonatal immune response, and the inability of the B cells to produce antibodies against antigens like bacterial polysaccharide.

1.2.4 DENDRITIC CELLS

Dendritic cells (DC) are professional antigen presenting cells (APC), essential for initiating an adaptive immune response. After taking up a foreign antigen in peripheral tissue, DC process and display it on MHC complexes on their surface. They upregulate the expression of activation markers and MHC complexes and migrate to the draining lymph node where they present the antigen together with co-stimulatory molecules to T cells. This process initiates an adaptive immune response (Steinman 1991; Banchereau & Steinman 1998).

Human neonatal DC (differentiated from cord blood monocytes) display a phenotype that is similar to their adult counterparts (surface CD11c expression, etc.). However, Goriely et al. showed that after their activation, expression of the important maturation markers HLA-DR, CD40, CD80 and CD86 are lower compared to adult DC. Neonatal DC also display diminished phagocytic capacity, which is essential for the uptake of antigens (Liu et al. 2001). Upon stimulation (LPS, CD40 ligation, poly I:C) they also produce very low amounts of IL-12. Due to this defect, neonatal DC are less potent to induce IFN-γ production in $CD4^+$ T cells (Goriely et al. 2001; Langrish et al. 2002; Landers et al. 2005). Because of that, neonatal DC are less effective in

inducing and sustaining T cell proliferation following antigenic stimulation (Langrish et al. 2002). In contrast to neonatal monocytes/macrophages, DC not only express similar amounts of TLR-4, but also similar amounts of TNF and IL-10 compared to adult DC upon LPS stimulation. Therefore, the reduced IL-12 expression, resulting in lower IFN-γ production, is probably determined intrinsically. That the reduced IL-12 production of neonatal DC contributes to the skewing of the immune response towards Th2 was shown by Arulanandam and colleagues. They could induce a Th1 response by using IL-12 as an adjuvant (Arulanandam et al. 1999).

Deficient DC and monocytes/macrophages are the reason for the diminished neonatal IFN-γ production (Chirico 2005). Not only are both cell types producing less pro-inflammatory cytokines (IL-12, TNF, IL-1, IL-6), they are producing equal (DC) or even higher amounts (macrophages) of anti-inflammatory IL-10 compared to adult cells. This most likely is a major contributing factor for the Th2 bias of the neonatal immune response.

1.2.5 NEUTROPHILS

Neutrophils are often described as the first line of defense of the innate immune system since they are the first leukocytes to be recruited to the site of infection. These cells contain bacterial and fungal infections by phagocytosis and digestion, secretion of antimicrobial substances (degranulation), and catching and killing pathogens with so called neutrophil extracellular traps (NET) (Segal 2005; Hickey & Kubes 2009).

In order to migrate to the site of infection neutrophils follow an increasing gradient of chemotactic factors. Neonatal neutrophils display only 33 – 50% of the chemotactic ability of their adult counterpart (Wolach et al. 1998). In neutrophils from term and more so from preterm infants, several deficiencies in chemotaxis were found (Anderson et al. 1981; Carr et al. 1992; Klein et al. 1977; Pahwa et al. 1977; Wolach et al. 1998; Carr et al. 2000). First of all, in very preterm infants, the total neutrophil cell mass is decreased (Carr et al. 2000). Second, rolling adhesion (migration) to activated endothelium and transmigration to the subendothelial tissue are decreased in cells from newborn infants compared to adult cells (Anderson et al. 1991). Third, the formation of lamellipodia and directed movements towards a stimulus are impaired in neonatal cells (Anderson et al. 1981). Chemotaxis in term, especially in

preterm infants, is further impaired by lower expression of L-selectin which controls neutrophil rolling along the endothelium (Anderson et al. 1991; Mariscalco et al. 1998). In addition to that, neonatal neutrophils display a reduced ability to polymerize monomeric G-actin, which would (at least partially) explain the impaired migratory abilities (Sacchi et al. 1987; Harris et al. 1993; Merry et al. 1998). Interestingly enough, neutrophil chemotaxis improves very quickly after birth, and reaches adult values in about 10 days. This development takes considerably longer in very preterm infants (Carr 2000).

Wolach et al. showed that although the superoxide anion (O_2^-) production in neonatal neutrophils is not impaired, their bactericidal activity (killing of *E. coli*) is just 33% of the adult cells (Wolach et al. 1998). Furthermore, neonatal neutrophils are incapable of NET formation (Yost et al. 2009)

Upon infection, most neutrophils are rapidly recruited from the storage pool in the bone marrow to fight off infections. Also the generation of new neutrophils in the proliferative pool, consisting of proliferating pluripotent myeloid and unipotent neutrophil progenitor cells is increased (Cairo 1989; Berner 2005). Christensen et al. performed *in vivo* experiments, where neonatal and adult rats were infected with GBS followed by an analysis of the neutrophil proliferative pool, the neutrophil storage pool, the circulating blood neutrophil concentration and the immature to total neutrophil ratio in the blood. They showed that adult rats develop neutrophilia (>300% of circulating mature neutrophils compared to non-infected controls) 24 h post infection. The adult neutrophil storage pool decreased in the beginning (to 65%) but increased above 100% after 48 h of infection. And although the neutrophil proliferative pool itself didn't increase, the number of neutrophil progenitors and proliferating cells in the bone marrow increased (300%). The neutrophil response in the neonatal rats depicted a distinctly different picture. In contrast to the adult animals, neonatal rats developed severe neutropenia (aggravated by the fact that 90% of circulating cells were immature) after 15 h of infection. Also the neutrophil storage pool depleted rapidly (30% after 2h; 9% after 15 h compared to controls). The dramatic decrease of the neutrophils in both blood and bone marrow was exacerbated by the reduction of neutrophil progenitors and proliferating cells in the bone marrow (48%) after 15 h (Christensen et al. 1982). An explanation for neutropenia and rapid depletion of the bone marrow storage pool in human term and pre-term infants could be the proliferation rate of neonatal neutrophil progenitors. These cells proliferate at a much higher level compared to adult cells (cells in proliferative state: 55% to 7%). This high (possible maximum) level of proliferation

could mean that there is no possibility to increase the proliferation in case of infection (Christensen et al. 1986).

It is generally acknowledged that, although reduced chemotaxis and bactericidal activity play a role, the crucial factor for the deficient neutrophil activity in neonates is the small (25% of adult cell number, suggested by animals studies) and rapidly exhausted neutrophil storage pool (Chircio et al. 2005; Melvan et al. 2010) and possibly also the inability to increase progenitor proliferation.

1.3 HUMANIZED MOUSE MODEL

Immune responses, drug and vaccine efficacies as well as disease progression are complex processes and can only be studied *in vivo*, not *in vitro*. Studying the human immune response *in vivo* is very limited and severely restricted by ethical and legal restrictions as well as technical constraints (Shultz et al. 2007). Therefore, various scientists claim that there is the growing need for appropriate animal models to study human hematopoiesis, immunity, graft rejection, human specific viruses, infections, vaccines and treatments etc. *in vivo* (Shultz et al. 2005; Shultz et al. 2007). A number of pathogens are either specific for humans or causing human-specific immune responses, which diverge from the responses in other animals. Examples for these infectious agents are human immunodeficiency virus (HIV), Epstein Barr virus (EBV), Dengue virus, hepatitis B virus (HBV), hepatitis C virus (HCV), *Plasmodium falciparum* and *Mycobacterium tuberculosis*. To study HIV infection, primates like chimpanzees, which are closely related to humans have been used. However, chimpanzees are not only expensive and experiments using these animals are burdened with ethical concerns, infected animals also don't mirror the human disease progression, since chimpanzees don't develop acquired immune deficiency syndrome (AIDS) (Shultz et al. 2007; Watanabe et al. 2007; Legrand et al. 2009; Shultz et al. 2011).

The most common animal for research is the mouse (*mus musculus*), which has been and still is enabling many important research advances. The advantages of mice as a model system are: high homology with humans, completely sequenced genome, easy genetic manipulation (transgenic animals), quick reproduction, and being small animals, they are relatively inexpensive to breed and easily maintained (Adinstruments 2012). However, despite the high homology between humans and

mice, and all the above-mentioned benefits, the mouse is often not a very suitable model for the human immune system. Mestas and Hughes describe more than 60 differences between the human and the murine immune system (Mestas & Hughes 2004). They include differential expression of TLR 2/3/9/10, different Ig isotypes and CD1 genes, size of leukocyte populations (human: 30-50% lymphocytes and 50-70% neutrophils vs mouse: 75-90% and 10-25%), different expression of receptors (e.g. FcαRI and FcγRIIA/C), surface proteins (CD4 only on human macrophages) as well as other proteins and factors (e.g. granulysin only in humans). Furthermore, there are also differences of the effects of certain proteins and other factors (e.g. macrophage nitric oxide production induced by IFNγ and LPS (mouse) vs IFNα/β, IL-4 and anti-CD23 (human)). These differences between mouse and human might explain why virtually no treatment that had a significant impact in murine models of sepsis worked in the following 25 clinical trials in patients suffering from sepsis (Unsinger et al. 2009). All these studies show the need for a small animal model that resembles the nature of the human immune system, and may therefore be used to study human specific pathogens and immune responses as well as hematopoiesis.

In order to study human biological processes *in vivo*, mice need to be 'humanized'. This can be done e.g. by engraftment with cells isolated from human tissue (e.g. fetal liver, bone marrow, thymus), peripheral blood mononuclear cells (PBMC) or $CD34^+$ hematopoietic stem cells (HSC) (Shultz et al. 2007). The hematopoietic stem cells can be obtained from several sources: the bone marrow of adult donors (1 HSC per 10^5 cells) is the classic source of stem cells. A second option is to mobilize HSC by injection of certain cytokines (e.g. granulocyte colony stimulating factor (G-CSF)) and to collect the $CD34^+$ cells by filtering the peripheral blood of donors. Another source for human HSC is the umbilical cord blood, which - unlike adult peripheral blood – is rich in HSC. $CD34^+$ cells can also be acquired from fetal tissues, like liver and bone marrow (Stem cell information NIH 2001; Laughlin 2001; Schmitz & Barrett 2002; Shultz et al. 2005).

Engraftment with human cells and/or tissue is only possible in immunodeficient host mice, which are at least limited, or at best unable to reject xenografts.

In 1962, the first immunodeficient mouse strain was discovered. A mutation in the *FOXN1* gene not only resulted in hairlessness (which has given the nude mouse strain its name), but also in the absence of a thymus. This defect results in a lack of functional T cells and Ig, except IgM. They further display a weak response to T cell-dependent antigens, but have increased amounts of NK cells. Nude mice have been

used for xenografts, mostly human solid tumors and tumor cells. Subsequently these models have been used to study the effects of various treatments and drugs on tumor growth and investigate tumor immunity. However nude mice have been replaced in most research areas by severe combined immune deficiency (SCID) mice (Fogh & Giovanella 1978; Caretto et al. 1989; Holub 1992; Charles River 2007). One of the reasons being, that nude mice do not support the growth of transplanted human HSC, in contrast to SCID mice (Garnick et al. 1980).

In 1983 Bosma et al. discovered a mutation in the *Prkdc* (protein kinase, DNA activated, catalytic polypeptide) gene in CB17 mice, resulting in severe combined immunodeficiency (scid) (Bosma et al. 1983). A functional *Prkdc* gene is required for the activation of DNA recombinase enzyme, which in turn is essential for antigen receptor rearrangement. Since this mechanism is necessary for the development of mature T and B cells, both cell types are absent in C.B-17-*scid* mice (Greiner et al. 1998). Mosier et al. were the first to proof that engraftment with human PBMC was possible in C.B-17-*scid* mice (Mosier et al. 1988). McCune and colleagues followed promptly and established a new model by transplanting fetal hematopoietic tissues (human fetal liver, thymus, spleen and lymph nodes) under the renal capsule of these animals (McCune et al. 1988). Also, the successful engraftment with human HSC in C.B-17-*scid* mice has been shown (Lapidot et al. 1992).

Table 1: Research subjects using C.B-17-*scid* mice

Subject	Study
Tumor studies	Veronese et al. 1994
Human stem cell phenotype and differentiation	Kollman et al. 1994
	Heike et al. 1995
	Fraser et al. 1995
	McCune et al. 1996
Human gene therapy protocols	Akkina et al. 1994
	Yurasov et al. 1997
Human T cell differentiation and function	DiGiusto et al. 1996
	Roncarolo et al. 1996
Infection of human T cells with HIV	Jamieson et al. 1996
Homing of human myeloma cells into bone marrow	Urashima et al. 1997

Engraftment of human HSC in C.B-17-*scid* mice generates hu-SRC-SCID mice. SRC is the abbreviation of *scid*-repopulating cell, and characterizes a primitive human stem cell with the ability of multilineage repopulation of the bone marrow of irradiated immunodeficient mice (Larochelle et al. 1996).

Although the C.B-17-*scid* mice were used extensively in various fields of research (table 1), and also have provided valuable results, this model has several major limitations. The level of engraftment of human cells in the bone marrow is quite low (0.5-5% of total cell number) (Lapidot et al. 1992). For some cytokines and growth factors there is species cross-reactivity, however others are species-specific, so that the human stem and progenitor cells cannot utilize those from their murine host. Examples for species-specific cytokines are IL-3, stem cell factor (SCF) and granulocyte/monocyte colony stimulating factor (GM-CSF) (Greiner et al. 1998). This growth factor and cytokine-deficient microenvironment contributes heavily to the reduced proliferation and differentiation of human hematopoietic stem cells in the murine host (Bock et al. 1995). However, the microenvironment of the human cells is not the major reason for the poor engraftment of C.B-17-*scid* mice. The main problem is the rejection of the engrafted cells. Although lacking mature T and B cells, these mice have an enhanced innate immune system, comprised of increased levels of hemolytic complement and NK cell activity compared to C.B-17 wild type mice. This could be a compensation mechanism for the lack of the adaptive immune system (Shultz et al. 1995; Greiner et al. 1998; Macciarini et al. 2005). Aside from the poor engraftment of human cells, the C.B-17-*scid* mice display ‘leakiness’. This phenomenon, which occurs during aging, is the spontaneous rearrangement of antigen receptors, leading to the generation of mature murine T and B cells (Bosma et al. 1988).

Due to the leakiness and low engraftment, other immunodeficient mouse models were generated and investigated for engraftment of human cells and tissue. Since high NK cell numbers are a major factor for rejection of transplanted cells, *bg*/*nu*/*xid* mice have been generated. The beige (*bg*) mutation reduces the number of NK cells, the nude (*nu*) mutation prevents the development of mature T cells, and the *xid* mutation reduces the number of lymphokine activated killer (LAK) cells. Although these mice display higher engraftment of human colony forming units compared to C.B-17-*scid* mice, they did not prevail (Kamel-Reid & Dick 1988; Greiner et al. 1998). Additional models were RAG1- and RAG2-knockout mice, which are deficient for the V(D)J recombination activation gene (RAG) 1 and 2. Since both genes are essential for the V(D)J recombination in the generation of antigen receptors, both mouse

strains lack mature T and B cells (Mombaerts et al. 1992; Shinkai et al. 1992). In the end, C.B-17-*scid* mice were considered to be the mouse strain most suitable to be improved by modifications in order to increase engraftment levels (Greiner et al. 1998).

A more robust engraftment and also long-term repopulation of human cells is necessary for many scientific questions. Therefore C.B-17-*scid* mice have been backcrossed with various inbred mouse strains (C3H/HeJ; C57BL/6J; C57BL/6; DBS and NOD). The resulting animals have been engrafted with human PBMC, to evaluate the best strain background for human reconstitution (Hesselton et al. 1995; Greiner et al. 1998). The NOD-*scid* mice, resulting from crossing non obese diabetic (NOD/Lt) with C.B-17-*scid* mice, have displayed the best level of engraftment (5-10x higher than other strains) (Hesselton et al. 1995). NOD/Lt mice are a model for spontaneous autoimmune T cell mediated insulin-dependent diabetes mellitus (IDDM) which develops at the age of 4-6 weeks (Shultz et al. 1995). These animals show defective T cell as well as macrophage activation, resulting in low IL-2 and IL-1 production (Serreze & Leiter 1988). They have functional deficits in NK cells (Kataoka et al. 1983) and reduced monocyte/macrophage development and differentiation, including incomplete maturation upon IFN-γ stimulation, reduced proliferation, less mature phenotype, etc. (Serreze et al. 1993). Furthermore, NOD/Lt mice lack the complement protein C5, necessary for the formation of the membrane attack complex, and therefore display no complement lytic activity (Baxter & Cooke 1993).

In contrast to NOD/Lt, NOD-*scid* mice do not develop IDDM, since it is both mediated by and dependent on mature T cells, which are absent due to the *scid* mutation. Compared to C.B-17-*scid* mice, these animals show no hemolytic complement activity, and have a severely reduced NK cell activity, both endogenous and after stimulation with poly I:C. Furthermore, the NOD-*scid* strain is markedly less prone in developing ‘leakiness’. Only 10% of NOD-*scid* vs 90 % of C.B-17-*scid* mice develop detectable levels of immunoglobulin by 200 days of age. Furthermore NOD-*scid* mice maintain allogeneic skin grafts for several months. These findings indicate the absence of both mature B and T cells. These animals also display some defects of myeloid cells, like a significantly reduced IL-1 production upon LPS stimulation. The deficiencies, mostly the reduced NK cell and complement activity, explain the increased reconstitution of human cells compared to C.B-17-*scid* mice. Another factor, which furthers human HSC engraftment in NOD-*scid* mice, is the Signal-regulatory protein alpha (SIRPA) allele expressed on the macrophages due to the

NOD background. Due to a polymorphism in the IgV-like domain of *SIRPA,* the protein can bind to human CD47. This not only inhibits phagocytosis and secretion of proinflammatory cytokines like TNF, preventing graft rejection by murine macrophages, but is also thought to induce signaling pathways in human HSC that increase their survival and engraftment levels (Takenaka et al. 2007).

However, the increased engraftment levels come at a price. NOD-*scid* mice contain the murine leukemia provirus *Emv30* in the proximal region of chromosome 11. This provirus is not expressed in NOD/Lt mice, but induces spontaneous thymic lymphomas in NOD-*scid* mice after 5 months and is the major cause of death in aging NOD-*scid* mice which have a median survival of only 8.5 months (Shultz et al. 1995; Greiner et al. 1998).

Table 2: Research subjects using NOD-scid mice

Subject	Study
Hematopoiesis	LaRochelle et al. 1996
	Hogan et al. 1997
	Gan et al. 1997
Leukemia	Steele et al. 1997
	Appelbaum et al. 2001
Cysticercosis	Ito et al. 2001
Gene therapy	Woods et al. 2002
Sjögren's syndrome	Cha et al. 2002
Dengue fever	Bente et al. 2005
EBV infection and toxic shock syndrome	Melkus et al. 2006

Table 2 shows examples of studies where the NOD-*scid* model was used. Although this model is far superior in engraftment of human cells compared to nude and C.B-17-*scid* mice, it still possesses various drawbacks. Therefore, several mouse models have been developed to improve the generation of a functional human immune system in immunocompromised mice. One approach was the knockout of the β2 microglobulin (*B2m*) gene. This gene is required for MHC class I expression, and is essential for NK-cell development. Due to the total absence of functional NK cells in NOD-*scid B2m*$^{-/-}$ mice, they have moderate engraftment levels for human HSCs,

higher numbers of T cells and multiple human myeloid linages, although only in low numbers. However, like NOD-*scid* mice, they only develop immature human B cells, and due to the lack of NK cell activity, the mice develop, and die from T cell lymphomas faster (Christianson et al. 1997; Macchiarini et al. 2005; Shultz et al. 2007).

A number of additional immunodeficient mouse strains were generated, each having certain advantages but also disadvantages for engraftment of human tissue, lifespan, etc. Some strains have been based on the deficient *Prkdc* allele responsible for scid, e.g. C57BL/6-*scid bg* and BALB/c-*scid bg,* both featuring low NK cell function, but high levels of innate immunity resulting in low to very low engraftment with human HSC. Since the NOD background provides a very good basis for human cell engraftment, it has been used for various immunodeficient strains: NOD-*scid* and NOD-*scid B2m*$^{-/-}$ mice, described above; NOD-*scid* IL-3, GM-CSF, SCF transgenic mice, which express human hematopoietic factors, but still have low levels of human HSC engraftment; NOD-*Rag1*$^{-/-}$ and improved NOD-*Rag1*$^{-/-}$ *Prf1*$^{-/-}$ mice with low and very low NK cell activity, respectively. However, both strains display only limited levels of engraftment (Shultz et al. 2007). For a comprehensive review and references of all the immunodeficient mouse strains described above, see Shultz et al. 2007.

A breakthrough in generating immunodeficient mouse strains for humanization has been the introduction of a targeted mutation in the IL-2RG locus (*IL2rg),* also called common γ-chain (γc). The γc is not only an essential element of IL-2/4/7/9/15 and IL-21 receptors, but also required for signaling through these receptors. Lack or truncation of the γc results in seriously impaired T and B cell function and development and abolishes NK cell development altogether (Ito et al. 2002; Ishikawa et al. 2005; Shultz et al. 2007).

Two different mutated *IL2rg* have been implemented into several stains by backcrossing. One of the IL-2RG loci (*Il2rg*^{tm1sug}*)* produces a truncated protein, lacking the intracytoplasmic domain. This leads to the abrogation of all signaling through receptors containing the γc. The other IL-2RG locus (*Il2rg*^{tm1Wjl}) is an entire knockout, resulting in the complete absence of a γc. Introduction of mutated IL-2R γ-chain loci in NOD-*scid* mice generated NOG (NODShi.Cg-Prkdc^{scid} *Il2rg*^{tm1sug}/Jic [NOD/LtSz-scid IL2rg$^{-/-}$] with truncated γc) and NSG (NOD.Cg-Prkdc^{scid} *Il2rg*^{tm1Wjl}/Szj [NOD/Shi-scid IL2rg$^{-/-}$] without γc) mice. It was hypothesized that the presence of the truncated γc could lead to the binding of human cytokines, like IL-7 to murine cells,

bearing the correlating receptors. The retention of human cytokines by murine cells would in turn disturb and reduce the development of certain human leukocytes, in case of IL-7 this would be T cells. This theory could help explain why NSG mice display higher engraftment of human $CD45^+$ cells in spleen, bone marrow and thymus compared to NOG mice, although only by 10-20% (McDermott et al. 2010) (Shultz et al. 2007; McDermott et al. 2010). The resulting immunodeficient strains with $Rag2^{-/-}$ background are $H2d^{-}Rag2^{-/-}IL2rg^{-/-}$, BALB/c $Rag2^{-/-}IL2rg^{-/-}$. NSG and NOG mice have a long lifespan of >90 weeks since there is no thymic lymphoma development. This is most likely because the thymocytes, which generate the lymphomas, require IL-7 and IL-2 receptor signaling in order to expand (Shultz et al. 2005). There is also no sign of leakiness, even after irradiation, which generally enhances the sporadic development of T and B cells (Ballen et al. 2001). Due to the γc knockout, the strains display markedly increased engraftment levels of human cells (Shultz et al. 2007). Upon humanization with HSC from adult donors, NSG mice show 6-fold higher amounts of human $CD45^+$ cells in the spleen, 10-fold higher in BM, 100-200-fold higher in thymus and >60-200-fold higher in the peripheral blood compared to NOD-*scid* mice (Shultz et al. 2005). Transplantation of HSC into NSG mice following irradiation results in the generation of human granulocytes, monocytes/macrophages, NK cells, plasmacytoid and myeloid DCs, mature T and B cells, and even erythrocytes and platelets (Ishikawa et al. 2005; Shultz et al. 2005; Shultz et al. 2007; Unsinger et al. 2009). The human T cells found in the NSG mice develop by progressing through the expected stages of intrathymic development (CD4 CD8 double-negative, CD4 CD8 double-positive and finally CD4 or CD8 single positive) (Shultz et al. 2005; Shultz et al. 2007). In contrast to T cells from humanized NOD-*scid* mice, T cells from NSG mice display a complex T cell receptor (TCR) repertoire with high levels of TCR rearrangements. They are much more abundant in numbers and there are also regulatory T cells (T_{reg}) present (Shultz et al. 2005; Shultz et al. 2007). T cells from NSG mice display human leukocyte antigen (HLA)-dependent cytotoxicity (killing of allogeneic lymphoblastoid cells), mount a delayed-type hypersensitivity (DTH) response, and proliferate after stimulation. Furthermore, B cells can undergo class switching and generate antigen specific IgM and IgG upon immunization with ovalbumin (OVA) (Shultz et al. 2005; Ishikawa et al. 2005; Unsinger et al. 2009).

Humanized NSG mice were used for various studies in different research fields (table 3), and although they represent a marked improvement to previous animal models, there are still ways to improve this particular model for translational research.

Table 3: Research subjects using NOD-*scid* γ-chain knockout mice

Subject	Study
Acute lymphoblastic leukemia	Agliano et al. 2008
Sepsis model	Unsinger et al. 2009
Dengue fever pathogenesis	Mota & Rico-Hesse 2009
	Mota & Rico-Hesse 2011
Malaria model	Jimenez-Diaz et al. 2009
Melanoma lung metastases	Carreno et al. 2009
ADCC against leukemia cells	Ito et al. 2009
Ovarian cancer	Bankert et al. 2011
Chemotherapy against hepatoblastoma	Lieber et al. 2011
Breast cancer model	Wege et al. 2011
GVHD model	Covassin et al. 2011
Treatment for rhabdomyosarcoma	Tahan et al. 2012
Disease progression of HIV	Long & Stoddart 2012
HIV therapy	Vets et al. 2012
	Dubrovsky et al. 2012

In order to further enhance the engraftment of human HSC or PBMC, the residual murine myeloid cells (macrophages, granulocytes and DC) should be eliminated. This can be achieved by treating the animals with liposome encapsulated dichloromethylenebisphosphonate or specific antibodies prior to transplantation with human cells (Shultz et al. 2007). Studies also showed that administration or transgenic expression of human hematopoietic growth factors and cytokines (e.g. IL-3, SCF and GM-CSF) improves engraftment and differentiation of human HSC in NSG mice. Other cytokines like IL-7 facilitate the function and development of lymphocytes, in this case T cells (Shultz et al. 2007; Andre et al. 2010; Takagi et al. 2012).

1.4 BACKGROUND ON TREATMENT OPTIONS

1.4.1 LUNG MATURATION - BETAMETHASONE

Liggins and Howie have been the first, who used antepartum glucocorticoid treatment in a clinical trial to prevent respiratory distress syndrome in premature infants (Liggins & Howie 1972). Before the widespread use of glucocorticoids for fetal lung maturation, respiratory distress syndrome (RDS) has been a main cause of neonatal death. RDS occurs due to inadequate production and presence of surfactants in the fetal lung before 32 to 34 weeks of gestation. Surfactants are produced by type II alveolar cells. They are composed of the surfactant proteins SP-A, SP-B and SP-C and several lipid species, the primary lipid being Dipalmitoylphosphatidylcholine (DPPC). Surfactants coat the alveoli with a lipid/protein-monolayer, thereby reducing the surface tension to near 0 (Longo 1993). This is called compliance (ease of expansion of the lungs) and essential for a markedly reduced respiratory effort. Furthermore, surfactants help the lung maintaining a large alveolar surface area, where gas exchange can take place (Schürch et al. 1992). Therefore, lack of surfactants, occurring in premature infants, leads to a collapse of alveoli during expiration, and the following inspiration requires considerable effort. This quickly induces fatigue, leading to decreased respiratory effort, followed by hypoxia, cyanosis, acidosis and finally death (Purandare 2005).

Since the 1970s, antepartum glucocorticoids are the recommended practice to prevent RDS and intraventricular hemorrhage (IVH) in preterm infants (NIH Consens Statement 1994). Studies in fetal sheep have shown that Betamethasone treatment markedly decreased cerebral blood flow in all brain regions except the hippocampus 24 h, and less pronounced 48 h post injection. This effect is mediated by the vasoconstrictory impact of Betamethasone on fetal cerebral blood flow. This may explain the reduction of IVH after glucocorticoid treatment (Schwab et al. 2000).

Meta-analysis of 18 studies confirmed that prophylactic glucocorticoids reduce incidence and severity of RDS, IVH and neonatal mortality of preterm infants born at 24 to 34 weeks of gestation (Crowley 2000). The commonly utilized glucocorticoids are Dexamethasone or Betamethasone. They were chosen due to their long half-lives, limited mineral corticoid activity and both also readily cross the placenta (Goldenberg 2002). However, since Baud et al. determined that Betamethasone is

more effective in reducing periventricular leukomalacia and also IVH compared to Dexamethasone, the better choice seems to be Betamethasone (Baud et al. 1999). The standard therapy regimen is 12 mg Betamethasone given twice, 24 h apart, to the mother (Goldenberg 2002; Peltoniemi et al. 2006).

Although it is unknown if glucocorticoid therapy increases the maternal and/or neonatal infection, it is generally acknowledged, that the beneficial effect of preventing RDS, IVH and therefore also neonatal death outweighs the potentially greater risk of infection (NIH Consens Statement 1994).

1.4.2 TOCOLYSIS - INDOMETHACIN

Preterm delivery by definition occurs between 20 to 37 weeks of gestation. The preterm delivery rate in the US is about 11% and varies in Europe between 5% and 7%. Although mortality based on prematurity decreased due to improved neonatal intensive care, it still remains a leading cause of death (60-80% of death of neonates without congenital anomalies). Preterm deliveries primarily result from spontaneous preterm labor (40-50%), premature rupture of membranes (25-40%) or obstetrically indicated preterm delivery (20-25%) (Goldenberg 2002). Even with intensive care, neonates born before 22 weeks of gestation are incapable of surviving. The survival of neonates at a gestational age of 22 weeks is rare. However, with a gestational age of 23 weeks, the approximate survival rate is already 25%, with 24 weeks 50%, with 25 weeks 70% and about 80% for neonates born 26 weeks after gestation (Goldenberg 2002). It is evident that delaying or preventing preterm labor in the timeframe between a gestational age of 20 to 26 weeks greatly enhances the infants probability to survive. There are a number of tocolytic agents available for delaying time of delivery. These include Ritodrine, Terbutaline, magnesium sulfate, Nifedipine, Atosiban and Indomethacin. These drugs have different mechanisms of action. Ritodrine and Terbutaline stimulate β_2 receptors, which results in an increase in intracellular cAMP. This inhibits the myosin light chain kinase, inducing uterine smooth muscle relaxation. The relaxation leads to the inhibition of uterine contractions and therefore temporarily arrests premature labor. Nifedipine is a calcium channel blocker, inhibiting calcium influx into the smooth muscle cells and thereby inhibiting contractions. Magnesium sulfate is a calcium antagonist, which also inhibits contractions and stopping premature labor. Atosiban is an oxytocin antagonist, which inhibits oxytocin-induced uterine contractions and thereby

preventing delivery (Goldenberg 2002; DeHeus 2008; Mediglyphics). Indomethacin is a non-steroidal anti-inflammatory drug (NSAID) that inhibits both the cyclooxygenase (COX)-1 and 2 (Woods et al. 2001; Sekar & Corff 2008). Both convert arachidonic acid into prostaglandin (PG)-G, which is quickly converted into PGH. PGH then serves as a precursor from which all other prostaglandins originate (Perrone et al. 2010). COX-1 is constitutively active in most cell types and produces so called protective prostaglandins (PG), which preserve the integrity of the stomach lining and maintain normal renal function among others. COX-2 is inducible and it produces PG which play a role in ovulation, the birth process and inflammation. PG, especially PGE_2, which is mostly produced by monocytes in humans, has been shown to exert effects on both cellular and humoral immune responses and inflammation (Goodwin et al. 1978; Goodwin & Ceuppens 1983; Vane et al. 1998; Thuresson et al. 2001; Suleyman et al. 2010). The role of PGs in labor is stimulation of myometrial contractions, cervical softening, and induction of enhanced levels of myometrial gap junctions, which increase intracellular calcium levels and thereby enhance myometrial activity (Husselein 1984; Riemersma et al. 1998). As with the above mentioned tocolytics, studies using Indomethacin to block labor show very contradicting results regarding efficacy and side effects. However, Loe et al. performed a meta-analysis of 28 studies, and concluded that Indomethacin therapy did not significantly increase the rate of IVH, bronchopulmonary dysplasia, premature closure of the ductus arteriosus and perinatal mortality, which were all side effects, mentioned in other studies. But he also did not exclude adverse outcomes, since the limited statistical power of the 28 studies did not allow that (Loe et al. 2005). Suarez et al. described that most studies claiming that Indomethacin increases the risk of IVH use the drug as a second line tocolytic, when the first one fails. This procedure increases the risk of IVH. In addition, animal studies showed that Indomethacin even protects the fetus from IVH (Suarez et al. 2001). Combining Indomethacin with another tocolytic also increases the risk for necrotizing enterocolitis in infants, whereas the use of Indomethacin alone does not (Parilla et al. 2000). Other studies indicate that in 10-50% of fetuses exposed to Indomethacin, premature closure of the ductus arteriosus occurs. This can lead to pulmonary hypertension and even heart failure in the fetus, and mostly happens when the drug is administered for more than 48 h and at higher gestational age (>32 weeks) (Goldenberg 2002; Giles 2007; Perrone et al. 2010). Since prostaglandins, especially PGI_2 and PGE_2 are important for regulation of kidney function (e.g. increase of renal blood flow, salt and water excretion), renal dysfunction such as anuria, increased serum creatinine concentrations and even renal microscopic lesions have been reported after prenatal

Indomethacin exposure (Norton et al. 1998; Goldenberg et al. 2002). Although renal dysfunction is a serious side effect, Indomethacin does not seem to cause negative long-term effects. A study on neonates treated with Indomethacin for patent ductus arteriosus did show increased levels of serum creatinine, decreased glomerular filtration rate and 24% of infants even displayed acute renal failure on day 2 and 7 upon Indomethacin treatment. However, after 30 days the renal function was normal in all infants (Akima et al. 2004).

1.5 AIM

The aim of this study was to determine the effect of Betamethasone and Indomethacin treatment on the human neonatal immune system during an ongoing infection. As described above, Betamethasone is the standard treatment for promoting fetal lung maturation of premature infants in the clinic. Indomethacin is one of the tocolytics, which are routinely used to prevent premature birth in the clinic. Although, both drugs are routinely used in the clinic, not much is known about their effect on the neonate in regards of organ damage, or their effect on the neonatal immune system and disease progression. Therefore, I generated a new infection model using humanized mice, to mimic the naïve human neonatal immune system and subsequently tested both treatment options. Humanized NSG mice were infected with GBS, animals were treated with Betamethasone or Indomethacin and the effects of both drugs on clearance of live bacteria, migration and proliferation of immune cell populations, immune cell function (cytokine and nitric oxide production) and organ damage was analyzed.

2 MATERIAL & METHODS

2.1 METHODS

2.1.1 ANIMALS

The animals used for this study were NOD.Cg-Prkdc^{scid} Il2rg^{tm1Wjl}/Sz (NOD-*scid* IL2R^{null}, NSG) mice, which were obtained from Jackson Laboratories, USA. Mice were kept and bred in a specific pathogen free animal facility at the University Hospital Regensburg.

2.1.2 HUMANIZATION OF MICE

Neonatal mice (0-2 days old) were irradiated with 1 gray. This process is called conditioning and necessary to clear stem cell niches in the bone marrow, which can subsequently be settled by human hematopoietic stem cells (HSC). These human CD34$^+$ stem cells were purified from human cord blood as follows:

Fresh human cord blood, containing citrate to prevent coagulation, was mixed with PBS in a ratio 1:1. The diluted blood is carefully layered on 15 ml Pancol (Pan Biotech, Aidenbach, Germany) in a 50 ml Falcon tube (Sarstedt, Nümbrecht, Germany) and centrifuged at 600 rcf, room temperature (RT) for 30 min. After density gradient centrifugation, the following layers are visible from top to bottom: the plasma layer, the so-called buffy coat (containing mono-nuclear cells (MNC) and platelets), the Pancol layer, and a pellet of erythrocytes and granulocytes. The MNC could easily be harvested from the buffy coat using a 5 ml pipette (Sarstedt). MNC were transferred into 25 ml PBS + 2 mM EDTA to prevent clotting and to dilute Pancol which can be harmful for MNC when exposed to for a longer period of time. After centrifugation for 10 min at 300 rcf, 4°C, MNC were resuspended in 5 ml PBS + 2 mM EDTA and counted. Cell suspension was diluted 1:100 with Trypan blue solution (Sigma-Aldrich) and counted using a Neubauer counting chamber (HBG Precicolor, Giessen, Germany). For purification of human CD34$^+$ hematopoietic stem cells from cord blood MNC, MACS cell separation (Miltenyi Biotech, Bergisch Gladbach, Germany) was utilized. The cell suspension was centrifuged, supernatant was

removed and MNC were resuspended in MACS buffer (table 8) (150 µl/10^8 MNC). After adding CD34 Microbeads (Miltenyi Biotech) and MACS Fc Block (Miltenyi Biotech) (50 µl beads and block/10^8 cells), cells were incubated 30 min at 4°C. Then MNC were washed with MACS buffer (10 ml / 10^8 cells), centrifuged for 10 min at 300 rcf, 4°C, supernatant was removed, and labeled MNC were resuspended in MACS buffer (250 µl/10^8 cells). A MACS MS Separation Column (Miltenyi Biotech) was placed in the magnetic field of a MACS Separator (Miltenyi Biotech) and rinsed with 500 µl MACS buffer. Labeled MNC suspension was applied over a 40 µm cell strainer and passed through the column. The effluent was reapplied onto the column and passed through a second time to increase yield. Subsequently, the column was washed 3x with 500 µl MACS buffer. The column was removed from the Separator and placed on a 15 ml Falcon tube (Sarstedt). Cells were flushed out by applying 1 ml MACS buffer and pushing the plunger into the column. In order to increase the purity of the magnetically labeled $CD34^+$ stem cells, they were passed over a second column (as described above). MNC in the effluent were frozen and stored (see 2.9). After purification, 10 µl of the cell suspension were stained (table 8 staining C) for flow cytometric analysis to determine purity. Stem cells were counted by diluting 10 µl of the cell suspension 1:10 with trypan blue solution. The remaining cells were centrifuged at 300 rcf, 4°C for 10 min, and resuspended in RPMI 1640 medium (Pan Biotech, Aidenbach, Germany) ($2x10^5$ stem cells per 50 µl).

Purified $CD34^+$ stem cells were transplanted into previously conditioned NSG neonates. 50 µl cell suspensions, containing $2x10^5$ cells, were injected intrahepatically using a BD SafetyGlide Insulin syringe (BD Biosciences, Franklin Lakes, USA). The $CD34^+$ human hematopoietic stem cells generated a complete human immune system in the transplanted, humanized mice. After approximately 6 weeks, when the generation of the human immune system was completed, peripheral blood (pb) was taken from each mouse and analyzed using flow cytometry (table 4, staining T and M) to determine the level of reconstitution.

2.1.3 GROWING AND QUANTIFYING BACTERIA FOR INFECTION

Stock cultures of GBS were prepared using the Mikrobank Bacterial Storage System (Prolab Diagnostics, Richmond Hill, Canada) according to manufacturer's protocol. GBS (reference stain ATCC 13813 received from Department of Microbiology, University Hospital Regensburg) were plated on blood agar plates and grown

overnight at 37°C. Subsequently, bacteria were scraped off the plate using an inoculation loop and used to inoculate cryopreservative in Mikrobank vials containing plastic beads. Vials were inverted 4–5 times to distribute the bacteria on the beads. Cryopreservative was aspirated and vials containing inoculated beads were stored at -80 °C.

In order to grow GBS for infection of animals or for *in vitro* experiments, 2 blood agar plates were inoculated with one inoculated bead each and incubated overnight at 37°C. Bacteria were scraped off the plate, transferred into 1 ml PBS and vortexed vigorously. GBS suspension was diluted with PBS and adjusted to an optical density (OD) of 0.400 using a Nano Photometer (Implen, Munich, Germany). The bacteria suspension was serially diluted starting at 10^{-1} down to 10^{-6}. Dilutions 10^{-4}, 10^{-5} and 10^{-6} were plated on blood agar plates and incubated at 37°C overnight. Colonies on plates were counted and calculated to ensure that the suspension contained appropriate amount of GBS.

2.1.4 INFECTION AND TREATMENT OF ANIMALS

Humanized or non-humanized NSG mice were infected with different doses of GBS. For determining appropriate infectious doses for humanized mice, the animals were injected with different amounts of live bacteria ($1x10^5$, $5x10^5$, $1x10^6$, $1x10^7$, $5x10^7$, $1x10^8$). For each dose, the bacteria suspension was adjusted with PBS, so that 1 ml PBS contained the appropriate amount of live bacteria. Each mouse was then infected by injecting 1 ml of GBS suspension intraperitoneally using a Plastipak 1 ml syringe (BD, USA) in combination with a 27 G Microlance 3 needle (BD Biosciences).

Animals that were infected with 10^7 GBS for 24 h (short term infection) received either vehicle control (PBS) or 5 mg/kg Betamethasone (Essex pharma, Munich, Germany) intraperitoneally 3 h post infection. Mice that obtained 10^6 GBS and were killed either 3 d (intermediate infection) or 7 d (long term infection) after infection received either vehicle control (PBS), 5 mg/kg Betamethasone or 3 mg/kg Indomethacin (Euro OTC Pharma, Bönen, Germany) 24 h as well as 48 h post infection.

2.1.5 PREPARATION OF BLOOD, SINGE CELL SUSPENSIONS AND TISSUE FROM MICE

Mice were anesthetized and blood samples were taken retrobulbarly. For flow cytometric analysis, 100 µl pb were mixed with 20 µl 0.5 M EDTA. The remaining pb was collected in a 1.5 ml reaction tube and allowed to clot at 4°C, to obtain serum for cytokine analysis (see 2.18). After bleeding, mice were killed by cervical dislocation. Using a 10 ml BD Discardit II syringe (BD Biosciences) in combination with a 22G BD Microlance needle (BD Biosciences), the peritoneum was rinsed with 10 ml FACS buffer to obtain peritoneal lavage containing peritoneal exudate cells (PEC).

One femur, spleen, two kidneys, liver, mesenteric lymph nodes (mLN), lung and brain were removed and placed in PBS (Pan Biotech). Approximately one fourth of the spleen and liver, half of a kidney and the brain and a whole mLN were embedded for histological analysis (see 2.13-15). The remaining part of the organ was weighted, passed through a 40 µm cell strainer (BD Biosciences) using a 2 ml BD Discardit II syringe plunger (BD Biosciences), and washed 2x with 10 ml PBS. The ends of the femur were clipped off and the bones were rinsed with RPMI 1640 medium using a 5 ml BD Discardit II syringe (BD Biosciences) in combination with a 27G BD Microlance needle (BD Biosciences). The extracted bone marrow was passed through a 40 µm cell strainer (BD Biosciences) using a 2 ml BD Discardit II syringe plunger (BD Biosciences). Subsequently, 200 µl of the resulting single cell suspensions were removed and kept for colony forming unit (CFU) detection (see 2.7). The remaining single cell suspensions were centrifuged at 300 rcf, 4°C for 10 min. Supernatants were discarded and the cells were resuspended in residual PBS and counted. Afterwards, 10^6 cells were stained for flow cytometric analysis (see 2.8).

2.1.6 PERCOLL CELL SEPARATION

In order to be able to conduct flow cytometric analysis of single cell suspensions of lung and liver, a density gradient cell separation was conducted to separate leukocytes from lung epithelial cells or hepatocytes, respectively. 100% Percoll (GE Healthcare, Uppsala, Sweden) was diluted with RPMI 1640 medium to 70% and 40% Percoll. Samples of single cell suspensions of liver and lung were centrifuged at 300 rcf, 4°C for 10 min, and supernatant was discarded. Each sample was resuspended

in 5 ml 40% Percoll and carefully underlayed with 6 ml 70% Percoll using a glass Pasteur pipette (Brand, Wertheim, Germany). This Percoll gradient was centrifuged at 1000 rcf, 20°C for 20 min. Due to density separation, the following layers were generated: An upper band, containing almost exclusively epithelial cells or hepatocytes, respectively, a middle layer containing few cells (mixed population of MNC) and a lower band, containing the majority of MNC. The upper band was removed completely. Both middle and lower bands were transferred into a new 15 ml Falcon tube containing 5 ml PBS. Cells were centrifuged at 300 rcf, 4°C for 10 min, supernatant was removed, cells resuspended in residual PBS and counted.

2.1.7 DETECTION OF COLONY FORMING UNITS IN VARIOUS ORGANS

In order to detect live bacteria (CFU) peritoneal lavage (PEL) and single cell suspensions of bone marrow (BM) (from femur), spleen, kidney, liver, lung and brain were diluted and plated on blood agar plates. PEL and single cell suspensions were serially diluted from 10^0 to 10^{-4} by mixing 100 µl of each sample with 900 µl PBS. Each dilution was subsequently plated on blood agar plates and incubated over night at 37°C. Bacteria colonies were counted the next day, and the number of GBS per g organ (or per ml for PEL and BM) was calculated using the following formula:

$$\frac{\text{(number of CFU) x (dilution factor) x 10 x (volume of cell suspension in ml)}}{\text{(weight of organs in g)}}$$

2.1.8 STAINING FOR FLOW CYTOMETRY

First, 10^6 cells of single cell suspensions from BM, mLN, spleen, PEL, purified liver and lung (see 2.5,6) were adjusted to 100µl using FACS buffer (table 8). These cell suspensions or 100µl pb respectively, were incubated with 2 µl human serum for 15 min to block unspecific binding sites. Subsequently, cells were incubated with antibodies according to the manufacturer's protocol (dilutions see table 5) for 45 min at 4°C in the dark. Subsequently, erythrocytes in the samples of spleen, BM, liver, lung and pb were lysed using a 1:10 dilution of BD FACS Lysing Solution (BD Biosciences) with deionized H_2O for 10 min in the dark. 2 ml FACS buffer were applied to each sample followed by 10 min centrifugation at 300 rcf, 4°C, and

supernatant was discarded. For FACS staining M and T 0.06 µg (0.3 µl) Streptavidin APC-Cy7 (FITC) was applied for 15 min. Samples were washed with 2 ml FACS buffer, centrifuged at 300 rcf, 4°C for 10 min, and supernatant was removed. Finally, labeled cells were resuspended in residual buffer in FACS tube by vortexing and analyzed using a BD LSR II Flow Cytometer (BD Biosciences).

For analysis of FACS data, BD FACSDiva software (BD Biosciences) was used.

Table 4: FACS stainings

Antibody stainings

staining	FITC	PE	PerCP	APC	Pe-Cy7	APC-Cy7
T	CD4	CD19	CD3	CD8	CD45 RA	CD27 biotin
M		CD66	CD33	CD45	HLA-DR	CD80 biotin
C	CD3	CD34	CD33	CD56		
V	CD3	CD66	CD33	CD56	CD19	
K		CD86	CD33	CD45		

Isotype controls

Iso T	CD4	CD19	CD3	IgG1	IgG2b	IgG1 biotin
Iso M		IgG2b	CD33	CD45	IgG2	IgG1 biotin
Iso C	no isotype control necessary					
Iso V	no isotype control necessary					
Iso K		IgG2b	CD33	CD45		

2.1.9 Freezing of MNC

MNC were centrifuged at 300 rcf, 4°C for 10 min. Supernatant was removed and cells were resuspended in 800 µl RPMI 1640 medium. MNC were transferred into a 2 ml Cryo Tube (Nunc, Wiesbaden, Germany) and mixed with 800µl cold freezing medium (2x) (table 8). Cryo tubes were immediately put into Nalgene Cryo 1°C Freezing Container (Nalgene, Penfield, USA) and stored at -80°C overnight. Cryo

tubes were transferred into gaseous phase of liquid nitrogen for long term storage at -178 to -150°C.

2.1.10 IN VITRO *DIFFERENTIATION OF MONOCYTES AND SUBSEQUENT STIMULATION*

Humanized mice were anesthetized and killed by cervical dislocation. Femurs and tibias were surgically removed and placed in cold RPMI 1640 medium. The ends of the femurs and tibias were clipped off and single cell suspensions were prepared as described above (see 2.5). The resulting single cell suspensions of bone marrow derived cells (BMDC) were counted by diluting 10 µl 1:100 with Trypan blue solution. BMDC were seeded at a density of $5x10^5$ cells/cm^2 in Falcon 6 well-plates (BD Biosciences), and cultivated in Macrophage SFM (Invitrogen, Carlsbad, USA) + 50 ng/ml M-CSF (R&D Systems, Minneapolis, USA). Medium was changed after 24 h and again after 3 d to avoid activation of the macrophages. After cultivation of BMDC 7 d under these conditions, the monocytes differentiated into bone marrow derived macrophages (BMDM). They were subsequently stimulated with 100 ng/ml LPS and 1 µg CpG (Metabion, Martinsried, Germany) for 24 h. To determine their ability to differentiate and develop a mature/activated phenotype, the cells were analyzed using flow cytometry (table 4, staining K) and their phenotype was inspected microscopically.

2.1.11 RESTIMULATION OF PEC FROM INFECTED HUMANIZED MICE

Humanized mice were infected with 10^7 GBS for 24 h. Afterwards, PEC were extracted using peritoneal lavage and counted. 10^6 cells were seeded in 24 Multiwell plates (BD, USA). Cells from uninfected mice (control), infected mice treated with PBS (PBS) and infected mice treated with Betamethasone (BETA) were either incubated in RPMI 1640 Glutamax (Invitrogen, Carlsbad, USA) + 10% FBS (Pan Biotech) alone (-) or restimulated with Medium containing 10^7 live GBS (+). After 1 h at 37°C, plates were spun down (300 rcf, 4°C for 10 min) and medium was completely removed and stored at -80°C for nitrite measurement (see 2.17). One ml fresh RPMI Glutamax + 10% FBS, containing 0.1 mg/ml Gentamicin (Sigma-Aldrich, Taufkirchen, Germany) was applied to each well. After incubating the PEC for 24 h in

total, plates were spun down (300 rcf, 4°C for 10 min), medium was removed for nitrite measurement.

2.1.12 CLEARANCE AND SURVIVAL OF CORD-BLOOD DERIVED MNC

MNC were extracted from fresh cord blood as described above (see 2.2) and counted. 10^6 cells were seeded in 24 Multiwell plates (BD Biosciences) each containing 1 ml RPMI 1640 Glutamax (Invitrogen) + 10% FBS (Pan Biotech). To test the effect of drugs on clearance of bacteria, either PBS (vehicle control), 1 µg/ml Betamethasone or 1 µg/ml Indomethacin were added before applying 10^7 GBS to each well (batch A). Samples were incubated at 37°C for 4 h. To analyze the influence of both drugs on MNC cultured with GBS for 24 h and 48 h, 10^6 cells were incubated with 10^5 live GBS and Chloramphenicol (2.5 µg/ml) was applied to suppress bacterial growth (batch B). As internal control GBS without MNC were incubated as described for batch A for 4 h (batch C). As second internal control MNC were also incubated without GBS as described for batch A for 4h, 24 h and 48 h (batch D). After incubation, clearance of bacteria (batch A and B) and survival of GBS (Batch C) were determined by plating 10^{-4}, 10^{-5} and 10^{-6} dilutions of each well on blood agar plates, incubating them overnight at 37°C and counting them.

To determine the effect of treatment together with bacteria (batch A and B) or treatment alone (batch D) on survival of MNC, cells from each well were counted and analyzed using flow cytometry. Therefore, MNC were resuspended in each well by pipetting up and down, before transferring them into a 2 ml reaction tube (Sarstedt, Germany). Then, adherent cells were collected by adding 500 µl PBS and scraping them off using a cell scraper (Sarstedt). Cells were counted, centrifuged at 300 rcf, 4°C for 10 min, supernatant was removed and cells were resuspended in residual medium and stained for FACS analysis (table 4, stain V).

2.1.13 PREPARATION AND SECTIONING OF PARAFFIN-EMBEDDED TISSUE SAMPLES

Tissue samples of spleen, kidney, liver, mLN, lung and brain were put into Rotilabo-embedding cassettes (Carl Roth, Karlsruhe, Germany) and incubated in 5% paraformaldehyde.

The tissue samples were dehydrated by transferring them sequentially in 30%, 50%, 70%, 80%, 90%, 95% and 100% ethanol (EtOH) (J.T. Baker, Griesheim, Germany) for 2 h each. In order to ensure that all water is substituted with EtOH, the samples were put into an additional 100% EtOH solution. Subsequently tissue samples were cleared by incubating them 3x in xylol (Merck, Darmstadt, Germany) for 1h. Tissues were placed in melted paraffin (56–58°C) for 1.5 h and subsequently transferred into a fresh container containing melted paraffin for additional 1.5 h to ensure that tissue samples were completely infiltrated with paraffin. After the infiltration, the samples were placed in an embedding mold and grouted with melted paraffin to form a block. These paraffin-tissue blocks were allowed to cool and stored at RT until sectioning.

Paraffin-tissue blocks were first trimmed to an optimal cutting surface and then 4 µm sections were prepared using a Leica RM2145 microtome (Leica, Wetzlar, Germany) according to manufacturer's protocol. Sections were cut and placed in a warm (42°C) HI1210 water bath (Leica) and fished out using Superfrost Plus microscope slides (Menzel, Braunschweig, Germany). Sections were air dried and subsequently used for immunohistochemistry and Hematoxylin & Eosin (H&E) staining.

2.1.14 IMMUNOHISTOCHEMISTRY OF PARAFFIN SECTIONS

Paraffin sections were deparaffinized by incubating them 2x 10 min in xylol. Sections were pretreated by incubation in 0.1 M citrate buffer, pH 7.3 (table 8) and heating them 30 min in a microwave at 320 W. For immunostaining the streptavidin–biotin–peroxidase complex method together with 3,3'-diaminobenzidine as chromogen was used. The staining was performed with a Ventana Nexes autostainer (Ventana, Tucson, USA) in combination with an iView DAB detection kit (Ventana) according to manufacturer's protocol. For detection the following antibodies were used: anti-CD45/LCA (Dako, Glostrup, Denmark) to stain human leukocytes, anti-CD3 (Thermo Scientific, Fremont, USA) to stain human T cells, anti-79a (Dako) to stain human B-cells and anti-CD68 (Dako) for staining human macrophages. Sections were analyzed using a Zeiss Axio Imager M1 (Zeiss, Wetzlar, Germany).

2.1.15 HEMATOXYLIN & EOSIN STAINING

Sections were fixed onto microscope slides by incubating them in acetone for 5 min at -20°C. Sections were air dried for 5 min at RT and rehydrated by incubation the sections 2x 1 min in 99% EtOH, 1 min in 96% EtOH and finally 1 min in 70% EtOH. Sections were incubated for 20 sec in Hematoxylin (Merck, Darmstadt, Germany) to stain the nuclei and subsequently washed 10 min in H_2O, before incubating them 20 sec with eosin (Carl Roth) to counterstain eosinophilic structures (mostly cytoplasm). Sections were washed again for 10 min in H_2O before dehydrating them using EtOH. Therefore sections were incubated 1 min in 70% EtOH, 1 min in 96% EtOH and 2x 1 min in 99% EtOH before submerging them in xylol. For mounting, the sections were taken out of the xylol and mounted using Entellan (Merck). Afterwards sections were air-dried and analyzed using a Zeiss Axio Imager M1 (Zeiss).

2.1.16 CYTOSPIN AND STAINING OF PEC

PEC from PEL (see 2.5) were counted (dilution 1:10) and adjust $2x10^5$ cells with RPMI 1640 medium (Pan Biotech) + 10% FCS (Pan Biotech) to a total volume of 200 µl. Superfrost Plus microscope slides (Menzel) were mounted with Shandon paper card (Thermo Scientific) and Shandon Cytofunnel (Thermo Scientific) and held together with Shandon Cytoclip (Thermo Scientific). Samples were applied on Cytofunnels and centrifuged for 6 min at 600 rpm, RT in a Shandon Cytospin 4 Cytocentrifuge (Thermo Scientific) and air dried at RT.

For staining of cytospins a Diff-Quick Staining Kit (Medion Diagnostics, Düdingen, Switzerland) was utilized. The first step of staining was fixation of cytospins by immersing slide for 10 sec in Diff-Quick Fixative. Cytospins were transferred into Diff-Quick Solution 1, containing Eosin, for 20 sec. Subsequently slides were immersed in Diff-Quick Solution 2, containing Thiazine, for 20 sec before rinsing them gently with distilled water. Slides were blotted and air dried at RT before analyzing them using a Zeiss Axio Imager M1 (Zeiss).

2.1.17 Assay for measuring nitrite accumulation (NO production)

For measuring NO production of myeloid cells *in vitro*, nitrite accumulation in PEC supernatant of GBS infected humanized mice was measured after restimulation of cells with GBS (see 2.11). First, Griess reagent was prepared by mixing Griess solution A (table 8) and B (table 8) 1:1. For the standard curve, 10 mM $NaNO_2$ stock solution (table 8) was diluted to 100 µM using ddH_2O. The resulting 100 µM $NaNO_2$ solution was serially diluted 1:2 (6x) down to 1.56 µM using RPMI 1640. From each dilution 100 µl were applied onto a 96 well plate (BD Biosciences) in triplicate. Also 100 µl of RPMI 1640 were applied in triplicate as blank. Supernatant samples were applied (100 µl in triplicate). Afterwards, 100 µl Griess reagent were added to each well and the OD was measured at 550 nm using an Emax Endpoint ELISA Microplate Reader (Molecular devices, Sunnyvale, USA).

2.1.18 Cytokine detection

In order to determine cytokine production of human leukocytes in humanized mice, animals were bled retrobulbarly. The blood was allowed to clot at 4°C for 30 min and subsequently centrifuged at 3000 rcf, 4°C for 10 min. Serum was removed and centrifuged again at 10000 rcf, 4°C for 10 min to pellet contaminating cells and debris. Pure serum was removed and stored at -80°C until cytokine analysis.

Serum samples were sent to Multimetrix, Regensburg, Germany for analysis. There a multiplex cytokine analysis was conducted, analyzing the serum cytokine levels of IFNγ, TNF, IL-1β, IL-6, IL-8 and IL-10.

2.2 MATERIALS

Table 5: Antibodies for flow cytometry

Antibody	Fluorochr.	Clone	Isotype	Manufacturer	Dil.
anti-human CD19	Pe	HIB19	mouse IgG1, κ	BD Biosciences	1:20
anti-human CD27	Biotin	0323	mouse IgG1, κ	eBioscience, San Diego, USA	1:50
anti-human CD3	FITC	UCHT1	mouse IgG1, κ	BD Biosciences	1:20
anti-human CD3	PerCP-Cy5.5	OKT3	mouse IgG2a, κ	eBioscience	1:20
anti-human CD33	PerCP-Cy5.5	P67.6	IgG1	BD Biosciences	1:20
anti-human CD34	Pe	581/CD34	mouse IgG1, κ	BD Biosciences	1:20
anti-human CD4	FITC	SK3	IgG1	BD Biosciences	1:20
anti-human CD45	APC	HI30	mouse IgG1, κ	BD Biosciences	1:20
anti-human CD45RA	Pe-Cy7	HI100	mouse IgG2b, κ	eBioscience	1:50
anti-human CD56	APC	B159	mouse IgG1, κ	BD Biosciences	1:20
anti-human CD66	Pe	B1.1/CD66	mouse IgG2a, κ	BD Biosciences	1:20
anti-human CD8a	APC	HIT8a	mouse IgG1, κ	Biolegend, San Diego, USA	1:20
anti-human CD80	Biotin	2D10.4	mouse IgG1, κ	eBioscience	1:50
anti-human CD86	Pe	IT2,2	mouse IgG2b, κ	eBioscience	1:20
anti-human HLA-DR	Pe- Cy7	LN3	mouse IgG2b, κ	eBioscience	1:50
Streptavidin	APC-Cy7			BD Biosciences	1:333

Table 6: Isotype controls for flow cytometry (Dilution see Table 5)

Antibody	Fluorochrome	Clone	Isotype	Manufacturer
mouse IgG1	APC		mouse IgG1, κ	eBioscience
mouse IgG1	Biotin		mouse IgG1, κ	eBioscience
mouse IgG1	Pe	MOPC-21	mouse IgG1, κ	Biolegend

Antibody	Fluorochrome	Clone	Isotype	Manufacturer
mouse IgG1	Pe-Cy7		mouse IgG1, κ	eBioscience
mouse IgG1	PE-Cy5.5		mouse IgG1, κ	eBioscience
mouse IgG2b	Pe	MPC-11	mouse IgG2b, κ	Biolegend
mouse IgG2b	Pe-Cy7		mouse IgG2b, κ	eBioscience

Table 7: Antibodies for histology

Antibody	Clone	Manufacturer	Dilution
anti-human CD3	SP	Thermo Scientific, Fremont, USA	1:300
anti-human CD45	2B11-PD7/26	Dako, Glostrup, Denmark	1:600
anti-human CD68	P6M1	Dako, Glostrup, Denmark	1:100
anti-human CD79a	JCB117	Dako, Glostrup, Denmark	1:20

Table 8: Buffers, Solutions and Media

Buffers, Solutions and Media	Application	Composition
Acid-Citrate-Dextrose (ACD)	Cell culture	37 mM $C_6H_8O_7.H_2O$ 75 mM $Na_3C_6H_5O_7.2H_2O$ 0,12 M $C_6H_{12}O_6$
Ammonium-Chloride-Potassium (ACK) lysis buffer	Miscellaneous	0,15 M NH_4Cl 10 mM $KHCO_3$ 0,1 mM EDTA in ddH_2O
BD FACS Lysing Solution 1x	Miscellaneous	10 % BD FACS Lysing Solution 10x in ddH_2O
Blood agar plates	Miscellaneous	4 % (w/v) Columbia Agar (Merck) 8 % defibrinated sheep blood in ddH_2O
Citrate buffer (0.1 M; pH 7.3)	Histology	0.1 M $Na_3C_6H_5O_7.2H_2O$ in ddH_2O adjust pH value to 7.3 with NaOH
PBS (phosphate buffered saline w/o Ca &Mg)	Miscellaneous	PAA, Pasching, Austria

Buffers, Solutions and Media	Application	Composition
EDTA stock solution (0,5 M pH 7.9)	Miscellaneous	0.5 M EDTA adjust pH value to 7.9 with NaOH
FACS buffer	Flow cytometry	2 % (v/v) FCS 2 mM EDTA in PBS
Freezing medium (2x)	Cell culture	20 % (v/v) DMSO 10 % (v/v) FCS 25 % (v/v) Deltadex 40 5 % (v/v) ACD 40 % (v/v) RPMI medium
Griess solution A	Measuring Nitrite	1 % (w/v) $C_6H_8N_2O_2S$ 5 % (v/v) H_3PO_4 in ddH_2O
Griess solution B	Measuring Nitrite	0,1 % (w/v) $C_{10}H_7NHCH_2CH_2NH_2.2HCl$ in ddH_2O
MACS buffer	Cell separation	0.5 % (w/v) BSA 2 mM EDTA in PBS
$NaNO_2$ stock solution	Measuring Nitrite	10 mM $NaNO_2$ in ddH_2O
Paraformaldehyde (PFA) 4%	Flow cytometry	4 % (v/v) PFA 2.5 mM $Ba(OH)_2$ 0.4 mM $CaCl_2$ 50 mM $C_{12}H_{22}O_{11}$ 0.1 M NaH_2PO_4 in ddH_2O
PBS (10x)	Miscellaneous	1.5 M NaCl 83 mM Na_2HPO_4 17 mM NaH_2PO_4 (pH 7.4) in ddH_2O
Percoll (100 %)	Cell separation	10 % (v/v) PBS (10x) 90 % (v/v) Percoll (GE Healthcare)
RPMI + 10% FCS	Cells culture	10 % (v/v) FCS (Pan Biotech) in RPMI 1640 Glutamax (Invitrogen)

Table 9: Chemicals, Reagents and Kits

Chemicals and Reagents	Application	Manufacturer
2-Mercaptoethanol	Cell culture	Sigma-Aldrich, Taufkirchen, Germany
2-Propanol	Miscellaneous	Merck, Darmstadt, Germany

Chemicals and Reagents	Application	Manufacturer
$Ba(OH)_2$ (Barium hydroxide)	PFA	Merck, Darmstadt, Germany
Bovine serum albumin (BSA)	MACS	Sigma-Aldrich, Taufkirchen, Germany
$C_{10}H_7NHCH_2CH_2NH_2.2HCl$ (2-(1-Naphthylamino)ethylamine dihydrochloride)	Measuring Nitrite	Sigma-Aldrich, Taufkirchen, Germany
$C_6H_8N_2O_2S$ (Sulfanilamide)	Measuring Nitrite	Merck, Darmstadt, Germany
$C_{12}H_{22}O_{11}$ (Sucrose)	PFA	Sigma-Aldrich, Taufkirchen, Germany
$C_6H_{12}O_6$ (Dextrose)	ACD	Serva, Heidelberg, Germany
$C_6H_8O_7.H_2O$ (Citric acid)	ACD	Merck, Darmstadt, Germany
$CaCl_2$ (Calcium chloride)	PFA	Merck, Darmstadt, Germany
CD34 Micro Bead Kit	MACS	Miltenyi Biotech, Bergisch Gladbach, Germany
Celestan 4 mg (Betamethasone)	Miscellaneous	Essex pharma, Munich, Germany
CpG-1648 odn	*In vitro* stimulation	Metabion, Martinsried, Germany
Deltadex 40	Freezing of cells	Deltaselect, Munich, Germany
Diff-Quick Staining Kit	Diff-quick staining	Medion Diagnostics, Düdingen, Switzerland
Dimethyl sulfoxide (DMSO)	Freezing of cells	Applichem, Gatersleben, Germany
Eosin G (0,5%)	Histology	Carl Roth, Karlsruhe, Germany
Entellan	Histology	Merck, Darmstadt, Germany
Ethanol (100%)	Miscellaneous	J.T. Baker, Griesheim, Germany
Ethylenediaminetetraacetic acid (EDTA)	Miscellaneous	Applichem, Gatersleben, Germany
Fetal bovine serum (FBS)	Miscellaneous	Pan Biotech, Aidenbach, Germany
Gentamicin 50 mg/ml	Restimulation	Sigma-Aldrich, Taufkirchen, Germany
Hematoxylin	Histology	Carl Roth, Karlsruhe, Germany

Chemicals and Reagents	Application	Manufacturer
HCl 37%	pH adjustment	Merck, Darmstadt, Germany
H_3PO_4 (Phosphoric acid)	Measuring Nitrite	Merck, Darmstadt, Germany
Indomethacin (5g)	Miscellaneous	Euro OTC Pharma, Bönen, Germany
iView DAB detection kit	Histology	Ventana, Tucson, USA
$KHCO_3$ (Potassium bicarbonate)	ACK lysis	Roth, Karlsruhe, Germany
Lipopolysaccharides from Escherichia coli 0127:B8 (LPS)	Cell culture	Sigma-Aldrich, Taufkirchen, Germany
Macrophage SFM	Cell culture	Invitrogen, Carlsbad, USA
M-CSF (E.coli expressed)	Cell culture	R&D Systems, Minneapolis, USA
Mikrobank Bacterial Storage system	Storage of GBS	Prolab Diagnostics, Richmond Hill, Canada
Na_2HPO_4 (Disodium phosphate)	PBS	Merck, Darmstadt, Germany
NaH_2PO_4 (Sodium Phosphate)	PBS, PFA	Merck, Darmstadt, Germany
$Na_3C_6H_5O_7.2H_2O$ (Sodium citrate)	ACD	Merck, Darmstadt, Germany
NaCl (Sodium chloride)	PBS	Merck, Darmstadt, Germany
$NaNO_2$ (Sodium nitrite)	Measuring Nitrite	Merck, Darmstadt, Germany
NH_4Cl (Ammonium chloride)	ACK lysis	Merck, Darmstadt, Germany
Pancol human	MACS	Pan Biotech, Aidenbach, Germany
Paraformaldehyde 36,5 – 38%	PFA	Sigma-Aldrich, Taufkirchen, Germany
Percoll (density 1.131 g/ml)	Miscellaneous	GE Healthcare, Uppsala, Sweden
RPMI 1640 L-Glutamine	Miscellaneous	Pan Biotech, Aidenbach, Germany
RPMI 1640 GlutaMAX	Cell culture	Invitrogen, Carlsbad, USA
Trypan blue (0,2% in 0,9% NaCl)	Cell culture	Sigma-Aldrich, Taufkirchen, Germany
Xylol (>98 pure)	Histology	Merck, Darmstadt, Germany

Table 10: Expandable material

Material	Application	Manufacturer
4-well chamber slide	Cytochemistry	Nunc, Wiesbaden, Germany
BD Discardit II 2 ml, 5 ml, 10 ml, 20 ml (syringes)	Miscellaneous	BD Biosciences, Franklin Lakes, USA
BD Falcon 40 µM Cell Strainer	Miscellaneous	BD Biosciences, Franklin Lakes, USA
BD Microlance 3 20G, 22G, 27G (cannulas)	Miscellaneous	BD Biosciences, Franklin Lakes, USA
BD Plastipak 1 ml (syringes)	Miscellaneous	BD Biosciences, Franklin Lakes, USA
Biosphere Filter Tips 200 µl, 1000 µl	Miscellaneous	Sarstedt, Nümbrecht, Germany
Bottle-Top-Filter 500 ml, 0,2 µm	Miscellaneous	Nalgene, Penfield, USA
Cell culture plate (96 well)	Miscellaneous	Greiner, Kremsmünster, Austria
Cell scraper 25 cm	Cell culture	Sarstedt, Nümbrecht, Germany
Cord Blood System 150 ML CPD	MACS	Marco Pharma, Langen, Germany
Cryo Tube Vials	Cell culture	Nunc, Wiesbaden, Germany
Disposable latex gloves	Miscellaneous	Hartmann, Heidenheim, Germany
Disposable nitrile gloves	Miscellaneous	Hartmann, Heidenheim, Germany
Falcon Tubes (15 and 50 ml)	Miscellaneous	Sarstedt, Nümbrecht, Germany
Glass Pasteur pipette	Miscellaneous	Brand, Wertheim, Germany
Micro Pipettes 50 + 100 µl	Blood samples	Megro, Wesel, Germany
Microtest 96 well (plate)	ELISA	BD Biosciences, Franklin Lakes, USA
Microtome Blades R35 Type 50	Histology	Feather, Osaka, Japan
MS Columns (Separation columns)	MACS	Miltenyi Biotech, Bergisch Gladbach, Germany
Multiwell 24 well (plate)	Cell culture	BD Biosciences, Franklin Lakes, USA
Multiwell 6 well (plate)	Cell culture	BD Biosciences, Franklin Lakes, USA
Pipettes (2 ml, 5 ml, 10 ml, 25 ml)	Miscellaneous	Sarstedt, Nümbrecht, Germany
Reaction cups (1.5 and 2 ml)	Miscellaneous	Sarstedt, Nümbrecht, Germany
Rotilabo embedding cassettes	Histology	Carl Roth, Karlsruhe, Germany
Safe Seal Tips 10 µl, 20 µl	Miscellaneous	Biozym, Hessisch Oldendorf, Germany

Material	Application	Manufacturer
Shandon paper card	Cytospin	Thermo Scientific, Fremont, USA
Superfrost Plus Microscope slides	Histology	Menzel, Braunschweig, Germany
Tips (10µl, 100µl and 1000µl)	Miscellaneous	Sarstedt, Nümbrecht, Germany
Tube 5 ml (flow cytometry)	Flow cytometry	Sarstedt, Nümbrecht, Germany

Table 11: Lab equipment

Device	Application	Manufacturer
Accu-jet pro	Miscellaneous	Brand, Wertheim, Germany
Balance CP224S	Miscellaneous	Sartorius, Göttingen, Germany
Balance PJ400	Miscellaneous	Mettler-Toledo, Greifensee, Switzerland
Centrifuge 5417R	Miscellaneous	Eppendorf, Hamburg, Germany
Centrifuge 5810R	Miscellaneous	Eppendorf, Hamburg, Germany
Cold plate EG1130	Histology	Leica, Wetzlar, Germany
Cryo 1°C Freezing Container	Cell culture	Nalgene, Penfield, USA
EMax Endpoint ELISA Microplate Reader	ELISA	Molecular devices, Sunnyvale, USA
Finnpipette 0.2 – 2 µl	Miscellaneous	Thermo Scientific, Fremont, USA
Finnpipette 2 – 20 µl	Miscellaneous	Thermo Scientific, Fremont, USA
Finnpipette 20 – 200 µl	Miscellaneous	Thermo Scientific, Fremont, USA
Finnpipette 100 – 1000 µl	Miscellaneous	Thermo Scientific, Fremont, USA
Freezer (-20°C)	Miscellaneous	Liebherr, Kirchdorf an der Iller, Germany
Freezer (-80°C) Forma 900 series	Miscellaneous	Thermo Scientific, Fremont, USA
Hand counter T120	Miscellaneous	Baumer IVO, Villingen-Schwenningen, Germany
Implen Nano Photometer	Bacteria	Implen, Munich, Germany
Incubator BBD 6220	Cell culture	Heraeus, Hanau, Germany
Incubator WTC Binder	Miscellaneous	Binder, Tuttlingen, Germany

Device	Application	Manufacturer
Laminar flow KS 12	Miscellaneous	Thermo Scientific, Fremont, USA
Liquid nitrogen storage tank	Miscellaneous	German Cryo, Grevenbroich, Germany
MACS Multi Stand	MACS	Miltenyi, Bergisch Gladbach, Germany
Microscope (cell culture)	Miscellaneous	Carl Zeiss, Wetzlar, Germany
Microtome RM 2145	Histology	Leica, Wetzlar, Germany
Neubauer chamber improved	Miscellaneous	HBG Precicolor, Giessen, Germany
Rotilabo-Mini-Centrifuge	Miscellaneous	Carl Roth, Karlsruhe, Germany
Shandon Cytoclip	Cytospin	Thermo Scientific, Fremont, USA
Shandon Cytofunnel	Cytospin	Thermo Scientific, Fremont, USA
Shandon Cytospin 4 Cytocentrifuge	Cytospin	Thermo Scientific, Fremont, USA
Signal timer	Miscellaneous	Carl Roth, Karlsruhe, Germany
Ventana Nexes autostainer	Histology	Ventana, Tucson, USA
Water bath HI1210	Histology	Leica, Wetzlar, Germany
Water bath TW20	Cell culture	Julabo, Seelbach, Germany
Zeiss Axio Imager M1	Histology	Carl Zeiss, Wetzlar, Germany

Table 12: Software

Software	Company
Axio Vision 4.6	Zeiss, Wetzlar, Germany
BD FACSDiva software	BD Biosciences, Franklin Lakes, USA
Graph Pad Prism 4.0	Graph Pad Software, La Jolla, USA
Microsoft Office 2010	Microsoft Corporation, Redmond, USA
SoftMax Pro Data Acquistion & Analysis Software	Molecular devices, Sunnyvale, USA

3 RESULTS

3.1 GENERATION AND CHARACTERIZATION OF HUMANIZED MICE

After transplantation of human CD34$^+$ hematopoietic stem cells into neonatal NOD.*scid* IL2R^{null} (NSG) mice by intrahepatic injection (Fig. 1), the animals developed human CD45$^+$ leukocytes in all analyzed organs.

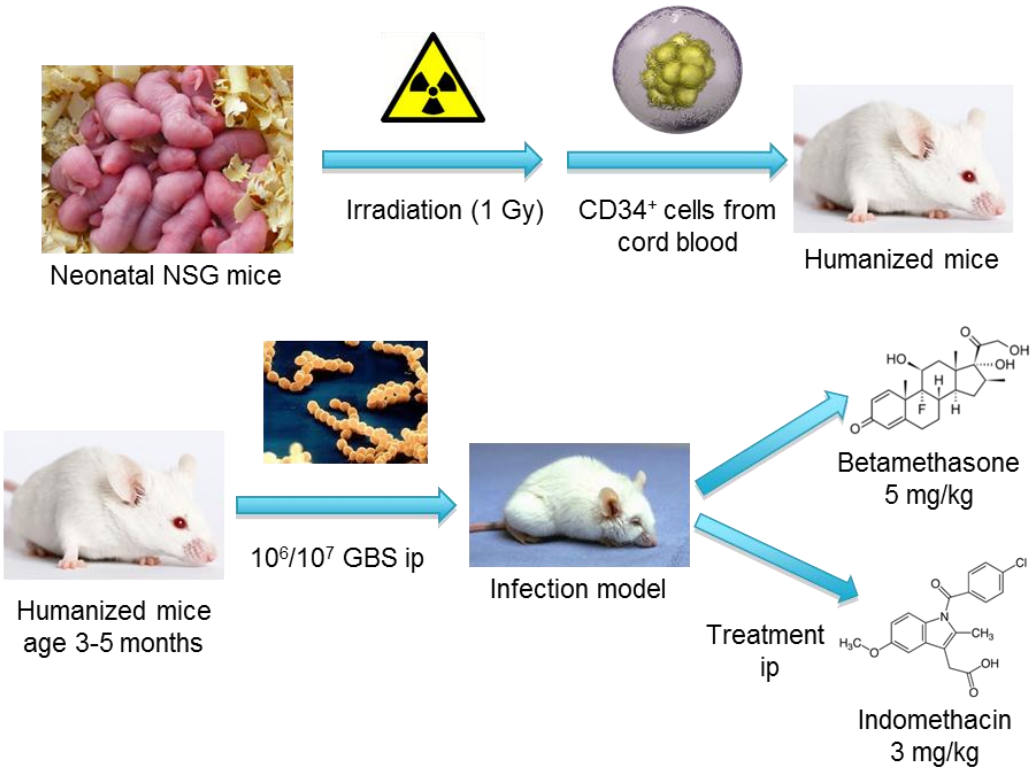

Fig. 1: *Schematic of humanization of NSG mice with human CD34$^+$ hematopoietic stem cells after conditioning (irradiation) and subsequent infection with GBS and treatment. Images: Biolegend; Environmental Health Services; Instituto de Bioquímica Clínica; Jackson Laboratories; Royal Society for the Prevention of Cruelty to Animals; Wikipedia.*

Cells positive for the human leukocyte marker CD45 were detected via flow cytometry in spleen, lung, liver, bone marrow (BM), mesenteric lymph nodes (mLN), peritoneum and peripheral blood (pb) (Fig. 2A). Human leukocytes constituted with an average of 41% viable cells in the lung, 50% in the pb, 59% in the BM, 64% in the spleen, 78% in the liver, and almost exclusively made up the mLN (91%). The peritoneum of naïve humanized NSG mice contained 7% of human CD45$^+$

leukocytes. The development of a complete human immune system was further monitored by the analysis of various immune cell subtypes. Staining of CD3 revealed considerable numbers of T cells in mLN (50% of live cells), liver (39%) and lung (30%). The pb (21%) and spleen (18%) had lower amounts, while peritoneum (6%) and BM (5%) contained low numbers of T cells (Fig. 2B). Whereas the proportion of T cells displayed higher variances, B cell numbers were more consistent, and varied between 39% of live cells in the spleen and 11% in the lung. The only exception was the peritoneum with 3% (Fig. 2C). Upon humanization, not only leukocytes of lymphoid linage, but also $CD33^+$ myeloid cells were present. Considerable numbers were detected in the bone marrow (18% of $CD45^+$ cells), lung (14%) and liver (12%), while pB (7%), peritoneum (4%) and spleen (3%) showed low amounts (Fig. 2D). Humanized mice only generated few CD66 expressing granulocytes. In most organs the proportion was less than 0.06% of $CD45^+$ cells, with the exception of the liver (0.5%) and even more so the BM (4.3%) (Fig. 2E). However, not only major subsets of human immune cells developed in the humanized mice. Examination of the human T cells revealed the presence of $CD3^+$ $CD4^+$ helper T cells (Fig. 2F) and $CD3^+$ $CD8^+$ cytotoxic T cells (Fig. 2G) indicating normal T cell development.

Histological analysis was performed to confirm the results from flow cytometry. Sections from spleen, mLN, liver, lung, kidney and brain were stained for human leukocytes (CD45), T cells (CD3), B cells (CD79a) and macrophages (CD68). Consistent with flow cytometric results, mLN and spleen contained very high numbers of human $CD45^+$ cells. Lung and especially the liver showed markedly reduced leukocyte counts. This was caused by the fact that prior to flow cytometric staining, the immune cells from lung and liver were enriched by density gradient centrifugation in Percoll. Considerable low numbers of human leukocytes were also present in the kidney. Humanized mice without infection showed no human $CD45^+$ leukocytes in the brain. Staining for T and B cells showed similar results. Human $CD68^+$ macrophages could be detected in most organs except the brain (Fig. 3).

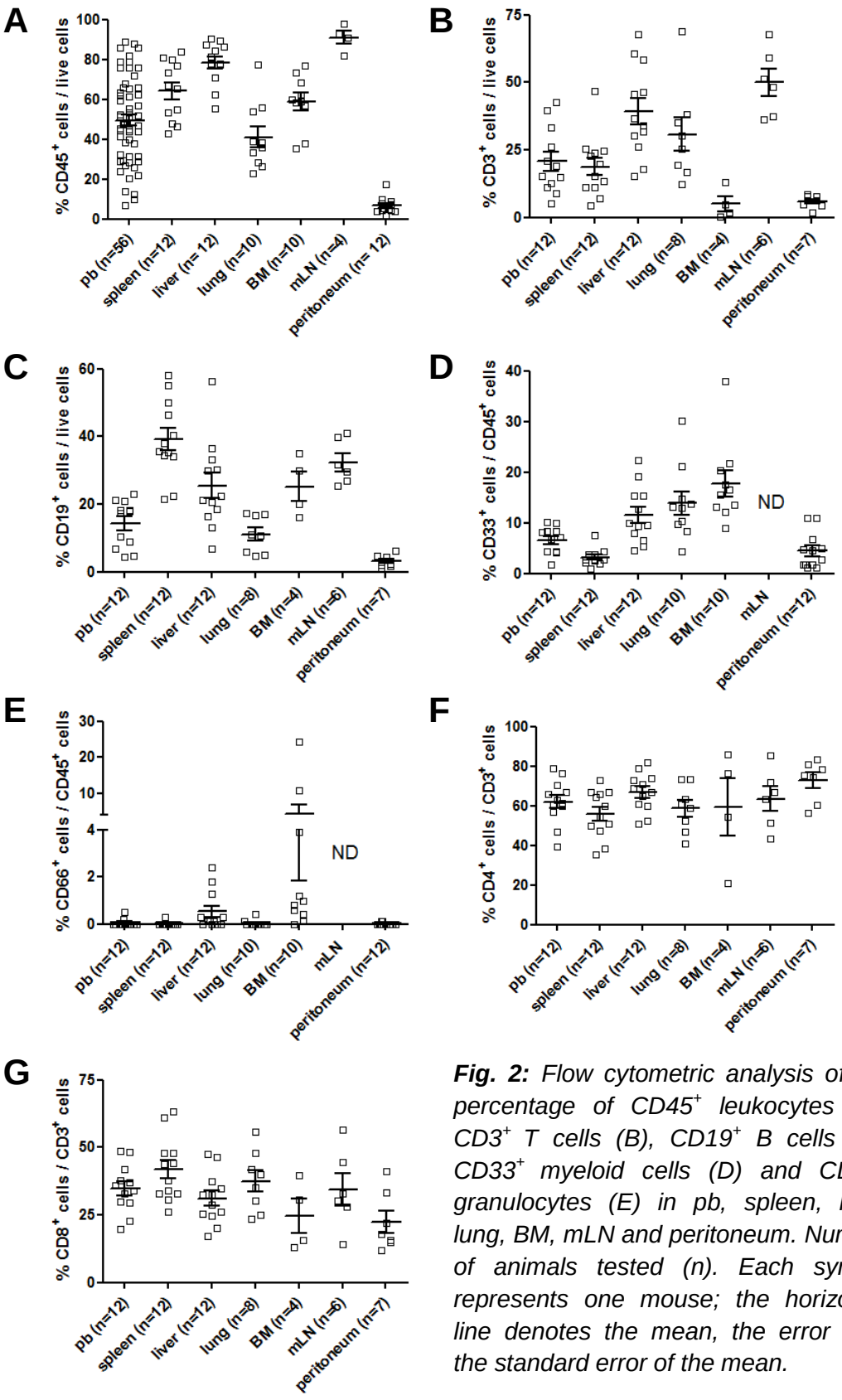

Fig. 2: *Flow cytometric analysis of the percentage of CD45$^+$ leukocytes (A), CD3$^+$ T cells (B), CD19$^+$ B cells (C), CD33$^+$ myeloid cells (D) and CD66$^+$ granulocytes (E) in pb, spleen, liver, lung, BM, mLN and peritoneum. Number of animals tested (n). Each symbol represents one mouse; the horizontal line denotes the mean, the error bars the standard error of the mean.*

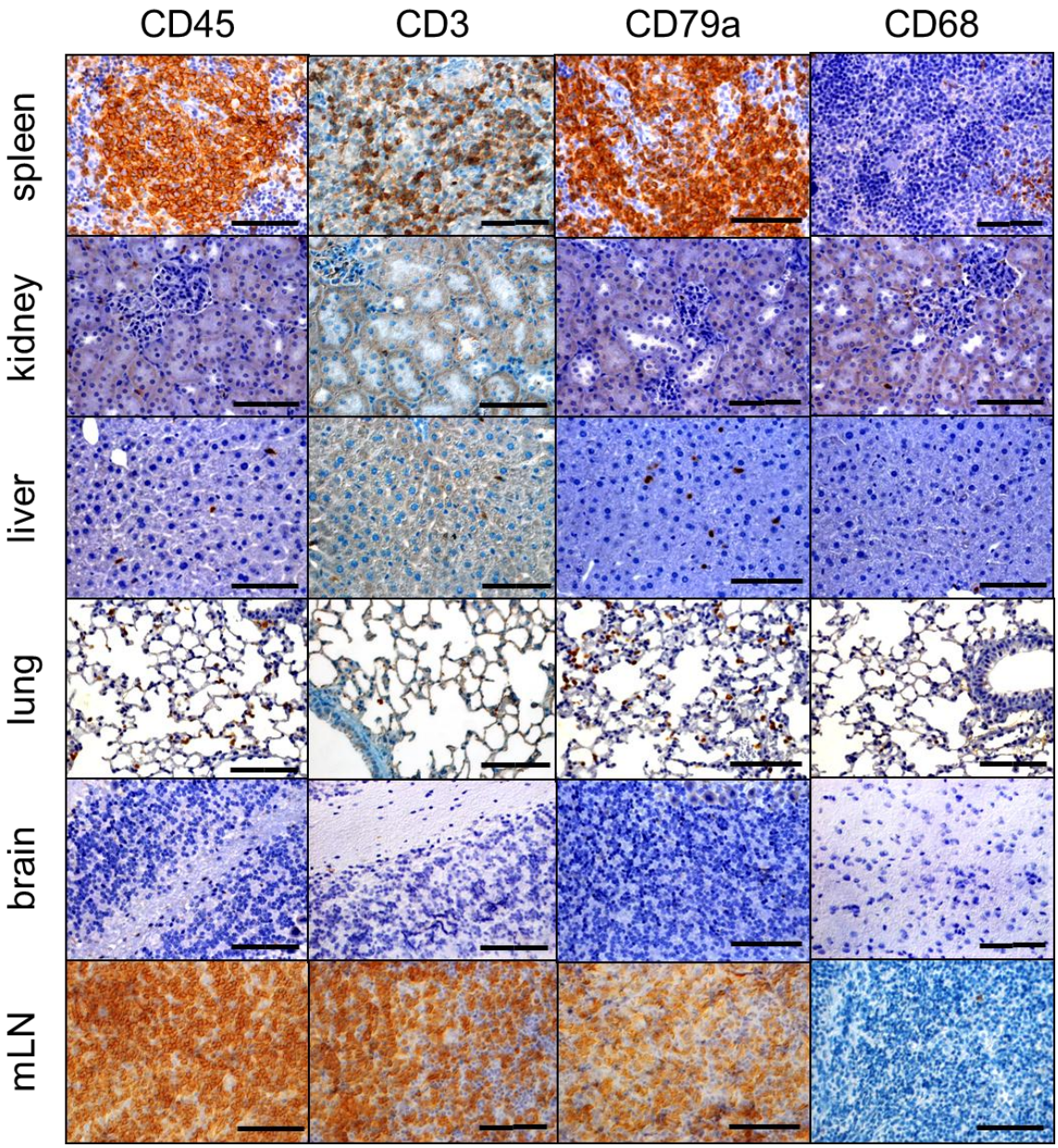

Fig. 3: *Immunohistochemical staining for CD45$^+$ leukocytes, CD3$^+$ T cells, CD79a$^+$ B cells and CD68$^+$ macrophages in spleen, kidney, liver, lung, brain, mLN of naive humanized mice. Animals were infected with moderate doses of GBS (10^6) and analyzed at day 3. Scale bar = 100 µm; objective used 40x.*

To monitor the development of the human immune system in the animals, blood was drawn starting 6-8 weeks post transplantation. While the human immune system with all immune cell subsets is already present at this point in time, the composition is still subject to change. A good example is the levels of T and B cells in the pb (Fig 4). Between 6 and 10 weeks after injection of $CD34^+$ hematopoietic stem cells, $CD19^+$ B cell percentages remained relatively constant at a high level, while $CD3^+$ T cell proportions rose very slowly. After 10 weeks, B cell percentages began to decline and T cell proportions increased more distinctively, until 30 weeks of age. Here the proportions of B and T cells were equal.

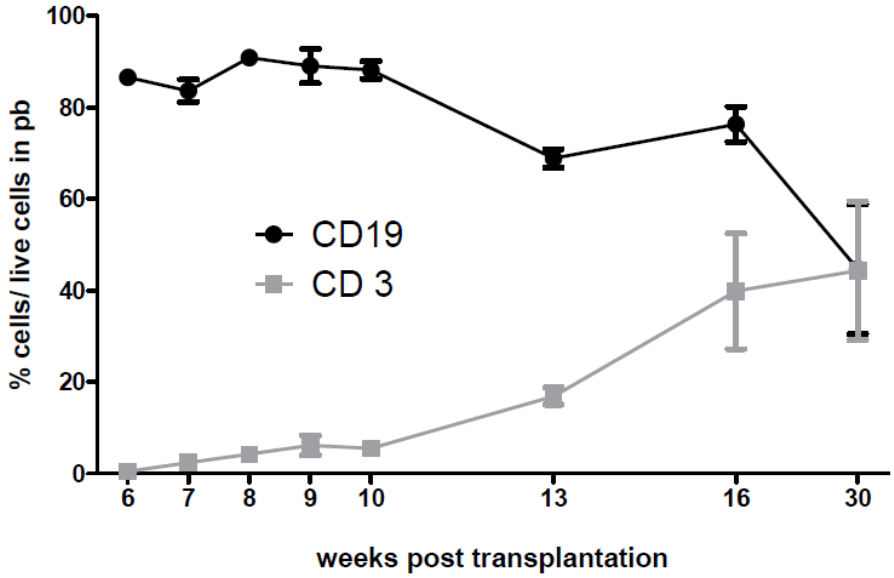

	6 weeks (n=10)	7 weeks (n=25)	8 weeks (n= 31)	9 weeks (n=9)	10 weeks (n= 15)	13 weeks (n=13)	16 weeks (n= 6)	30 weeks (n=3)
B cells	86.6 +/- 1.3	83.6 +/- 2.5	90.9 +/-1.4	89.1 +/- 3.7	88.1 +/- 1.9	68.9 +/- 2.1	76.3 +/- 3.8	44.7 +/- 14.2
T cells	0.5 +/- 0.2	2.4 +/- 0.8	4.2 +/- 1.1	6.2 +/- 2.2	5.5 +/- 1.6	16.9 +/- 1.9	39.9 +/- 12.7	44.3 +/- 15.1

Fig. 4: *Flow cytometric analysis of the percentage of $CD19^+$ B cells and $CD3^+$ T cells in pb of humanized mice between 6 and 30 weeks post transplantation of $CD34^+$ hematopoietic stem cells. Number of animals tested at each time point (n). Values in table are percentage of B or T cells of live cells (top) with standard error of the mean (bottom).*

Humanized mice have low proportions of myeloid cells (Fig. 2), mostly due to the lack of human specific growth factors for the myeloid linage (M-CSF, GM-CSF). Hence, the capacity of myeloid progenitors and monocytes to differentiate into functional macrophages was analyzed. Single cell suspensions from bone marrow of humanized mice were differentiated *in vitro* for 7 days to obtain macrophages. After 7 days, the cells were stimulated 24 h with 1 µM CpG and 100 ng/ml LPS. While only 33% of unstimulated cells expressed the maturation and activation marker CD86, stimulation induced the expression of CD86 in 81% of live $CD33^+$ cells (Fig. 5). This indicates that the differentiation of macrophages from humanized mice, as well as their functional maturation and activation is possible, given the presence of the appropriate growth factors and stimuli.

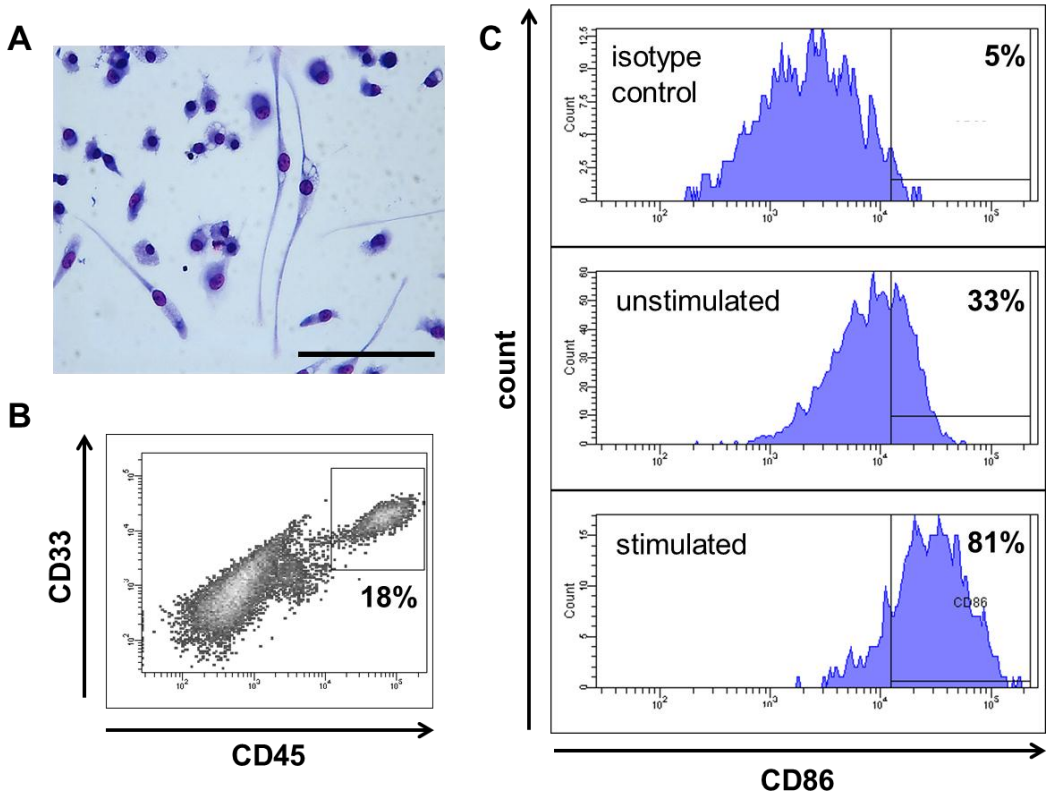

Fig. 5: *In vitro differentiation and stimulation of BMDM. Diff-Quick staining of cells after* in vitro *differentiation (A). Scale bar = 100 µm; objective used 40x. Flow cytometric analysis of $CD45^+$ $CD33^+$ myeloid cells after differentiation (B) and maturation and activation marker (CD86) expression of unstimulated and stimulated cells (C).*

3.2 INFECTION MODEL

3.2.1 CHARACTERIZATION OF GBS INFECTION IN HUMANIZED MICE

For infection of the humanized mice, GBS was grown on sheep blood agar plates and suspended in PBS. To be able to infect the animals with a standardized dose of bacteria, the correct amount of live GBS at a certain optical density (OD) had to be determined. A total of 12 independent experiments revealed that a solution at OD 0.400 contained $2x10^8$ live GBS (Fig. 6). In order to exclude possible complications with culturing, generation of bacterial suspension and adjustment of OD, and therefore incorrect doses, dilutions of the GBS suspension were plated and cultivated for each infection experiment.

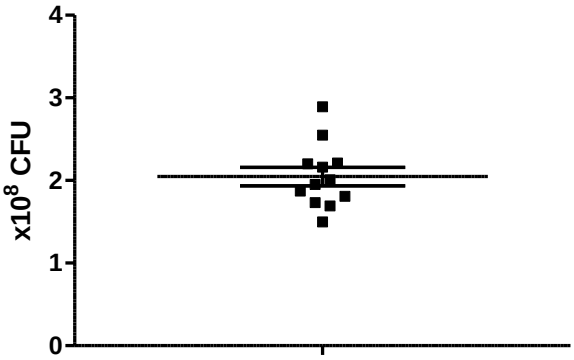

Fig. 6: *Number of CFU of a GBS suspension in PBS adjusted to the OD of 0.400. Each symbol represents one experiment (n=12); the horizontal line denotes the mean, the error bars the standard error of the mean.*

Humanized mice were a completely new animal model for GBS infections. Hence, a suitable infectious dose had to be determined. Animals were therefore injected intra peritoneally with various doses of bacteria and the survival was monitored. Infection with $5x10^8$ bacteria led to the death of all animals within 2 days. The doses $5x10^7$ and 10^7 resulted in the death of 75% of the animals at day 1 and day 2 respectively. Reduction of the number of injected pathogens drastically increased the rate of survival. While 10^6 GBS induced the death of 20% of mice, $5x10^5$ and lower doses lead to the death of less than 10% of infected animals (Fig. 7). For the analysis of the effects of an acute high dose infection, the dose of 10^7 GBS was chosen. Here animals could be challenged with a relatively high dose of live bacteria, but if they were killed 24 h after infection, 75% of live mice were available for analysis. In order

to be able to determine the effects of moderate to long term GBS infection on the immune system of humanized mice, the dose of 10^6 GBS was chosen. This dose represented a moderate amount of live bacteria, which still enabled the analysis of 80% of live mice 3d and 7d after infection.

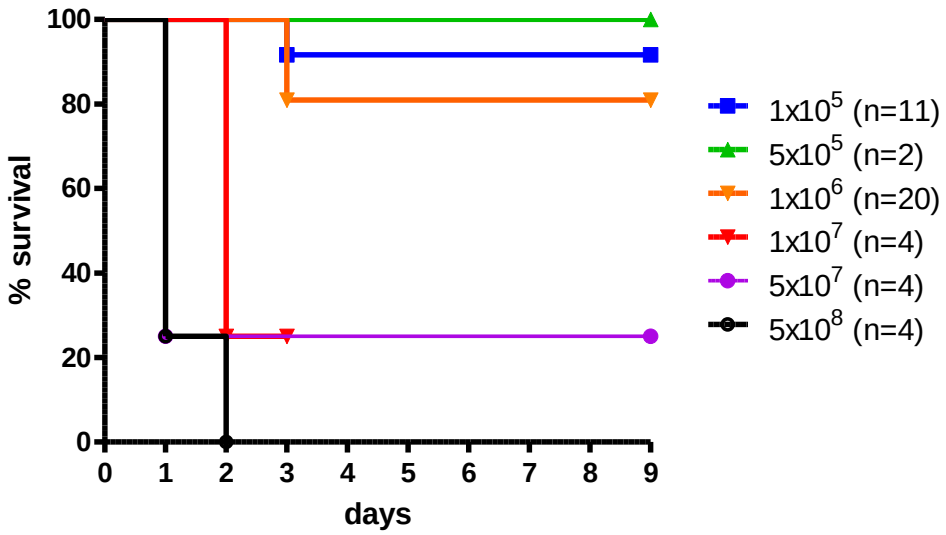

Fig. 7: *Survival in days of humanized mice infected with various doses of GBS from $1x10^5$ to $5x10^8$. Number of animals in each group (n).*

Although humanized NSG mice lack mature murine B, T and NK cells, they still feature murine cells of the myeloid linage. Especially granulocytes and macrophages are involved in fighting off bacterial infections. In order to ensure that the human immune system was the key player in coping with the GBS infection, neonatal NSG littermates were radiated with 1 Gy. Subsequently, half of the mice were transplanted with human $CD34^+$ hematopoietic stem cells. After approximately 3 months, when the human immune system in the humanized mice was fully developed, both groups (humanized and radiated only) were infected with 10^6 GBS and their survival was monitored. After 2 days, more than 90% (10/11) of the radiated only mice died, whereas 100% (11/11) of the humanized animals survived (Fig. 8). This indicated that the human immune system in the humanized mice plays a major role in fighting off the bacterial infection.

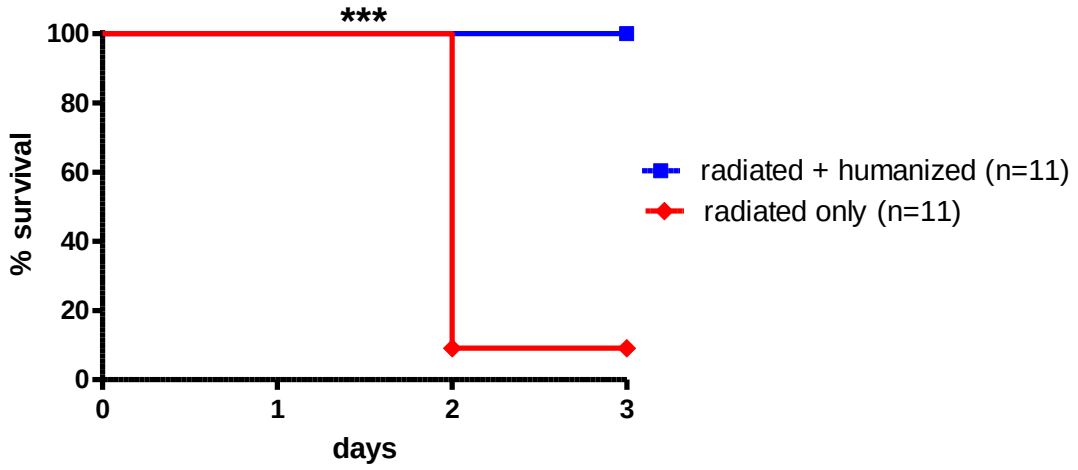

Fig. 8: *Survival in days of humanized (blue) and radiated only (red) mice infected with 10^6 GBS. Number of animals in each group (n=11). Statistical analysis: Log-rank (Mantel-Cox) test (***=p<0.0001)*

After determining suitable infectious doses and confirming the crucial role of the human immune system, humanized mice were infected with GBS and various parameters were analyzed.

3.2.2 Disease progression in GBS infected humanized mice

In order to analyze systemic distribution and clearance of live bacteria, various organs (spleen, kidney, liver, lung, brain, BM and peritoneum) were analyzed for colony forming units (CFU) (Table 13). After injection of GBS (either 10^6 or 10^7 CFU) intraperitoneally (ip), the bacteria rapidly spread systemically. After 24 h of high dose infection, none of the infected animals (n=10) was able to completely clear the pathogen from their system (supplement table 1). The peritoneum, as the site of initial infection harbored the highest amount of bacteria. At this time point, high CFU counts could also be found in the spleen, kidney, liver and lung. Lower numbers of live bacteria also spread into the BM and 6/10 animals showed low amounts of GBS in the brain. Three days after moderate dose infection, 4/10 mice managed to clear the GBS infection entirely. The remaining 6 animals featured the highest concentration of CFU in the liver, followed by the kidney. Low amounts of GBS were also found in BM, spleen and lung. Peritoneal cavities contained only minimal amounts of live bacteria. None of the infected animals displayed GBS in the brain.

Seven days post infection, more animals (4/6) were able to completely clear live GBS systemically. The remaining mice showed high amounts of GBS in the kidney. Low numbers of CFU were found in the peritoneum, the lung and even lower CFU counts were detected in BM and liver. Spleen and brain were entirely devoid of live bacteria after 7 days of infection.

Table 13: CFU per g of tissue (except in BM and peritoneal cavity where CFU were calculated per ml) in various organs of humanized mice infected with GBS.

	1d 10^7 GBS		**3d 10^6 GBS**		**7d 10^6 GBS**	
spleen	Mean	$8{,}71\times10^7$	Mean	$5{,}00\times10^2$	Mean	0
	SEM	$4{,}25\times10^7$	SEM	$5{,}00\times10^2$	SEM	0
	n	10	n	10	n	6
kidney	Mean	$2{,}38\times10^7$	Mean	$6{,}00\times10^3$	Mean	$4{,}19\times10^6$
	SEM	$1{,}15\times10^7$	SEM	$6{,}00\times10^3$	SEM	$4{,}19\times10^6$
	n	10	n	10	n	6
liver	Mean	$2{,}92\times10^7$	Mean	$2{,}69\times10^4$	Mean	$1{,}27\times10^1$
	SEM	$1{,}26\times10^7$	SEM	$2{,}65\times10^4$	SEM	$1{,}27\times10^1$
	n	10	n	10	n	6
lung	Mean	$4{,}03\times10^7$	Mean	$1{,}18\times10^2$	Mean	$2{,}22\times10^2$
	SEM	$1{,}50\times10^7$	SEM	$1{,}18\times10^2$	SEM	$2{,}22\times10^2$
	n	10	n	10	n	6
brain	Mean	$1{,}35\times10^5$	Mean	0	Mean	0
	SEM	$5{,}54\times10^4$	SEM	0	SEM	0
	n	10	n	10	n	6
bone marrow	Mean	$7{,}14\times10^5$	Mean	$7{,}40\times10^2$	Mean	$3{,}33\times10^1$
	SEM	$4{,}12\times10^5$	SEM	$6{,}18\times10^2$	SEM	$3{,}33\times10^1$
	n	10	n	10	n	6
peritoneal cavity	Mean	$3{,}62\times10^8$	Mean	$1{,}00\times10^1$	Mean	$7{,}20\times10^2$
	SEM	$2{,}21\times10^8$	SEM	$1{,}00\times10^1$	SEM	$7{,}20\times10^2$
	n	10	n	10	n	6

3.2.3 CHARACTERIZATION OF ORGAN DAMAGE AFTER GBS INFECTION

GBS sepsis generally leads to organ damage, especially in the lung and the brain of human neonates. Therefore spleen, kidney, liver, lung and brain in infected humanized mice were screened for histopathological changes. No changes were found in animals infected with moderate doses of GBS and also for high dose infected animals after 1 day (supplement Fig. 1-4; data not shown). However, high dose infected animals, which were moribund at day 2 showed leukocyte infiltration in the lung (Fig. 9A,B) and hemosiderin deposits in the spleen (Fig. 9C)

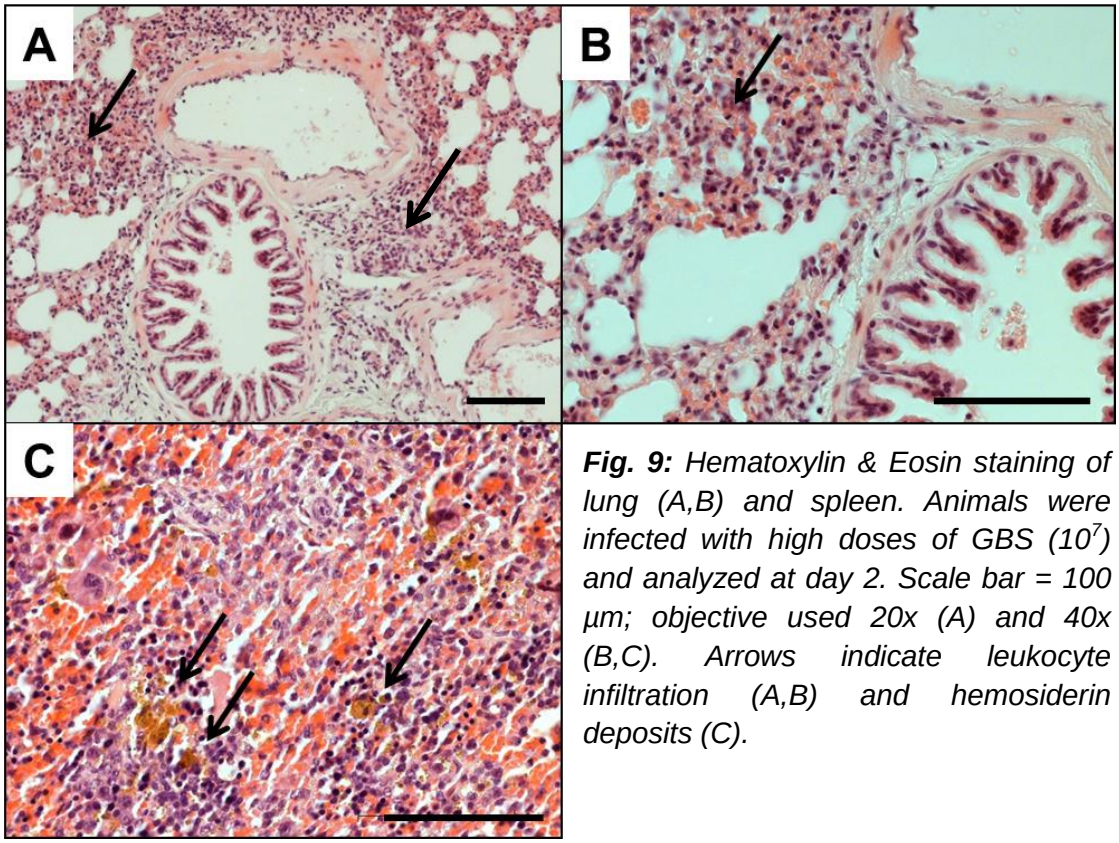

Fig. 9: *Hematoxylin & Eosin staining of lung (A,B) and spleen. Animals were infected with high doses of GBS (10^7) and analyzed at day 2. Scale bar = 100 µm; objective used 20x (A) and 40x (B,C). Arrows indicate leukocyte infiltration (A,B) and hemosiderin deposits (C).*

3.2.4 Effect of infection on cell count

For determining the general effect of GBS infection on cell proliferation and/or migration, the total cell count of different organs was determined. While infection with a high dose (10^7) of GBS induced a slight increase in splenocytes and a reduced cell count in the BM, these changes were not statistically significant (Fig. 10A). Infection with a moderate dose (10^6) of GBS induced an increase in total cell count in spleen and liver 3 days post infection, although not significant both times. However, the decrease in the amount of cells in the BM was significant (Fig. 10B). This effect was most likely caused by migration of leukocytes from the bone marrow into the periphery. Seven days after infection with a moderate dose of GBS, the increase in splenocytes was significant (Fig. 10C). This was probably caused by proliferation of lymphocytes in the spleen. The total cell count in the BM also increased compared to 3 days post infection, and began to align with the level of uninfected animals. This was most likely caused by proliferation of stem and progenitor cells.

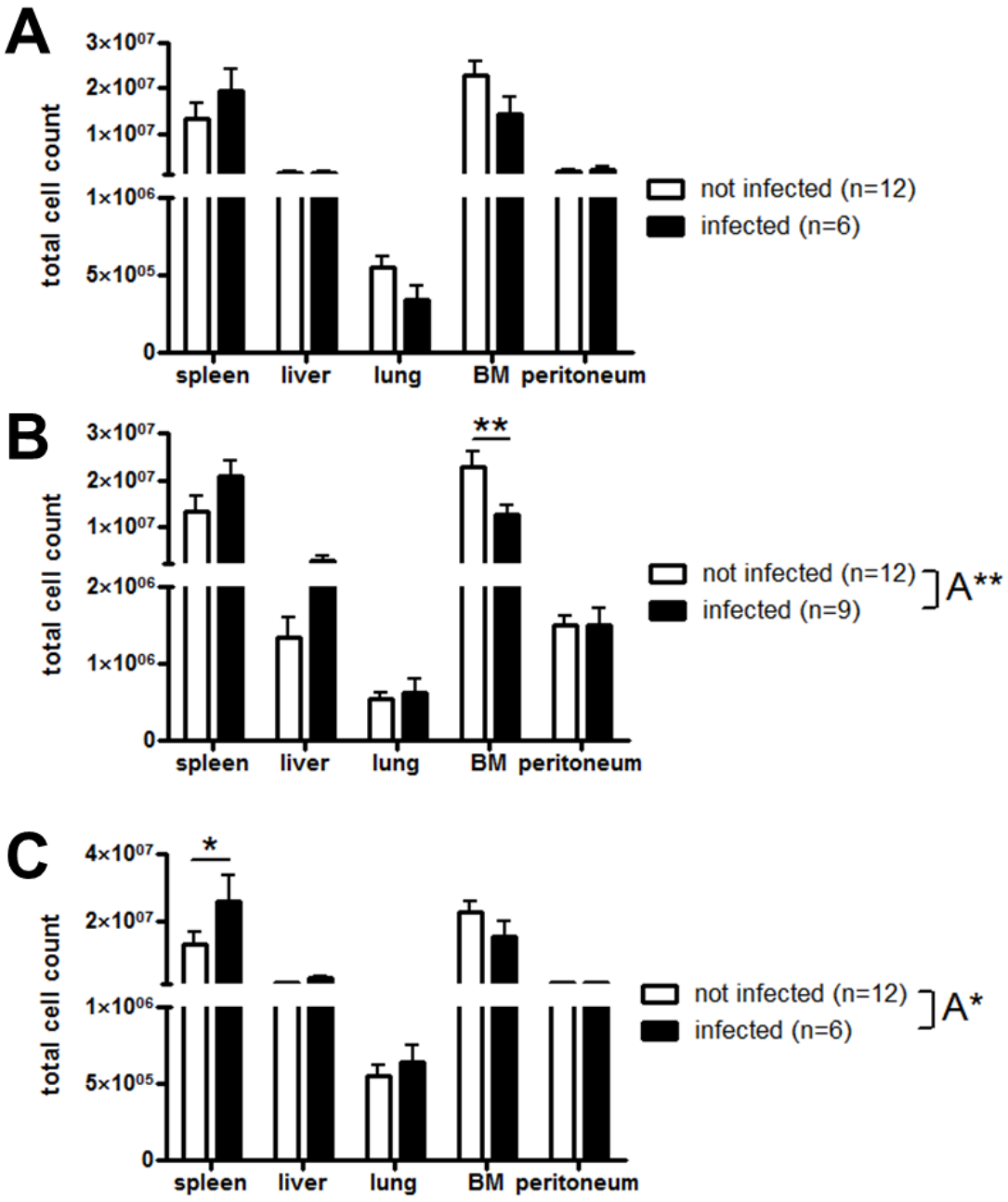

Fig. 10: *Total cell count of spleen, liver, lung, BM and peritoneum of humanized mice. After 1 day of high dose infection (10^7 GBS) (A), 3 days of moderate dose infection (10^6 GBS) (B) and 7 days of moderate dose infection (10^6 GBS) (C). Number of animals per group (n). Error bars denote the standard error of the mean. Statistical analysis: Two-way ANOVA (*=p<0.05; **=p<0.01) with Bonferroni posttest (*=p<0.05; **=p<0.01).*

3.2.5 RESPONSE OF THE HUMAN IMMUNE SYSTEM – MIGRATION AND PROLIFERATION

Aside from the changes in total cell count per organ, flow cytometric analysis was conducted to analyze the changes in immune cell populations. Although none of the changes in $CD45^+$ leukocytes were statistically significant, they coincided well with the changes in total cell counts (Fig. 11A). Infection led to a general increase in the number of human leukocytes in the spleen and the peritoneum. Moderate dose infection for 3 and 7 days decreased the number of $CD45^+$ cells in the BM but increased it in the liver (Fig. 11A). The number of $CD3^+$ T cells generally increased upon infection in the peritoneum and was probably the reason for the increased number of leukocytes there. Moderate dose infection also increased the T cell count in the liver after 7 days (Fig. 11B). The analysis of the two T cell subsets $CD3^+$ $CD4^+$ helper T cells and $CD3^+$ $CD8^+$ cytotoxic T cells revealed that the increase in T cells in the liver 7 days after moderate dose infection was mostly due to a rising helper T cell count and only a minor increase in cytotoxic T cells (Fig. 12). Changes in the T cell population were not statistically significant. High dose infection significantly increased the $CD19^+$ B cell count in the spleen and the BM. Moderate dose infection led to significantly elevated numbers of B cells in the spleen after 3 days and to a not statistically significant rise in the liver after 7 days (Fig. 11C). Increase of T and B cells most likely caused the increment of leukocytes in the liver after 7 days of moderate dose infection. The number of $CD33^+$ myeloid cells in the BM generally decreased after infection. This effect was accompanied by an increase in myeloid cells in the spleen as well as in the liver (Fig. 11D). Alterations in the myeloid cell population were not significant, however, they were present in all groups. GBS infection induced an increase in $CD66^+$ granulocytes in the BM which was significant after 3 days of moderate dose infection. Moderate dose infection for 7 days and high dose infection also resulted in the increment of granulocytes in the liver and spleen, but only by tendency (Fig. 11E).

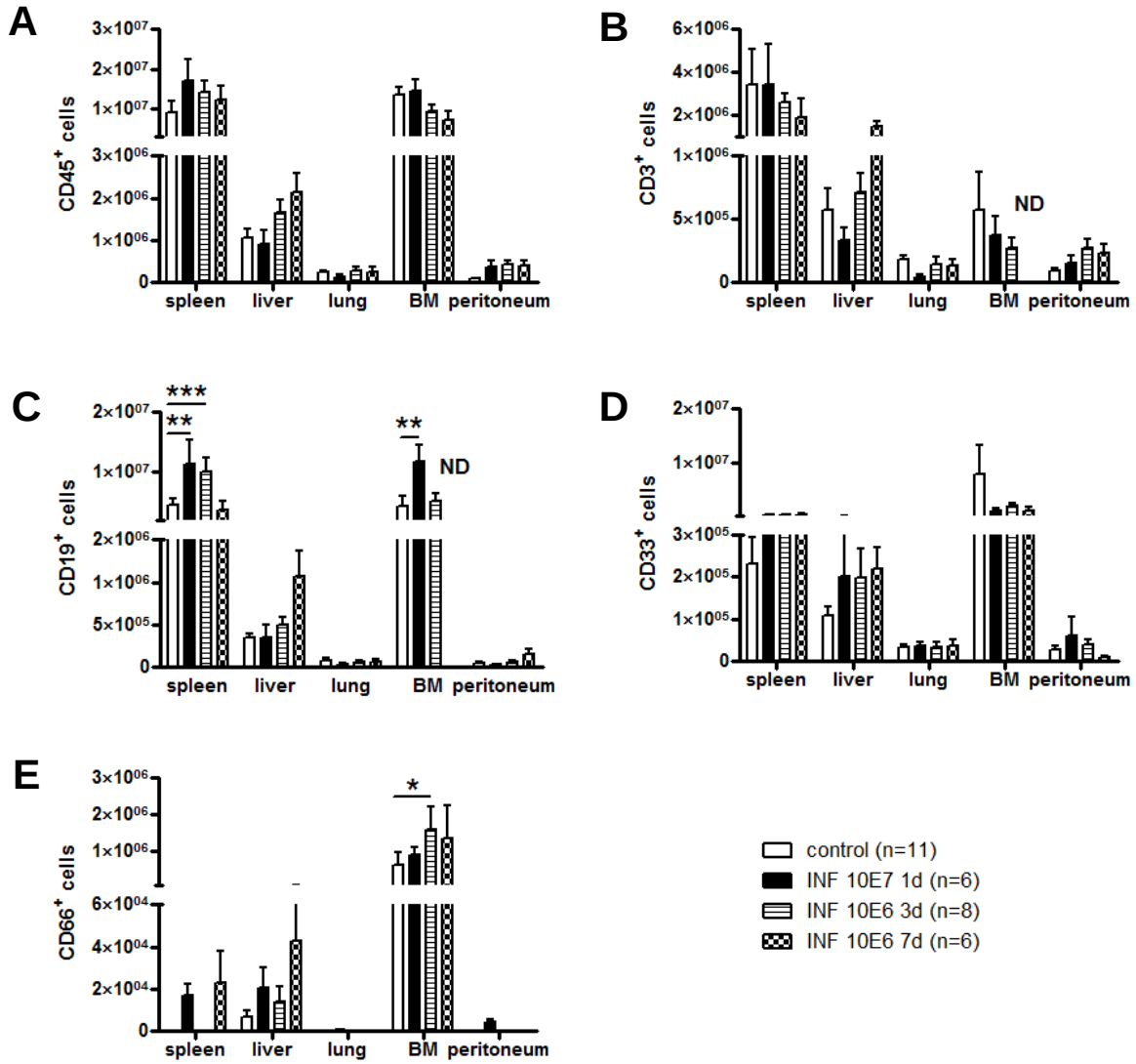

Fig. 11: *Flow cytometric analysis of the total amount of CD45$^+$ leukocytes (A), CD3$^+$ T cells (B), CD19$^+$ B cells (C), CD33$^+$ myeloid cells (D) and CD66$^+$ granulocytes (E) in spleen, liver, lung, BM and peritoneum. Animals were either not infected naïve mice (control), infected for 1 day with 10^7 GBS (INF 10E7 1d), infected for 3 days (INF 10E6 3d) or 7 days (INF 10E6 7d) with 10^6 GBS. Number of animals in each group (n). Statistical analysis: Two-way ANOVA with Bonferroni posttest (*=p<0.05; **=p<0.01; ***=p<0.001). ND means not determined.*

The human immune system that humanized mice develop is quite heterogenic. This can be seen in the high diversity of CD45$^+$ cells in the pb (Fig. 2A). Therefore, a direct comparison of the same animals before and after infection by analyzing their blood was conducted. Flow cytometric analysis showed no marked changes in the percentage of human leucocytes after 24 h of high dose and 7 days of moderate dose infection. However, a significant decrease in CD45$^+$ cells was determined 3 days after moderate dose infection (Fig. 13A). CD3$^+$ T cells were significantly elevated after 1 day (10^7 GBS) but remained unchanged after 3 days (10^6 GBS) (Fig.

13B). One day of infection with 10^7 GBS reduced the numbers of $CD19^+$ B cells in the pb significantly. Moderate dose infection with GBS showed the same picture after 3 days (Fig. 13C). Infection induced a significant increment in $CD33^+$ myeloid cell levels in all groups. However, the increase was most pronounced after high dose infection for 24 h (Fig. 13D). Moderate doses of GBS lead to a slight reduction of $CD66^+$ granulocytes after 3 days, but to an increase after 7d. High dose infection triggered a rise in granulocytes after 24 h (Fig. 13E).

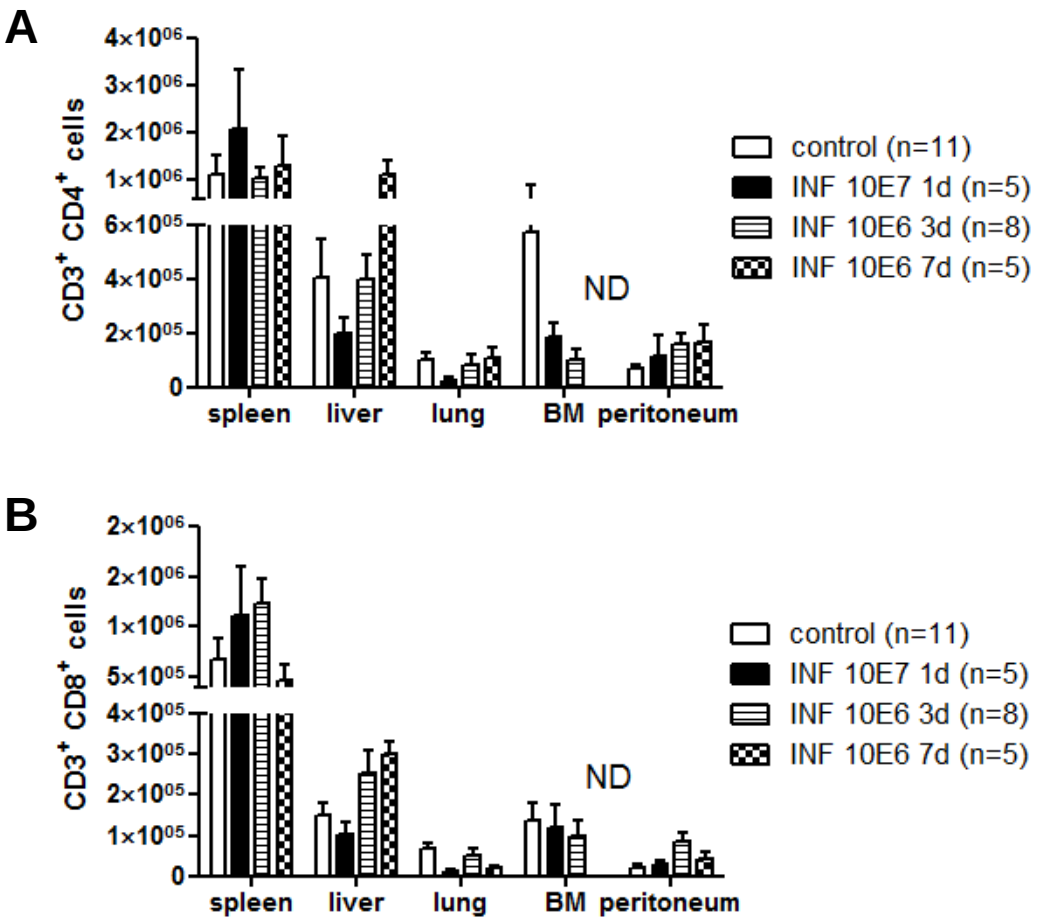

Fig. 12: *Flow cytometric analysis of the total amount of $CD3^+$ $CD4^+$ helper T cells (A) and $CD3^+$ $CD8^+$ cytotoxic T cells (B) in spleen, liver, lung, BM and peritoneum. Animals were either not infected naïve mice (control), infected for 1 day with 10^7 GBS (INF 10E7 1d), infected for 3 days (INF 10E6 3d) or 7 days (INF 10E6 7d) with 10^6 GBS. Number of animals in each group (n). Statistical analysis: Two-way ANOVA with Bonferroni posttest (no significance). ND means not determined.*

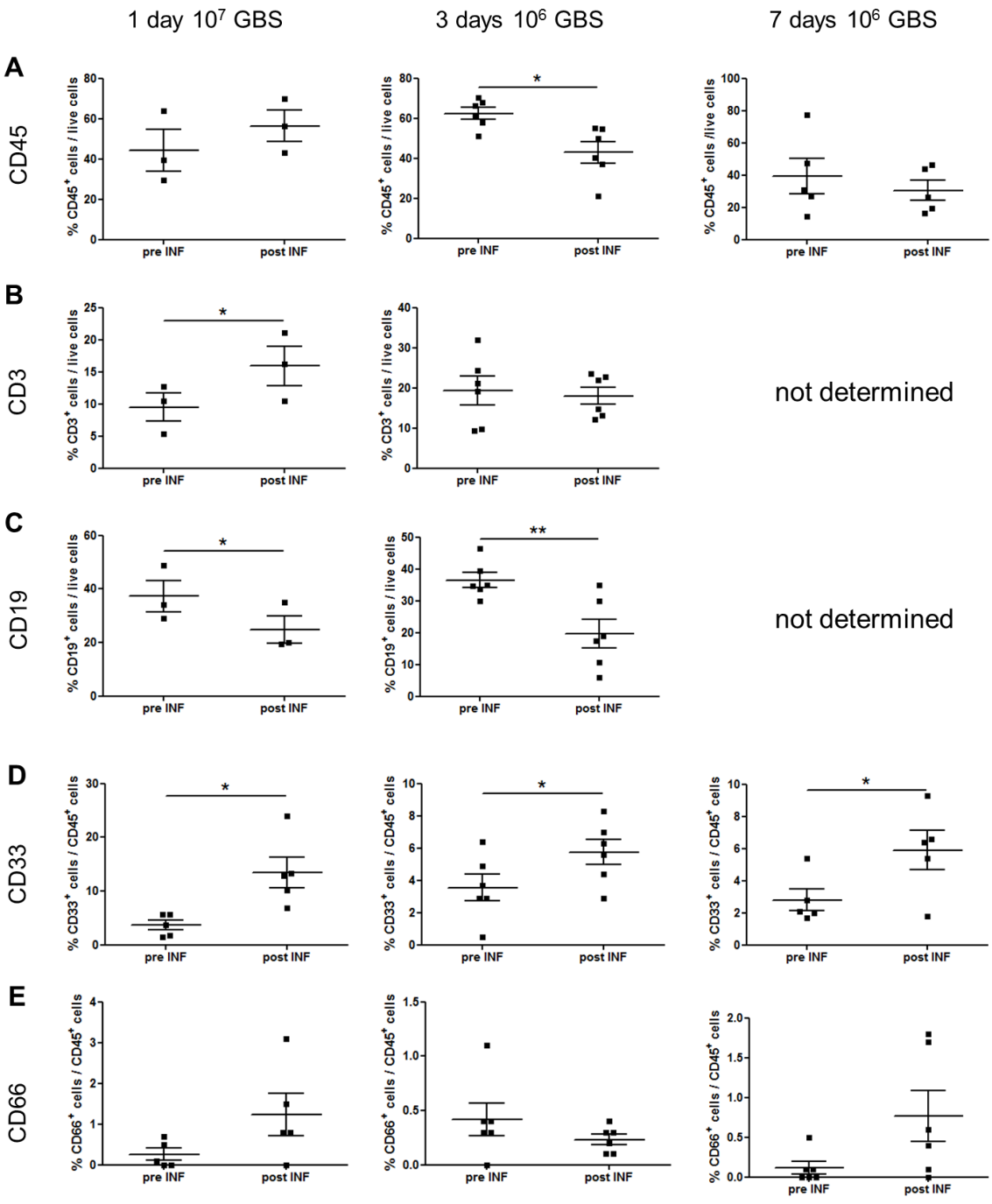

Fig. 13: *Flow cytometric analysis of CD45$^+$ leukocytes (A), CD3$^+$ T cells (B), CD19$^+$ B cells (C), CD33$^+$ myeloid cells (D) and CD66$^+$ granulocytes (E) in the pb before (pre INF) and after (post INF) infection. Animals were either infected for 1 day with 10^7 GBS (1 day 10^7), infected for 3 days (3 days 10^6) or 7 days (7 days 10^6) with 10^6 GBS. Number of animals in each group: n=3-5 (1 day 10^7), n=6 (3 days 10^6) and n=5 (7 days 10^6). Statistical analysis: Student's paired t test (*=p<0.05; **=p<0.01).*

The peritoneal cavity did not only represent the primary site of infection. Due to the low number of $CD45^+$ cells in naïve mice, this organ proved to be well suited to monitor the influx of human leukocytes and immune cell subsets during infection (Fig. 14). While high dose infection (10^7 GBS) induced increased levels of $CD45^+$ cells after 1d, moderate GBS doses led to significantly elevated amounts of human leukocytes in the peritoneum after 3 and also 7 days (Fig. 14A). Flow cytometry was used to further analyze the types of immune cells, which migrated into the peritoneum upon infection. After 1d, mostly myeloid cells and granulocytes were responsible for the elevated leukocyte levels. Three days post infection, migrated T cells and also myeloid cells comprised the majority of PEC. At 7 days of infection, T cells represented the major human immune cell population, followed by B cells, which constituted a minor population prior to that time point (Fig. 14B). Of note is the significant growth of the $CD66^+$ granulocyte population in the peritoneum after high dose infection, which was absent in moderate dose infection (Fig. 14C), whereas the increase in the amount of granulocytes in the BM was more pronounced in the 3 or 7 days of moderate dose infection compared to the relatively short time span (1 day) of high dose infection (Fig. 14D).

3.2.6 RESPONSE OF THE HUMAN IMMUNE SYSTEM – CYTOKINE PRODUCTION

After showing that the human immune cells in the animals responded to the infection by migration and proliferation, the production of human specific cytokines, which trigger those reactions, was analyzed. High doses of GBS induced the release of substantial amounts of the pro-inflammatory cytokines TNF, IFNγ, IL-1β and IL-6. Also the chemokine IL-8, which acts as a chemoattractant for neutrophils, was significantly elevated after 24 h. But not only the production and release of pro-inflammatory cytokines and chemokines were induced, also the anti-inflammatory cytokine IL-10, needed for counter-regulation of the inflammatory response, was released (Fig. 15A). Infection with moderate doses of GBS also triggered the release of cytokines and chemokines. On day 2 and day 3 post infection, TNF, IFNγ, IL-6 and IL-8 levels were slightly elevated. However, the changes were not significant and the cytokine and chemokine levels were rather low (except IL-8). IL-10 and especially IL-1β remained practically unchanged (Fig. 15B).

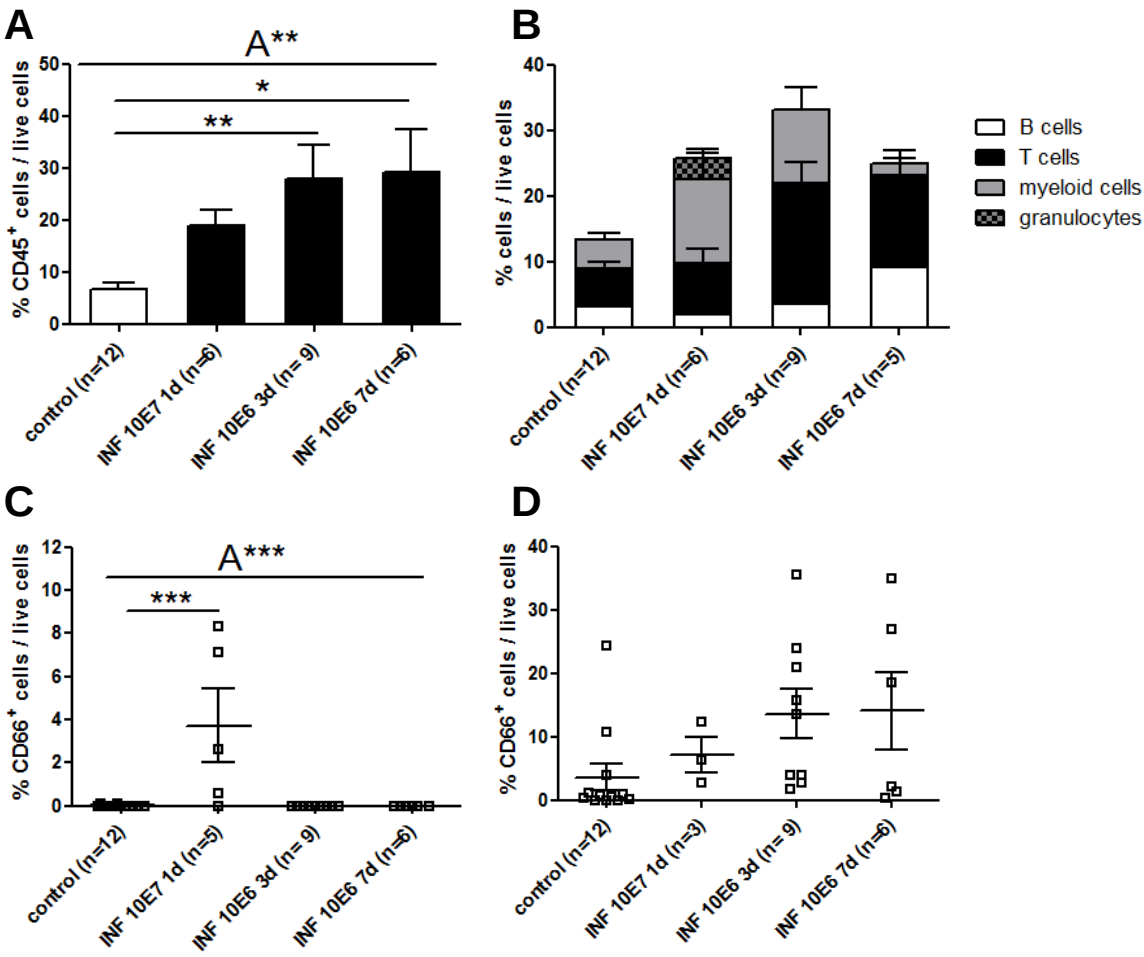

Fig. 14: *Flow cytometric analysis of CD45$^+$ leukocytes (A), and CD3$^+$ T cells, CD19$^+$ B cells, CD33$^+$ myeloid cells and CD66$^+$ granulocytes (B) in PEC after infection. Flow cytometric analysis of the relative changes in CD66$^+$ granulocytes in the PEC population (C) and BM cell population (D). Animals were either not infected (control), infected for 1 day with 10^7 GBS (INF 10E7 1d), infected for 3 days (INF 10E6 3d) or 7 days (INF 10E6 7d) with 10^6 GBS. Number of animals in each group (n). Each symbol represents one mouse; the horizontal line denotes the mean, the error bars the standard error of the mean. Statistical analysis: One-way ANOVA (A**= p<0.01, A***= p<0.001) with Tukey posttest (*=p<0.05; **=p<0.01; ***=p<0.001).*

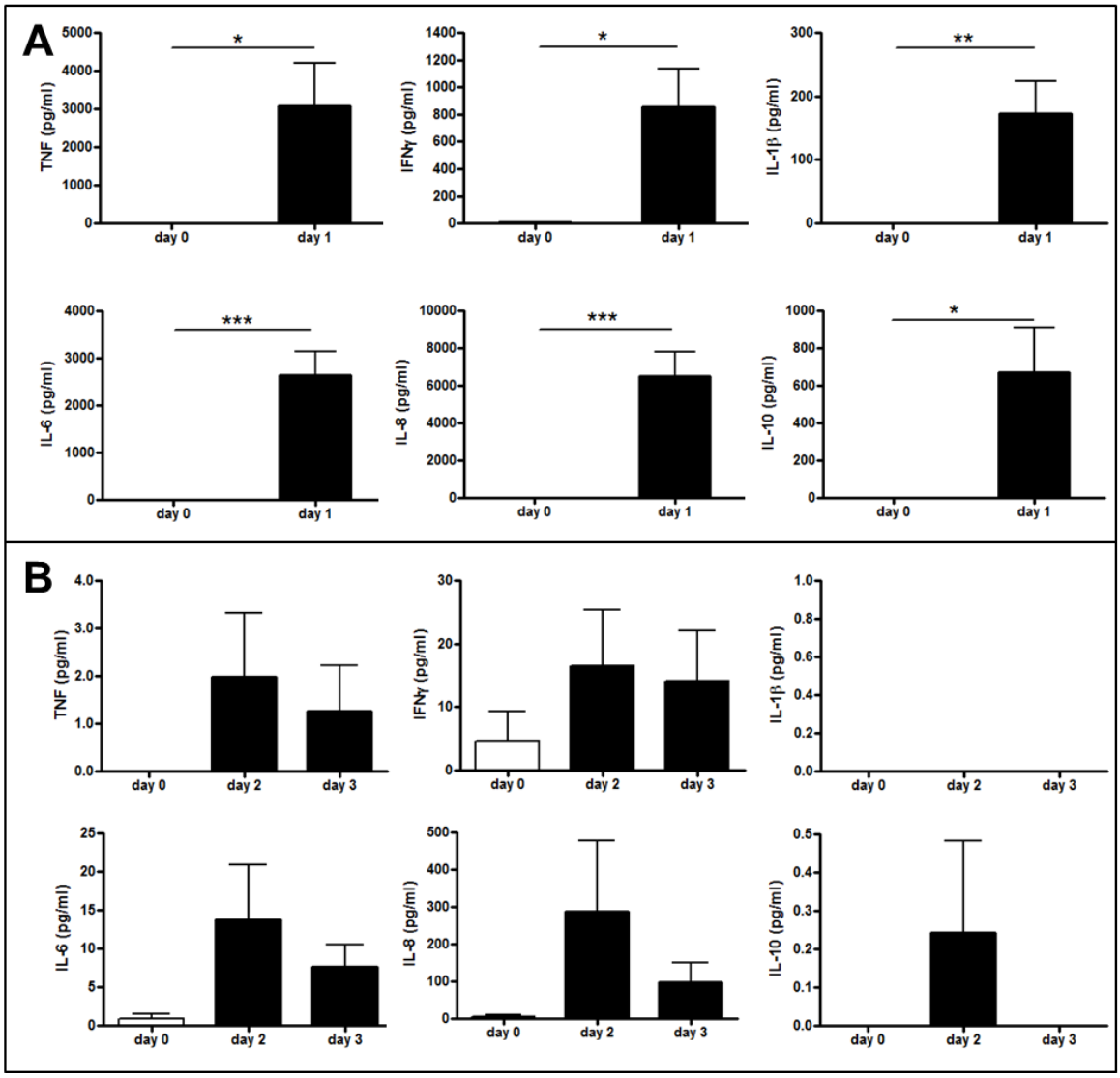

Fig. 15: *Multiplex analysis of the concentration (pg/ml) of TNF, IFNγ, IL-1β, IL-6, IL-8 and IL-10 in serum of uninfected (day 0) and infected (day 1, 2, 3) animals. Mice were either infected with 10^7 GBS and tested after 1 day (A) or infected with 10^6 GBS and analyzed at day 2 and 3 (B). Number of animals per group: (A) day 0 (n=8), day 1 (n=11); (B) day 0 (n=8), day 2 (n=12), day 3 (n=13). The error bars denote the standard error of the mean. Statistical analysis: (A) Student's unpaired t test (*=p<0.05; **=p<0.01; ***=p<0.001); (B) One-way ANOVA (no significant differences).*

3.3 EFFECT OF TREATMENT ON DISEASE PROGRESSION

3.3.1 TREATMENT REGIMEN

After establishing and analyzing the new animal model for GBS infection using humanized mice, the effect of treatment on disease progression (clearance of live bacteria, survival rate, organ damage) and effect on human immune system (migration and proliferation of leukocytes, cytokine production, clearance of GBS) was analyzed. The glucocorticoid Betamethasone is a drug routinely used for lung maturation in the clinic. The treatment regimen for human neonates is 2x 5 mg/kg given to the mother, 24 h apart. In the moderate dose GBS infection model (10^6 CFU for 3 or 7 days) the same regimen was used 24 h post infection (Fig. 16A). In the high dose infection model (10^7 GBS for 1 day) Betamethasone (5 mg/kg) was only given once, 3 h after infection due to the long biological half-life of 36-54 h (Tegethoff et al. 2009) (Fig. 16B). The non-steroidal anti-inflammatory drug Indomethacin is used for tocolysis. Since the LD50 of Indomethacin for mice is very low (11.8 mg/kg) (Material safety data sheet) and the treatment regimen for humans varies (Van Der Poole 1998), 3 mg/kg Indomethacin were given using the same regimen as Betamethasone.

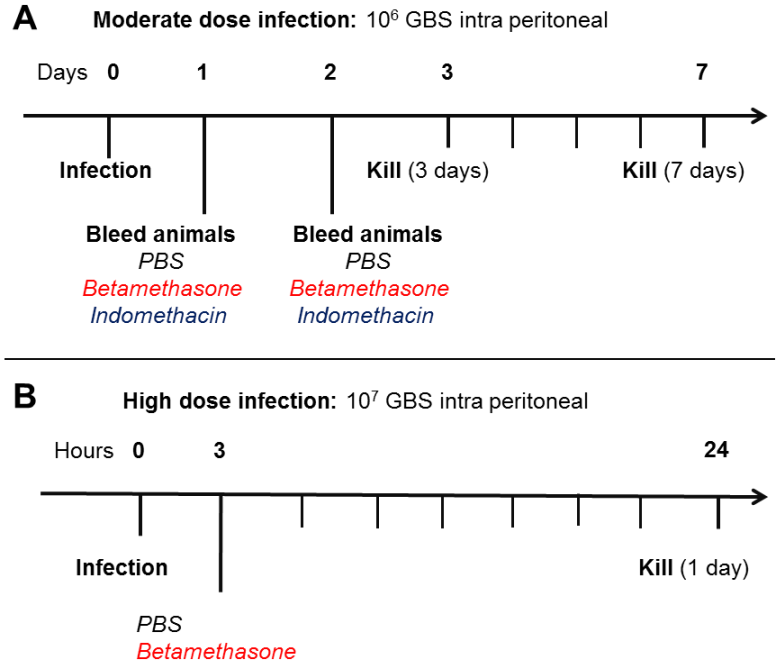

Fig. 16: *Schematic of the infection and the subsequent treatment regimen for the moderate dose (A) and high dose (B) infection model.*

3.3.2 *IMPACT OF TREATMENT ON CLEARANCE OF BACTERIA*

The clearance of live bacteria by immune cells is crucial for fighting off infections. Drugs which adversely affect the killing of pathogens usually exacerbate bacterial infections. Betamethasone treatment led to a significant reduction of the systemic CFU count (all analyzed organs combined) in the high dose infection model (10^7 GBS). It further led to an increased clearance in the peritoneum (significant), lung and spleen (Fig. 17A). The moderate dose infection model (10^6 GBS) displayed increased amounts of live bacteria with both drugs, 3 as well as 7 days after infection. At day 3, Betamethasone was responsible for a significantly higher systemic CFU count (all organs combined). Increased amounts of live bacteria were found in every organ except the peritoneum (Fig. 17B). While Indomethacin did not induce significantly higher CFU counts, treatment did result in increased amounts of live bacteria in kidney, lung and BM (Fig. 17C) 3 days post infection. Betamethasone treatment did not seem to have an effect on bacterial clearance 7 days after moderate dose infection (Fig. 17D). The effect of Indomethacin, 7 days post infection seemed to be a reduction in bacterial clearance (Fig. 17E).

GBS feature mechanisms to cross the blood brain barrier, and are known to cause meningitis. Therefore the presence of live bacteria in the brain, and the effect of treatment, was of special importance in our animal model. In the high dose infection model, 24 h post infection, 4/7 vehicle-treated animals and 4/8 Betamethasone-treated mice had live bacteria in the brain (Fig. 18A). Therefore treatment did not markedly affect the spreading of live GBS into the brain. In the moderate dose infection model however, CFU were detected only in animals which either received Betamethasone or Indomethacin. After 3 days, live bacteria were detected in 0/10 animals receiving PBS, in contrast to 3/10 receiving Betamethasone and 2/10 receiving Indomethacin (Fig. 18B). Seven days post infection, 1/2 mice in the Indomethacin treatment group had CFU in the brain. Animals in the PBS (n=6) and Betamethasone (n=3) treatment group were clean (Fig. 18C).

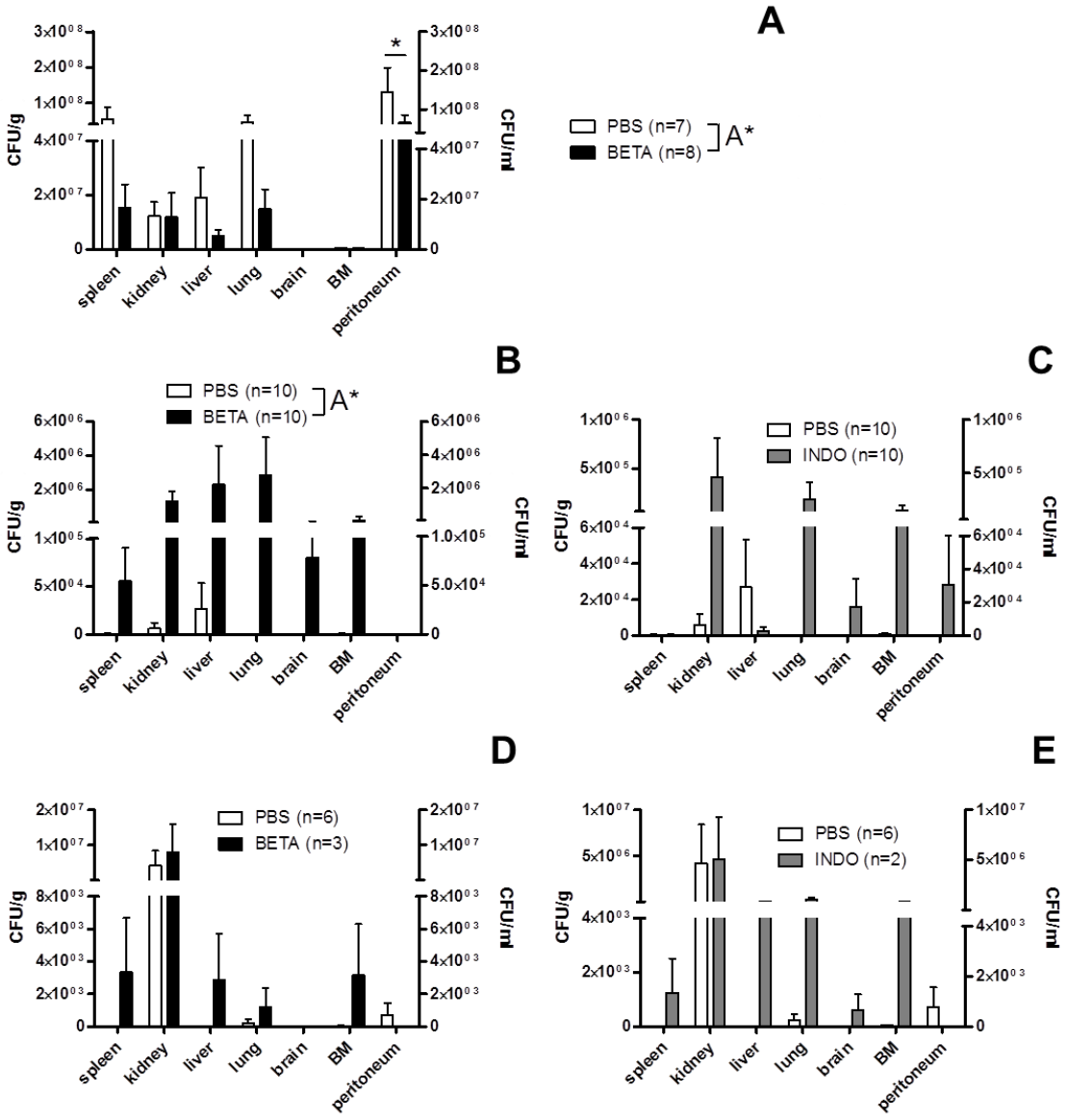

Fig. 17: *CFU count in spleen, kidney, liver, lung, brain, BM and peritoneum of infected and vehicle-treated (PBS) or infected and Betamethasone (BETA)- or Indomethacin (INDO)-treated mice. CFU count was calculated per g of tissue except for BM and peritoneal cavity where it was calculated per ml of cell suspension. Animals were either infected with 10^7 GBS and analyzed after 1 day (A) or infected with 10^6 GBS and analyzed at day 3 (B;C) or day 7 (D;E). Number of animals per group (n). The error bars denote the standard error of the mean. Statistical analysis: Two-way ANOVA (A*=*

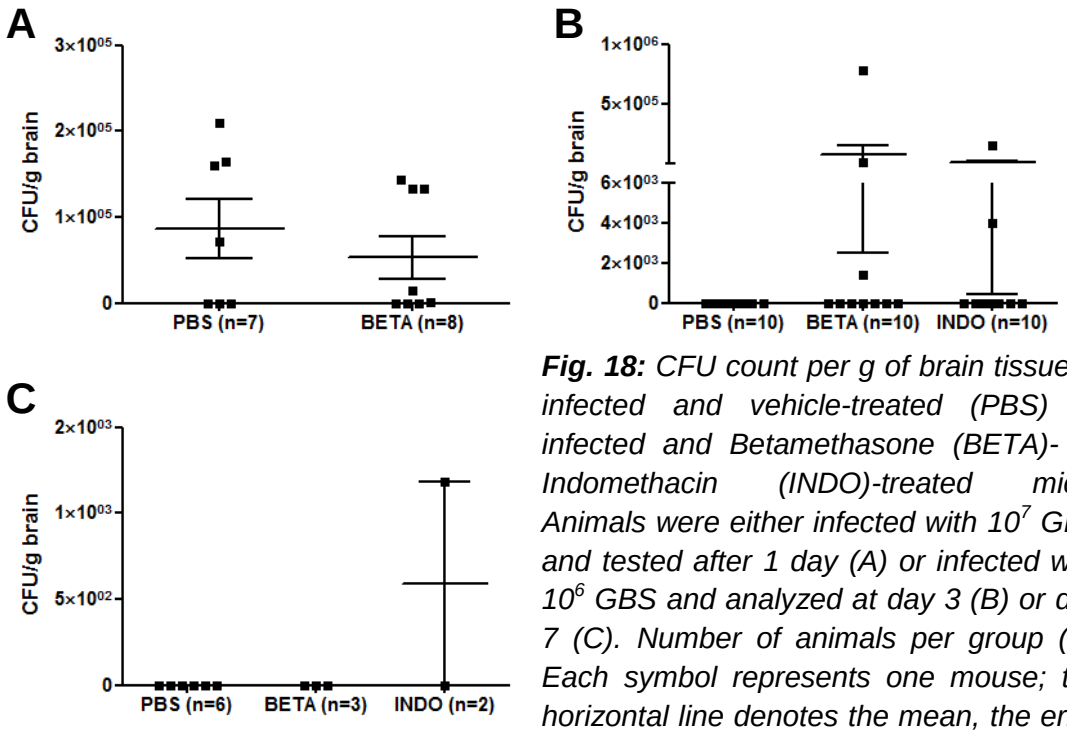

Fig. 18: *CFU count per g of brain tissue in infected and vehicle-treated (PBS) or infected and Betamethasone (BETA)- or Indomethacin (INDO)-treated mice. Animals were either infected with 10^7 GBS and tested after 1 day (A) or infected with 10^6 GBS and analyzed at day 3 (B) or day 7 (C). Number of animals per group (n). Each symbol represents one mouse; the horizontal line denotes the mean, the error bars the standard error of the mean. Statistical analysis: One-way ANOVA with Tukey posttest (no significant differences detected).*

3.3.3 Effect of treatment on total cell count

Betamethasone treatment did not affect the total cell count in high dose infected animals, 24 h after infection, except a slight decrease in PEC (Fig. 19A). In contrast, total cell count in the moderate dose infection model was affected by the treatment. Both drugs reduced the number of splenocytes significantly 3 days after infection (Fig. 19B). Furthermore, both drugs slightly decreased the leukocyte count in the liver. Treatment had no marked effect at day 7 in the moderate dose infection model (Fig. 19C).

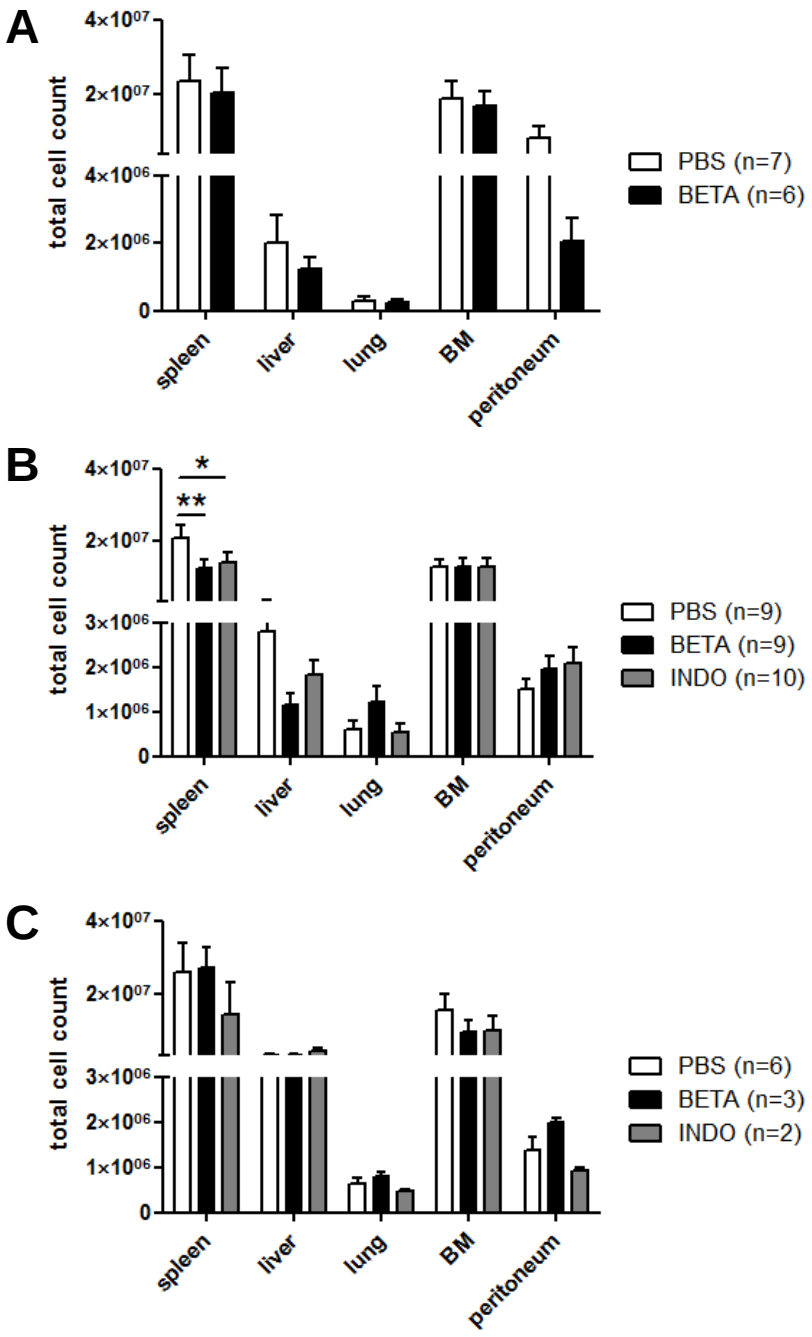

Fig. 19: *Total cell count of spleen, liver, lung, BM and peritoneum of infected and vehicle (PBS)-, Betamethasone (BETA)- or Indomethacin (INDO)-treated humanized mice. After 1 day of 10^7 GBS (A), 3 days of 10^6 GBS (B) or 7 days of 10^6 GBS (C). Number of animals per group (n). The error bars denote the standard error of the mean. Statistical analysis: Two-way ANOVA with Bonferroni posttest (*=p<0.05; **=p<0.01).*

3.3.4 EFFECT OF TREATMENT ON MIGRATION AND PROLIFERATION OF LEUKOCYTES

Flow cytometric analysis was used to determine if treatment affected the total amount of leukocytes and leukocyte subsets. This was done to analyze the effect of Betamethasone and Indomethacin on immune cell migration and proliferation during GBS infection.

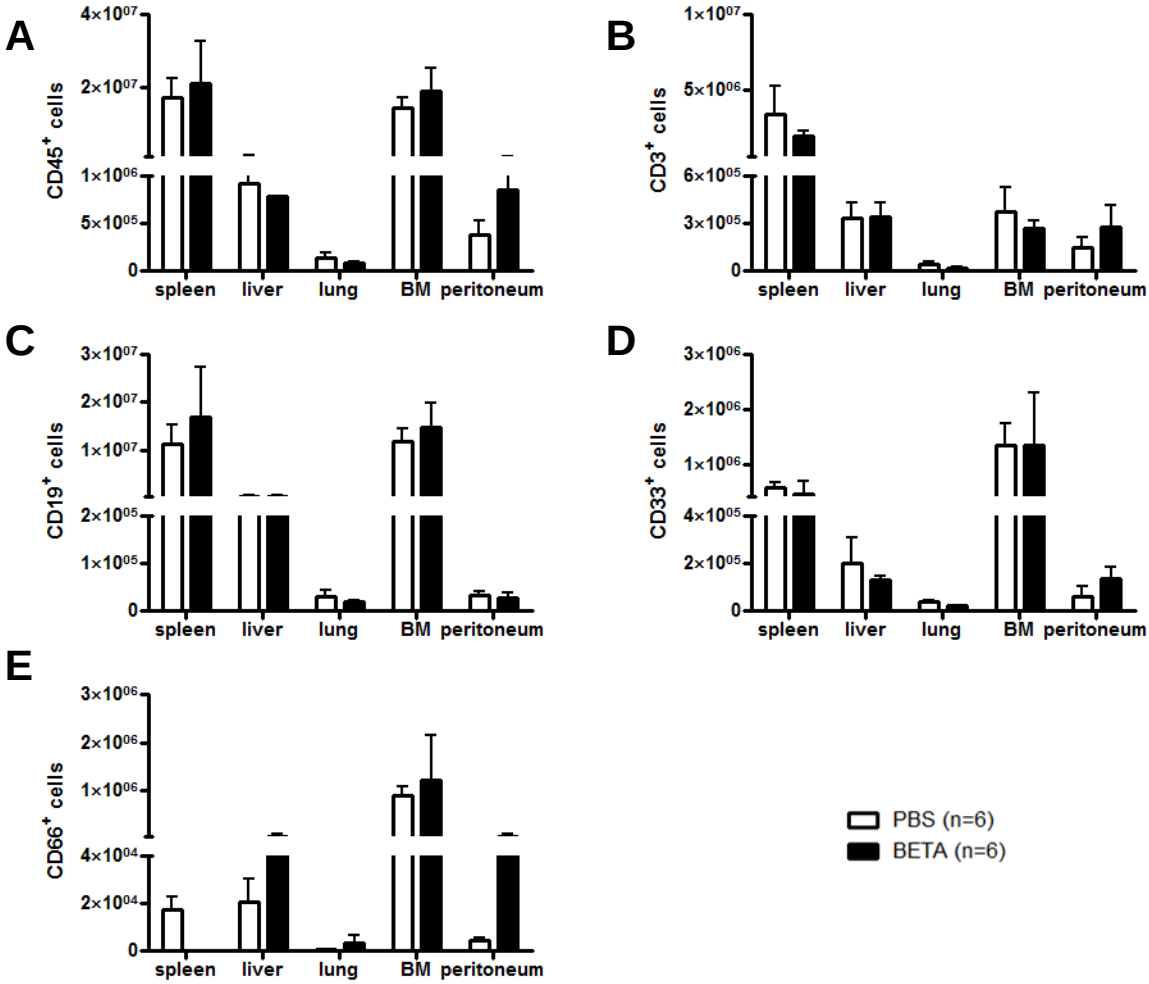

Fig. 20: *Flow cytometric analysis of $CD45^+$ leukocytes (A), $CD3^+$ T cells (B), $CD19^+$ B cells (C), $CD33^+$ myeloid cells (D) and $CD66^+$ granulocytes (E) in spleen, liver, lung, BM and peritoneum. Animals were high dose (10^7 GBS) infected, treated with either vehicle (PBS) or Betamethasone (BETA) and analyzed after 1 day. Number of animals per group (n). The error bars denote the standard error of the mean. Statistical analysis: Two-way ANOVA with Bonferroni posttest (no significant differences detected).*

In the high dose infection model (10^7 GBS, 24 h), Betamethasone treatment had no effect on total $CD45^+$ leukocyte count in all organs (spleen, liver, lung, BM) except the peritoneal cavity, where it led to increased amounts of leukocytes (not significant) (Fig. 20A). Unaffected by treatment were also $CD3^+$ T cell (Fig. 20B), B cell (Fig. 20C) and $CD33^+$ myeloid cell count (Fig. 20D). However, Betamethasone led to an increased amount of $CD66^+$ granulocytes in peritoneum and liver (not significant) and to the complete absence of this cell type in the spleen (Fig. 20E).

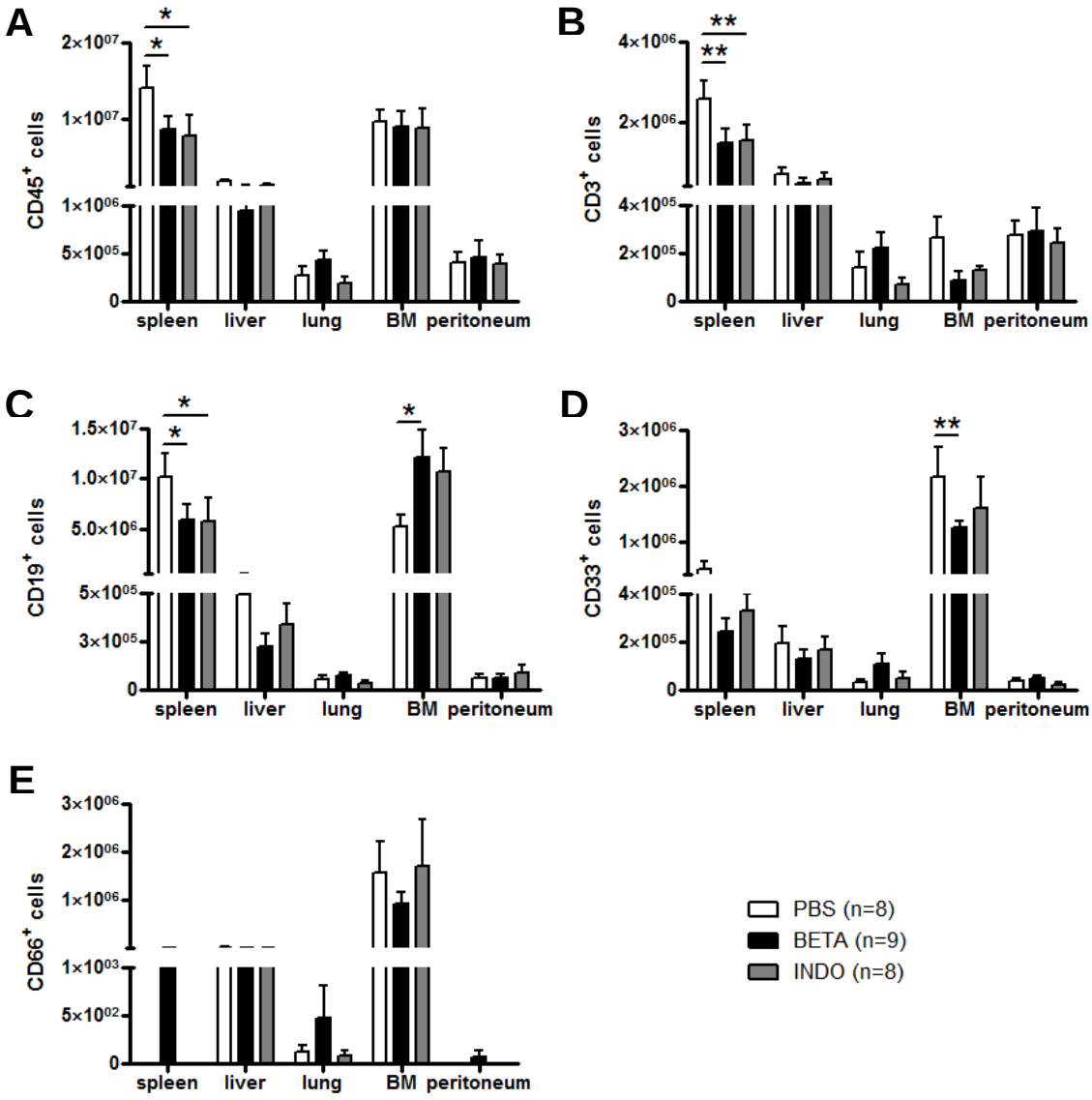

Fig. 21: *Flow cytometric analysis of $CD45^+$ leukocytes (A), $CD3^+$ T cells (B), $CD19^+$ B cells (C), $CD33^+$ myeloid cells (D) and $CD66^+$ granulocytes (E) in spleen, liver, lung, BM and peritoneum. Animals were infected with moderate doses of GBS (10^6), treated with (PBS), Betamethasone (BETA) or Indomethacin (INDO) and analyzed after 3 days. Number of animals per group (n). The error bars denote the standard error of the mean. Statistical analysis: Two-way ANOVA with Bonferroni posttest (*=p<0.05; **=p<0.01).*

In the moderate dose infection model (10^6 GBS) both drugs induced changes in leukocyte populations after 3 days. Both Betamethasone and Indomethacin led to a significant reduction in $CD45^+$ cell count in the spleen (Fig. 21A), which was explained by reduced amounts of T, B and myeloid cells. Furthermore, the two different treatments led to a significantly lower $CD3^+$ T cell count in the spleen, and also a slightly lower amount of T cells in the BM (Fig. 21B). Both drugs also induced a significant decrease in $CD19^+$ cells in the spleen and Betamethasone caused a significantly increased B cell count in the BM. Indomethacin had the same effect, but not significantly (Fig. 21C). $CD33^+$ myeloid cell counts in the spleen were lowered by both drugs, but only by tendency. Treatment also resulted in a reduction of myeloid cells in the BM, for Betamethasone this effect was significant (Fig. 21D). Betamethasone induced granulocytes in 1/9 of treated animals in peritoneum and spleen, which were completely absent in the other treatment groups (Fig. 21E).

After 7 days treatment did not induce significant changes. However, Betamethasone led to an increase in $CD45^+$ cells in the peritoneum in the moderate dose infection model (Fig. 22A), which was explained by an increase in T cell numbers (Fig. 22B). B cell (Fig. 22C), myeloid cell (Fig. 22D) and granulocyte populations (Fig. 22E) and were relatively unaffected by treatment.

Neither Betamethasone nor Indomethacin treatment had major effects on T cell subsets (Fig. 23). The pronounced increase in CD3+ CD8+ cytotoxic T cells in the spleen should not be considered important since it was the value of only one animal.

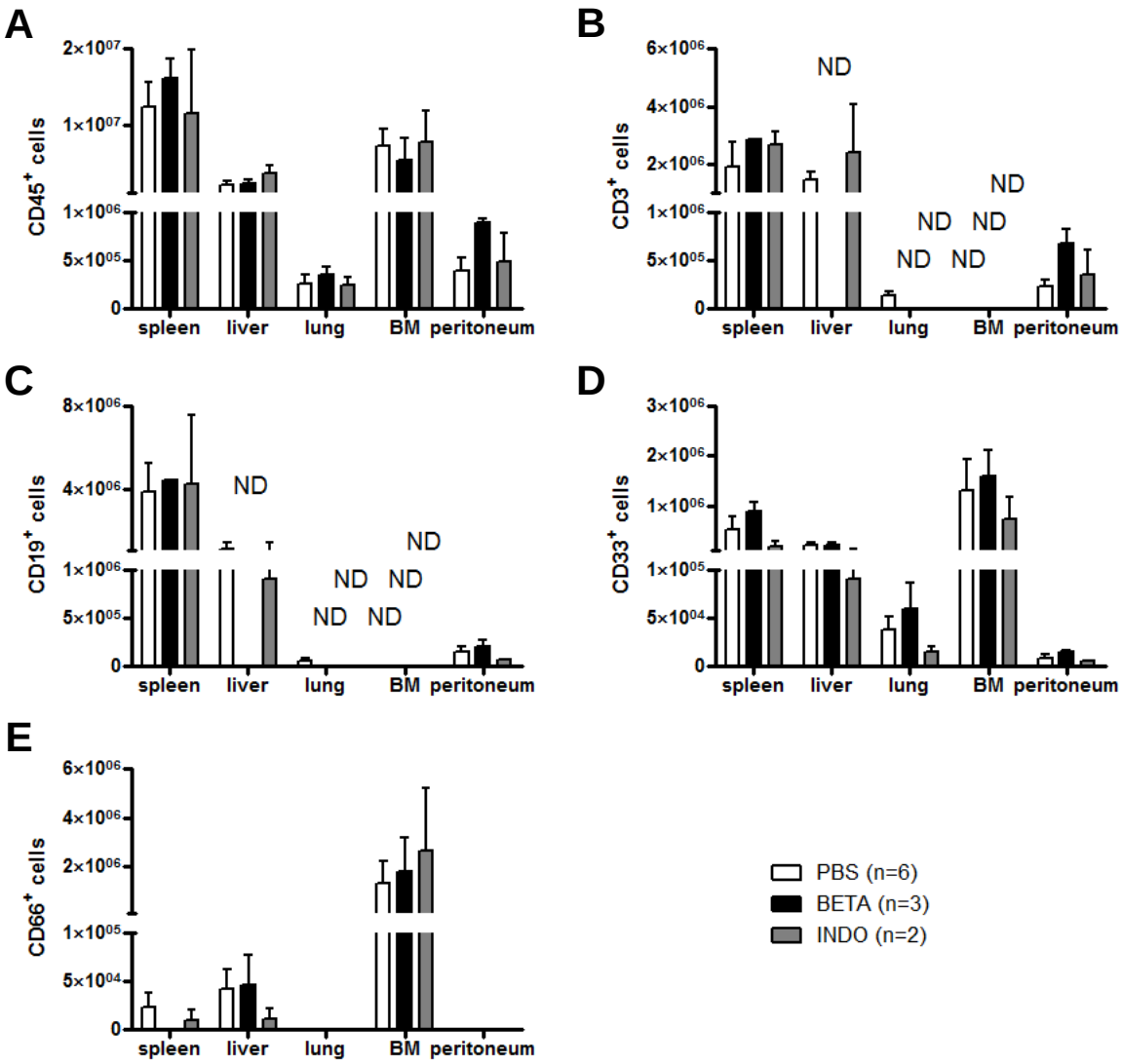

Fig. 22: *Flow cytometric analysis of CD45$^+$ leukocytes (A), CD3$^+$ T cells (B), CD19$^+$ B cells (C), CD33$^+$ myeloid cells (D) and CD66$^+$ granulocytes (E) in spleen, liver, lung, BM and peritoneum. Animals were infected with moderate doses of GBS (10^6) and treated either with vehicle (PBS), Betamethasone (BETA) or Indomethacin (INDO) and analyzed after 7 days. Number of animals per group (n). Exception: spleen INF 10E6 7d (CD19 and CD3) n=1. The error bars denote the standard error of the mean. Statistical analysis: Two-way ANOVA with Bonferroni posttest (no significant differences). ND means not determined.*

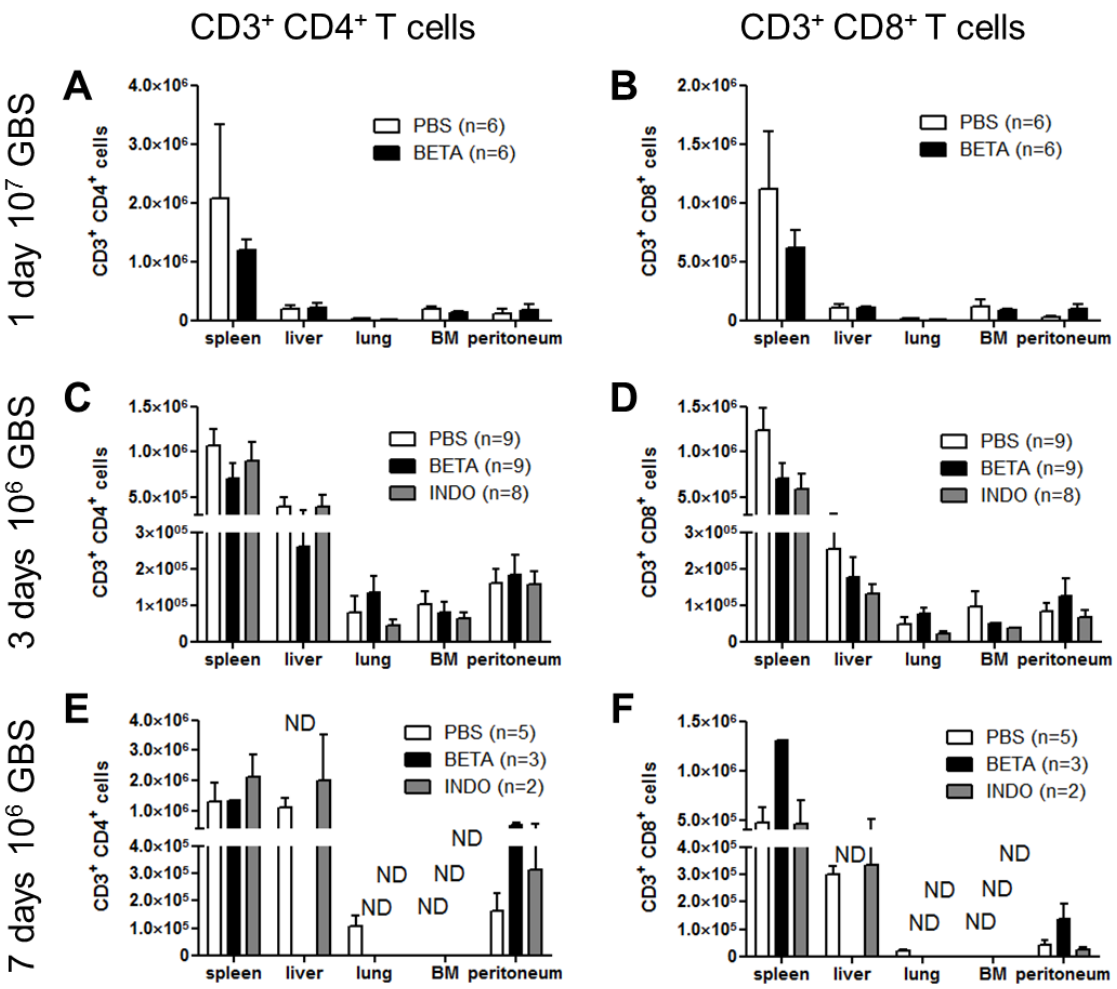

Fig. 23: *Flow cytometric analysis of the total amount of $CD3^+$ $CD4^+$ helper T cells (A,C,E) and $CD3^+$ $CD8^+$ cytotoxic T cells (B,D,F) in spleen, liver, lung, BM and peritoneum. Animals were infected with 10^7 GBS for 1 day (A,B), 10^6 GBS for 3 (C,D) or 7 days (E,F). The infected mice were either vehicle- (PBS), Betamethasone (BETA)- or Indomethacin (INDO)-treated and analyzed. Number of animals per group (n). Exception: spleen INF 10E6 7d (BETA) n=1. The error bars denote the standard error of the mean. Statistical analysis: Two-way ANOVA with Bonferroni posttest (no significant differences). ND means not determined.*

Due to the fact that pb can be drawn and analyzed before and after infection and treatment, this procedure enabled a direct comparison of immune cell populations in the same animal. Therefore, the heterogeneity of the human immune system in humanized mice had a lower impact, and slighter changes in cell populations, caused by treatment, were detectable.

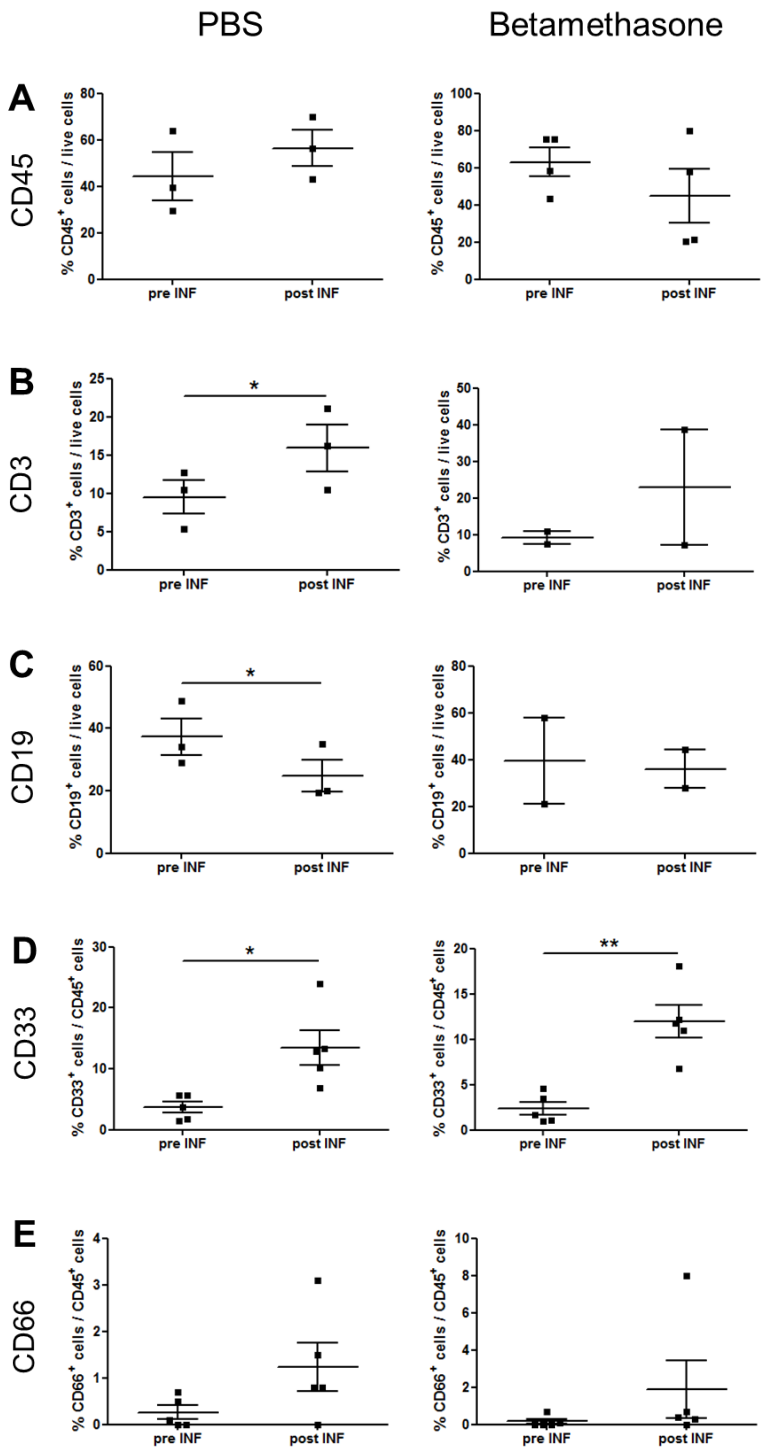

Fig. 24: *Flow cytometric analysis of CD45$^+$ leukocytes (A), CD3$^+$ T cells (B), CD19$^+$ B cells (C), CD33$^+$ myeloid cells (D) and CD66$^+$ granulocytes (E) in the pb before (pre INF) and after (post INF) infection. Animals were infected for 1 day with 10^7 GBS and received either vehicle (PBS) or Betamethasone once 3 h post infection. Number of animals per group: n=3-5 (PBS), n=2-5 (Betamethasone). Each symbol represents one mouse; the horizontal line denotes the mean, the error bars the standard error of the mean. Statistical analysis: Student's paired t test (*=p<0.05; **=p<0.01).*

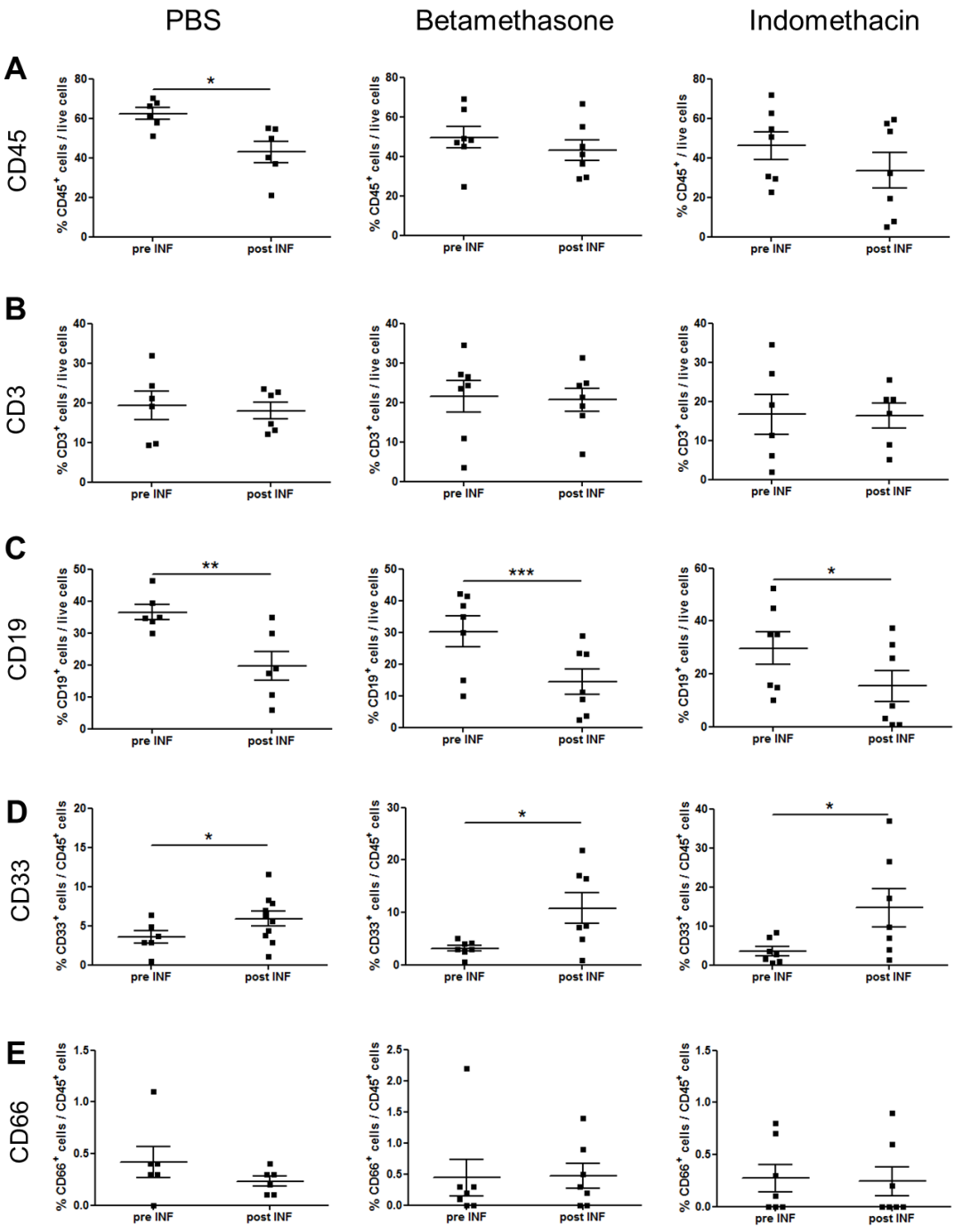

Fig. 25: *Flow cytometric analysis of CD45$^+$ leukocytes (A), CD3$^+$ T cells (B), CD19$^+$ B cells (C), CD33$^+$ myeloid cells (D) and CD66$^+$ granulocytes (E) in the pb before (pre INF) and after (post INF) infection. Animals were infected for 3 days with 10^6 GBS and received either vehicle (PBS), Betamethasone or Indomethacin twice (24 h and 48 h) post infection. Number of animals in each group: n=6 (PBS), n=7 (Betamethasone), n=6-7 (Indomethacin). Each symbol represents one mouse; the horizontal line denotes the mean, the error bars the standard error of the mean. Statistical analysis: Student's paired t test (*=p<0.05; **=p<0.01; ***=p<0.001).*

High dose infection (10^7 GBS) for 1 day had no major impact on $CD45^+$ leukocytes in the pb, neither with nor without treatment. $CD3^+$ T cells were elevated in both groups, however in untreated animals (PBS) this effect was significant. Infection led to a significant decrease in $CD19^+$ B cells, which was absent after Betamethasone administration. Treatment did not affect the significant rise in myeloid $CD33^+$ cells in the pb after high dose infection. Also, the slight rise in percentage of granulocytes was practically absent with Betamethasone treatment (Fig. 24).

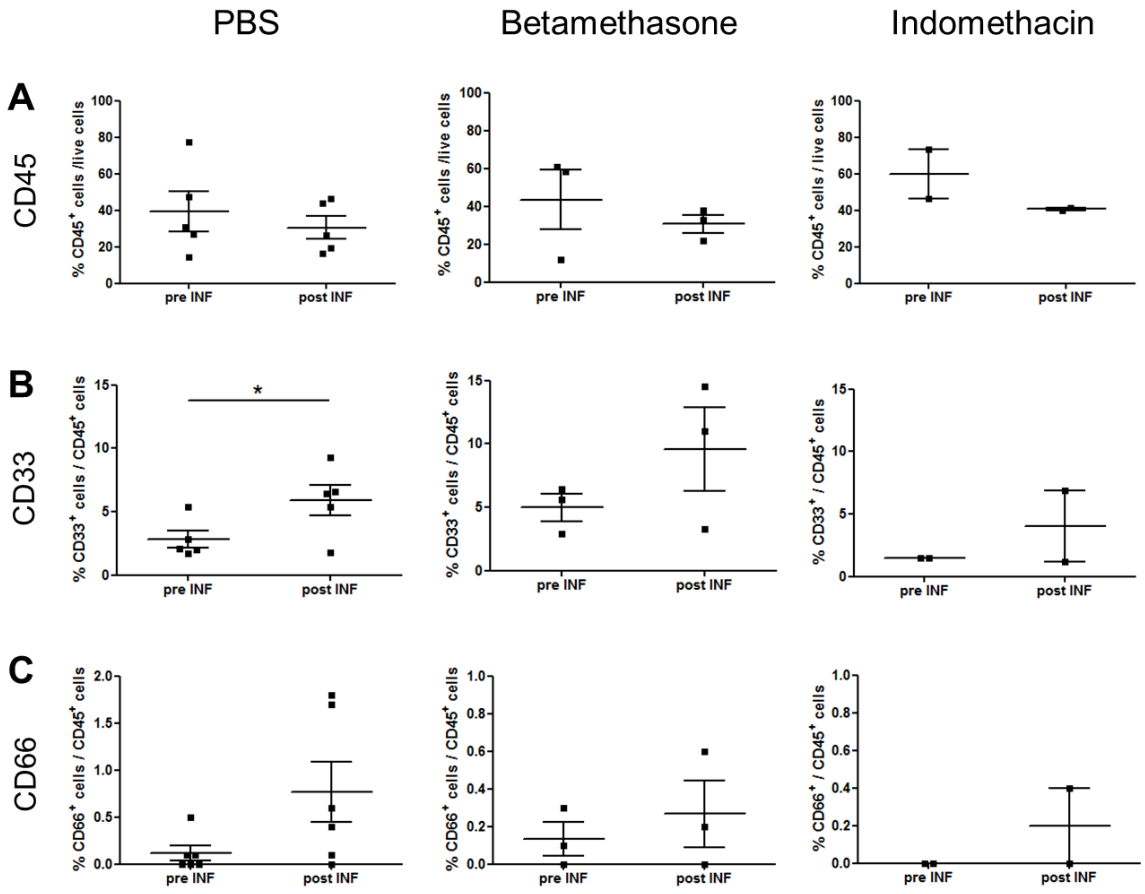

Fig. 26: *Flow cytometric analysis of $CD45^+$ leukocytes (A), $CD33^+$ myeloid cells (B) and $CD66^+$ granulocytes (C) in the pb before (pre INF) and after (post INF) infection. Animals were infected for 7 days with 10^6 GBS and received either vehicle (PBS), Betamethasone or Indomethacin twice (24 h and 48 h) post infection. Number of animals in each group: n=5-6 (PBS), n=3 (Betamethasone), n=2 (Indomethacin). Each symbol represents one mouse; the horizontal line denotes the mean, the error bars the standard error of the mean. Statistical analysis: Student's paired t test (no significant differences).*

In the moderate dose infection model (10^6 GBS) the amount of $CD45^+$ leukocytes in the pb decreased with Betamethasone and Indomethacin and also without treatment. However, a significant reduction was only observed in vehicle treated animals 3 days post infection. The size of the T cell population was unaffected while $CD19^+$ B cells significantly decreased in all 3 groups. Infection led to significantly increased levels of myeloid cells in all groups, but with Betamethasone and especially Indomethacin treatment, the percentage of $CD33^+$ cells was higher. The granulocyte population was quite low and heterogenic, but a slight reduction could be detected in animals which received vehicle only compared to no change in treated animals (Fig. 25).

After 7 days of moderate dose infection with GBS, the $CD45^+$ cell population in the pb was basically unaffected in all groups. An increase in myeloid cells was also observed in all groups, but it was only significant in vehicle treated animals. Furthermore, the granulocyte population was also slightly bigger after infection in all animals, but only by tendency (Fig. 26).

3.3.5 Effect of treatment on human immune response – cytokine production

Since treatment with Betamethasone and Indomethacin affected clearance of live bacteria and human immune cell populations, the effect of the drugs on the production and release of cytokines and chemokines, which serve as mediators of the immune response, was analyzed. Betamethasone reduced the amount of TNF, IFNγ and IL-6 in the bloodstream of high dose infected animals after 1 day (not significant). Indomethacin had no major effect at this time point (Fig. 27A). In the moderate dose infection model, 2 days post infection, Indomethacin induced significantly higher levels of the chemokine IL-8 in the serum. Treatment with both drugs also increased the level of IL-6 (not significant) (Fig. 27B). At day 3, the increased amount of IL-8 due to Indomethacin treatment was even more pronounced compared to day 2 in the moderate dose GBS infection model. Similar to day 2, the serum level of IL-6 was increased by both drugs (not significant) (Fig. 27C).

3.3.6 EFFECT OF TREATMENT ON HUMAN IMMUNE RESPONSE – NO PRODUCTION

In order to test the capability of NO production of PEC in humanized mice, animals (n=6) were infected with 10^7 GBS to induce infiltration of leukocytes into the peritoneum. The infected mice were treated with vehicle (n=3) or Betamethasone (n=3) 3 h post infection. After 24 h, the PEC were extracted and restimulated *in vitro* by culturing them for 1 h and 24 h respectively with 10^7 GBS, again either with vehicle (n=3) or Betamethasone (n=3). The subsequent nitrite measurement revealed that no measurable amount of NO was produced by the PEC (data not shown).

3.3.7 EFFECT OF TREATMENT ON DISEASE PROGRESSION – ORGAN DAMAGE

Infection alone (vehicle treated animals) did not result in significant organ damage in our GBS infection models (high dose for 1 day, moderate dose for 3 or 7 days). Furthermore, Betamethasone or Indomethacin treatment did not seem to have an adverse effect, since treated animals also did not display organ damage (Supplement Fig 1-4 + data not shown). In conclusion, treatment did not cause or increase organ damage in the infection models analyzed in this study.

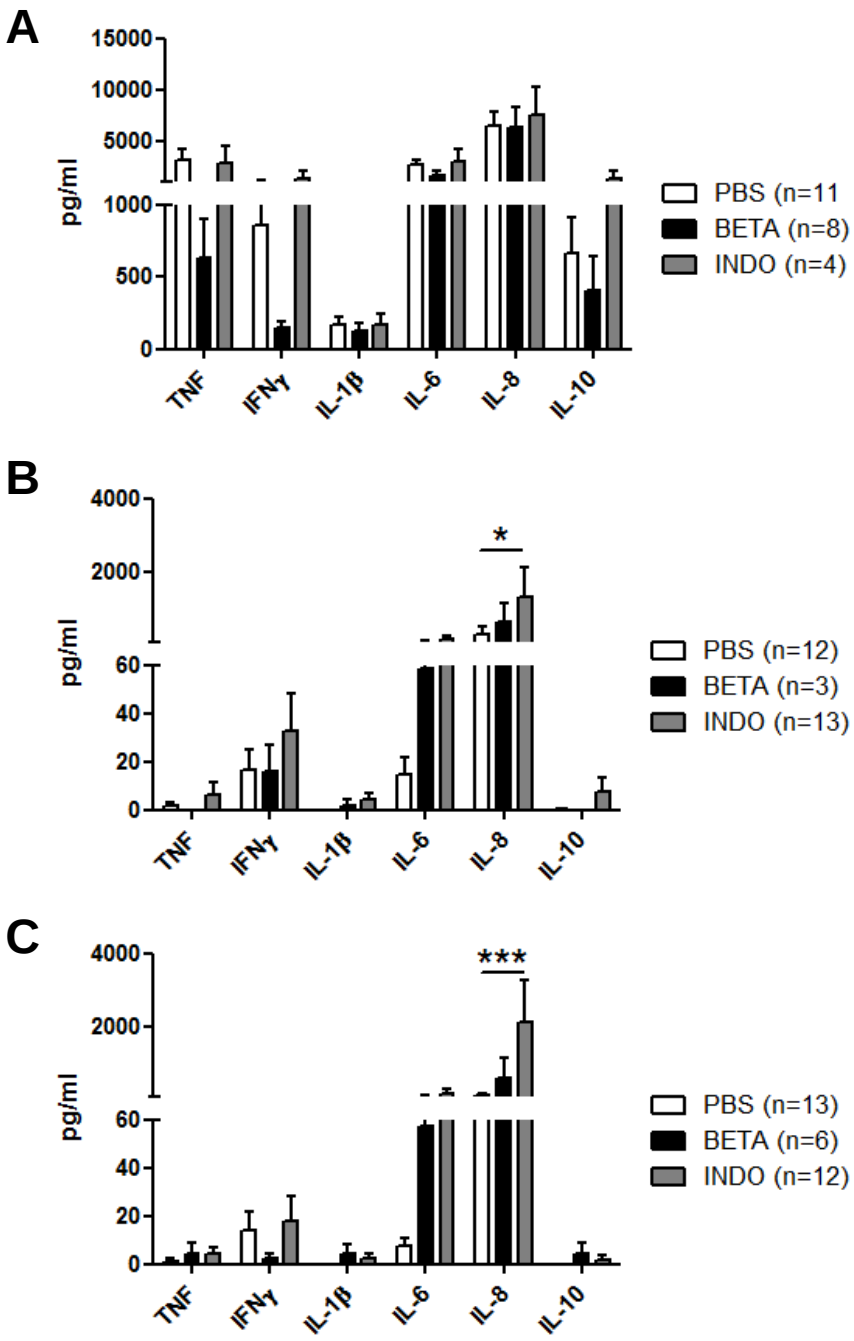

Fig. 27: *Multiplex analysis of the concentration (pg/ml) of TNF, IFNγ, IL-1β, IL-6, IL-8 and IL-10 in serum of infected animals treated with vehicle, (PBS), Betamethasone (BETA) or Indomethacin (INDO). Mice were either infected with 10^7 GBS, bled and tested after 1 day (A) or infected with 10^6 GBS and analyzed at day 2 (B) and 3 (C). Number of animals per group (n). Statistical analysis: Two-way ANOVA with Bonferroni posttest (*=p<0.05; ***=p<0.001).*

3.4 EFFECTS OF TREATMENT *IN VITRO*

Betamethasone or Indomethacin might exert a direct effect on the GBS itself, like facilitating growth, which would have increased their number in treated animals and led to the false assumption that the treatment reduced the clearance rate of the immune system (Fig. 17 B,C). To rule out a direct effect, 10^7 GBS were incubated either with vehicle alone (PBS), Betamethasone (1 µg/ml) or Indomethacin (1 µg/ml) for 4 h. In this timeframe, treatment did not significantly affect bacterial growth (Fig. 28).

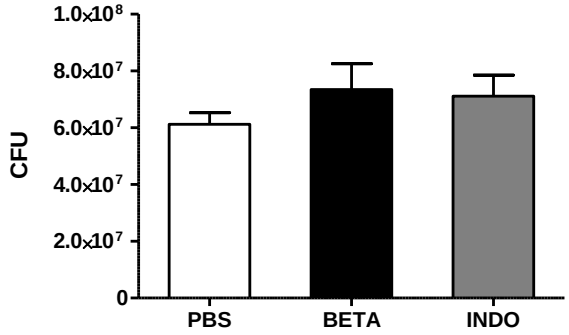

Fig. 28: *Colony forming units (CFU) of 10^7 GBS incubated alone for 4 h with either vehicle (PBS), 1 µg/ml Betamethasone (BETA) or 1 µg/ml Indomethacin (INDO). Statistical analysis: One-way ANOVA with Tukey posttest (no significant differences).*

In this study humanized mice were used as an animal model for the neonatal immune system. However, although the human immune cells in the animals feature similar deficiencies as neonatal leukocytes (see introduction), it was not certain, if genuine human neonatal immune cells behave similarly when challenged with GBS. Therefore, we also analyzed the bacterial clearance and the changes in immune cell populations of human neonatal MNC, isolated from cord blood, *in vitro*.

To mimic the high dose infection model, 10^6 MNC were incubated for 4 h with 10^7 GBS and either treated with PBS (vehicle), Betamethasone (1 µg/ml) or Indomethacin (1 µg/ml). The short timeframe was chosen to avoid bacterial overgrowth and death of the cultured MNC. At 4 h, bacterial clearance was unaffected by treatment (Fig. 29A). In order to incubate cord blood derived MNC together with GBS for extended periods of time, bacterial growth had to be abolished. To accomplish that, the bacteriostatic agent Chloramphenicol was used. Previous tests showed that the concentration of 2.5 µg/ml was high enough to completely inhibit bacterial growth but also low enough not to kill GBS at a density of 10^5/ml (Supplement Fig. 5). After 24 h of incubating MNC with GBS, Indomethacin treatment led to a reduced number of live bacteria, indicating increased bacterial clearance (not

significant) (Fig. 29 B). However, after an incubation of 48 h, treatment with both drugs resulted in reduced bacterial clearance, though not significantly (Fig. 29C).

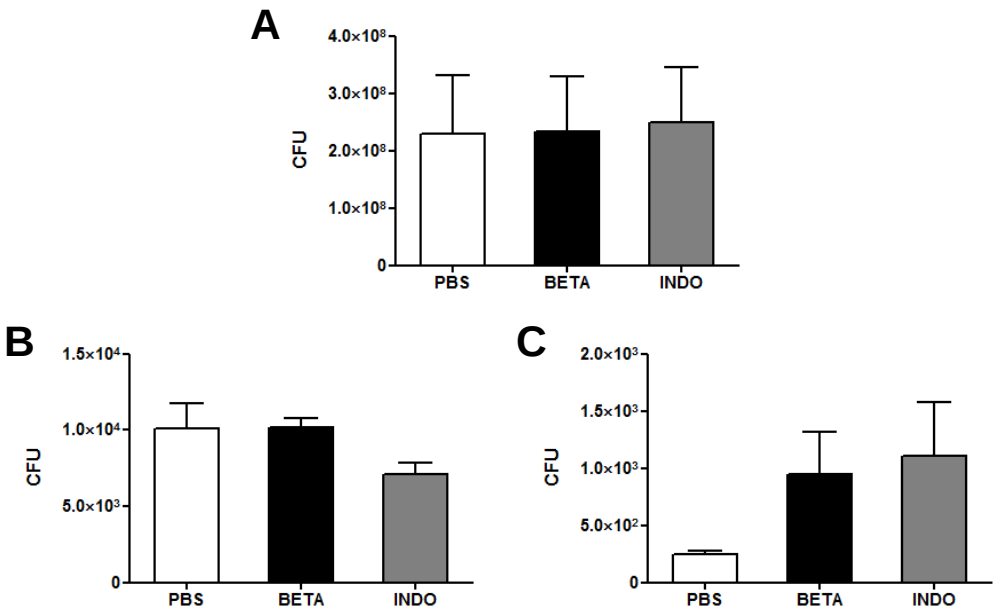

Fig. 29: *Colony forming units (CFU) of 10^7 GBS incubated with 10^6 MNC for 4 h and treated either with vehicle (PBS), 1 µg/ml Betamethasone (BETA) or 1 µg/ml Indomethacin (INDO) (A). CFU of 10^5 GBS incubated with 10^6 MNC for 24 h (B) or 48 h (C) with 2.5 µg/ml Chloramphenicol and treated either with vehicle (PBS), 1 µg/ml Betamethasone (BETA) or 1 µg/ml Indomethacin (INDO). Number of independent experiments (n); n=3 (A); n=2 (B,C). Statistical analysis: One-way ANOVA with Tukey posttest (no significant differences).*

In our animal model we also analyzed the effect of treatment on leukocyte subsets with and without the presence of GBS. Therefore, cord blood derived MNC were either cultured alone or together with GBS and treated either with vehicle (PBS), Betamethasone (1 µg/ml) or Indomethacin (1 µg/ml). When cultivated with high doses of GBS (10^7) for 4 hours, a reduction of the total cell count mostly due to the lower number of $CD33^+$ myeloid cells could be detected compared to the MNC that were cultured alone. An effect of drug treatment was not observed (Fig. 30A). Culturing of MNC with lower doses of GBS (10^5) for 24 h led to a markedly decreased total cell count because of the reduced number of T cells, myeloid cells and NK cells compared to MNC cultured alone. B cell count was relatively unaffected by the presence of live GBS. Treatment with both drugs led to an increased cell count in MNC incubated with GBS (not significant). No effect of treatment on the leukocyte subpopulations of the MNC that were cultured alone was observed (Fig. 30B). After 48 h, presence of GBS also led to a reduced total cell count, again due to the lower number of T cells, myeloid cells and NK cells compared to MNC cultured

without GBS. Furthermore, only treatment with Indomethacin resulted in higher total cell count (not significant). In the MNC cultured alone for 48 h, the total cell count was reduced compared to MNC cultured alone for 24 h. This was mostly caused by the reduced number of granulocytes. Interestingly enough, treatment with Betamethasone led to a reduced total cell count due to a reduction in the number of T cells (not significant) (Fig. 30C)

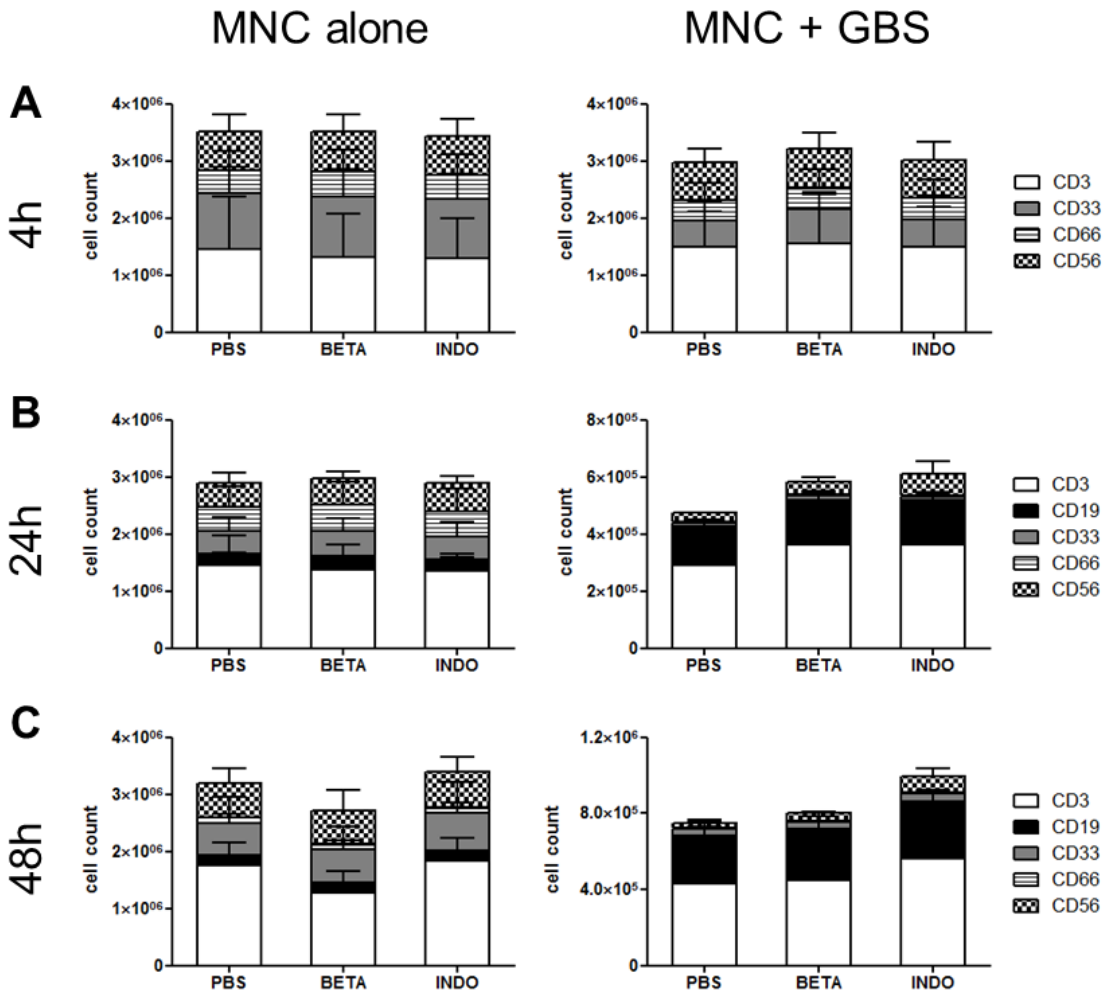

Fig. 30: *Flow cytometric analysis of $CD3^+$ T cells, $CD33^+$ myeloid cells, $CD66^+$ granulocytes and $CD56^+$ NK cells of cord blood derived MNC (10^6) incubated without and with 10^7 GBS for 4 h (A). Flow cytometric analysis of $CD3^+$ T cells, $CD19^+$ B cells, $CD33^+$ myeloid cells, $CD66^+$ granulocytes and $CD56^+$ NK cells of 10^6 MNC incubated without and with 10^5 GBS plus 2.5 µg/ml Chloramphenicol for 24 h (B) and 48 h (C). MNC were either treated with vehicle (PBS), 1 µg/ml Betamethasone (BETA) or 1 µg/ml Indomethacin (INDO). Number of independent experiments (n); n=3 for all incubations of MNC without GBS, n=3 for incubation of MNC with GBS for 4 h; n=2 for incubation of MNC with GBS for 24 h and 48 h. Statistical analysis: Two-way ANOVA with Bonferroni posttest (no significant differences detected).*

4 DISCUSSION

4.1 HUMANIZED MICE AS A GBS INFECTION MODEL

In this study I introduce a new model for GBS sepsis in neonates and analyzed the effect of Betamethasone and Indomethacin treatment in an ongoing bacterial infection. Only *in vivo* models allow the investigation of complex processes that occur during infection, like disease progression, clearance of bacteria in different organs, organ damage, leukocyte migration, hematopoiesis and the effect of treatment on these processes. Therefore, infection and sepsis studies are usually conducted using mice as an animal model since there are severe ethical as well as legal constraints for using human subjects (Shultz et al. 2007). However, although the mouse is a valuable research tool, there are more than 60 known differences in the immune system between mice and men (Mestas & Hughes 2004). Especially in sepsis, these differences seem to play an important role, since therapeutic treatments which have worked in animal studies failed in more than 25 clinical trials (Unsinger et al. 2009).

In order to combine the human immune system together with an *in vivo* model, the humanized mouse model was used for these experiments. Humanized mice feature all human immune cell subsets including granulocytes, monocytes/macrophages, plasmacytoid and myeloid DCs, NK, T and B cells as well as human erythrocytes and platelets (Ishikawa et al. 2005; Shultz et al. 2005; Shultz et al. 2007, Unsinger et al. 2009). Therefore the pathogen (GBS) interacts with human leukocytes, and the response of a human immune system can be analyzed. The second benefit of humanized mice is heterogeneity. Animals used in sepsis models are genetically identical from inbred strains and generally of the same sex, whereas human patients are of both sexes and genetically heterogenic. This could be one of the reasons why translating the results of animal studies of sepsis poses a problem (Pitts & Simpson 2010). I used mice as well as cord blood from both sexes. And since the cord blood for transplantation also stems from various human donors, the genetic heterogeneity is also ensured. Heterogeneity is also visible in the amount of leukocytes and immune cell subsets in the humanized mice (Fig. 2), which coincides at least basically with the broad leukocyte ranges of human neonates (Ikincioğullari et al. 2004). Due to the heterogeneity of the animals, significant differences due to infection and treatment are less frequent than in inbred animals. However, the results

from this study are probably more relevant and can be transferred onto humans more easily.

The first aim of this study was to analyze the distribution of human immune cells in the organs of humanized mice. This was done to ensure that leukocytes are present in lymphoid as well as other relevant organs and also to be able to compare the entire immune system of humanized mice and human neonates or adults. A direct comparison of leukocytes and leukocyte subsets in humanized mice and humans (adults and neonates) revealed that the relative size of B and T cell populations is similar in most organs (supplementary table 2-6). However, tissue macrophages in the lung and peritoneum and granulocytes in the pb and BM are underrepresented in the animal model, due to a lack of species-specific hematopoietic growth factors and a mouse microenvironment which seems to be suboptimal for human hematopoiesis, especially for the development of the myeloid linage (Shultz et al. 2007; Andre et al. 2010; Gille et al. 2012). Considering the important role of granulocytes and macrophages in fighting off bacterial infections, these differences can be seen as less-than-ideal for this model. However, to put this fact into perspective, even though there might be fewer myeloid cells present in humanized mice, these cells are functional. We could show that *in vitro* generated BMDM not only displayed a morphology similar to human donors (Möst et al. 1997) but also expressed the maturation marker CD86 after stimulation. Tanaka et al. recently showed that also the phagocytic activity and bacterial killing of BMDM of humanized mice are comparable to that of human macrophages (Tanaka et al. 2012).

Although humanized NSG mice feature a functional human immune system, they still possess a residual mouse immune system. However, due to the fact that 10/11 irradiated NSG mice died whereas all their humanized littermates survived the GBS infection (Fig. 8), there is a good case to believe that the remnants of the mouse immune system do not play a major role in resolving GBS infection. In addition the murine immune system of NSG mice lacks mature B, T and NK cells, the macrophages feature an immature phenotype, the DC are deficient and they also lack complement lysis due to a functional impairment of the complement factor C5 (Shultz et al. 1995; Türeci et al. 2003; Serbina et al. 2003; Shultz et al. 2005; Shultz et al. 2007).

In the first part of my thesis, I determined if the humanized mouse represents a suitable model for GBS infection. Our results revealed considerable reconstitution of human leukocytes in all analyzed organs, dose dependent survival and disease progression and that the residual mouse immune cells did not play a major role in resolving the GBS infection. This makes humanized mice the closest human like animal model currently available to study GBS infection and treatment effects *in vivo*.

4.2 EFFECTS OF GBS INFECTION IN HUMANIZED MICE

The second aim of this thesis was to analyze the effects of GBS infection on humanized mice and their human immune system (organ damage, changes in leukocyte populations due to proliferation and migration, cytokine production etc.). In the following paragraph I compare the changes in leukocyte subsets to humans and neonates (if possible), or other animal models in order to determine if the human immune system in humanized mice reacts to GBS infection (or bacterial infection in general) in a similar manner as the human (neonatal) immune system or a fully functional immune system of animal models.

4.2.2 ORGAN DAMAGE

In both the high dose (after 1 day) and the moderate dose infection model (after 3 and 7 days), no organ damage was detected. Since GBS is a major pathogen causing neonatal meningitis (Palys et al. 2006) we expected pathological changes in the brain. Studies using mice as an animal model for meningitis show that brain damage is accompanied by massive amounts of bacteria in the brain ($2x10^8$-$1x10^{10}$ CFU) (Mook-Kanamori et al. 2012). Infected humanized mice displayed considerably lower CFU counts (< $1x10^6$), which might explain the absence of organ damage in the brain. The hypothesis that high amounts of live bacteria are necessary to induce organ damage in humanized mice is supported by the fact that high dose infected animals, which displayed pathological changes in lung and spleen after 2 days of infection (Fig. 9) also featured high amounts of GBS in both organs (>$6x10^8$). The organ damage was also most likely responsible or contributed majorly to the high mortality in the high dose infection model.

4.2.3 CHANGES IN LEUKOCYTE POPULATIONS AND CYTOKINE PROFILE

T cells

Based on the literature, both humanized mice and human neonates feature very similar deficiencies. Since the amniotic cavity resembles a sterile environment, the majority of human neonatal T cells feature a naïve phenotype, which was also observed in $CD4^+$ and even more so in $CD8^+$ T cells in spleen, pb and lung of uninfected humanized mice. This was most likely caused by the specific pathogen free environment the mice were kept and bred in. Human neonatal T cells also express low amounts of IL-4 as well as IFN-γ upon activation and show lower proliferation compared to adult T cells, which is most likely attributed to their lower production of IL-2 (Schelonka & Infante 1998; Chalmers et al. 1998; Watson et al. 1991; Gasparoni et al. 2003).

Infected humanized mice did not display major changes in T cell populations except an increase in T cells in the pb after 1 day. That indicates a problem in the T cell function. Upon activation, T cells in humanized mice are known to produce low amounts of IFNγ, IL-4 and also IL-2 which corresponds well with their reduced proliferation (Watanabe et al. 2009). The reduced proliferation after antigenic stimulation could be one of the reasons why there was basically no increase in T cell numbers in infected humanized mice. To exacerbate the reduced proliferation capabilities, T cells in humanized mice are positively selected in the mouse thymus, and therefore have problems recognizing human MHC molecules (Watanabe et al. 2009). Another factor contributing to the reduced proliferation and T cell function in humanized mice are species specific cytokines produced by non-leukocyte cells. IL-7 is essential for T, B and dendritic cell development and also important for T cell homeostasis. It is produced primarily by stromal cells in thymus and bone marrow (Dittel & LeBien 1995; von Freeden-Jeffry et al. 1997; El Kassar et al. 2004; Mazzucchelli et al. 2004; Vogt et al. 2009). For survival and homeostatic proliferation of $CD8^+$ cytotoxic T cells, IL-15 is required (Surh & Sprent 2008). The combination of all these factors likely is the reason for the absence of proliferation of T cells in this infection model. There was also a lack of T cell migration in infected animals, which could have been caused or aggravated by a lack of human-specific chemokines and adhesion molecules in humanized mice (Macchiarini et al. 2005; Shultz et al. 2007).

B cells

According to the literature, human neonatal B cells share a variety of defects with their counterpart in humanized mice. Studies found that B cells from humanized mice mostly feature a naïve phenotype ($CD5^+$) and produce lower amounts of IgM and especially IgG, which most likely stems from a lack of germinal center formation and class switch (Lepus et al. 2009; Watanabe et al. 2009; Rajesh et al. 2010). Similar to humanized mice the naïve phenotype is also dominant in human neonatal B cells. They not only produce low amounts of Ig, these cells also mainly produce IgM and only little IgG and IgA after stimulation (Schelonka & Infante 1998; Splawski et al. 1991). Furthermore, animal studies have shown that structures, which are needed for B cell activation and antibody production against T cell dependent antigens, are missing at birth (Adkins et al. 2004), which implies that human neonates also lack germinal centers, which is similar to the situation in humanized mice.

Unlike T cells, B cells displayed both considerable proliferation and migration. After 1 day of GBS infection the $CD19^+$ B cells in spleen and BM increased while simultaneously decreasing in the pb (Fig. 11,13). After 3 days, a decrease in the pb coupled with an increase in the spleen was detected. Since other organs (liver, lung and peritoneum) were not affected, the logical explanation would be that the B cells migrated from the blood into the lymphoid structures (spleen and BM). A major contributing factor for the increase in B cells in the spleen after 3 days (possibly even after 1 day in BM and spleen) might have been proliferation. While fetal hematopoiesis takes place in the liver and spleen, the BM is the major site of hematopoiesis in adults. Although under certain conditions like irradiation, inflammation or infection with certain pathogens, extramedullary hematopoiesis, usually in spleen and liver, can occur. Lymphopoiesis and therefore B cell production in the BM is usually reduced in favor of increased myelopoiesis, especially granulopoiesis, which would explain the equal levels of B cells in animals infected for 3 days and in uninfected mice. However, extramedullary B cell lymphopoiesis can take place in the spleen, which might have been a contributing factor for the increased number of B cells on day 3 of GBS infection. The increase in hematopoiesis can be explained by the binding of TLR ligands (e.g. GBS cell wall components) to TLR on hematopoietic progenitors. (Tagaya et al. 2000; Nagai et al. 2006; Cain et al. 2009; Kim 2010; Bockstal et al. 2011). An additional contributing factor for the increased B cell count, 3 days post infection could have been TI activation and proliferation by mitogens. Peptidoglycan (part of the cell wall of GBS)

is a known TI antigen which induces proliferation and antibody production in B cells (Dziarski 1982; Caliot et al. 2012).

Myeloid cells

Human neonatal monocytes/macrophages display a reduced ability to kill GBS, and produce a lower amount of the cytokines IL-1β and IL-6 upon stimulation. Neonatal DC produce lower amounts of IL-12 and also feature reduced phagocytic activity (Pillay et al. 1994; Goriely et al. 2001; Liu et al. 2001; Marodi 2006). Although, the number of myeloid cells in humanized mice is generally limited, the phagocytic activity and bacterial killing of macrophages is comparable to their human counterpart (Andre et al. 2010, Tanaka et al. 2012). Furthermore, a direct comparison of monocytes from humanized NSG mice with neonatal human monocytes from cord blood revealed that phagocytic activity was identical and that basal expression of costimulatory molecules and the capacity to induce T cell proliferation was similar (Gille et al. 2012).

In this study, $CD33^+$ myeloid cells decreased in the BM, but increased in pb, spleen and liver at all three time points by tendency (Fig. 11,13). This suggests the migration of myeloid cells (predominantly monocytes) from the BM into the pb (transport medium) from where they were recruited into the organs to contain and combat the infection (Luster et al. 2005). Monocytes are generated from progenitor cells in the BM, which also serves as a reservoir from which monocytes are mobilized. Upon inflammation, mostly inflammatory monocytes emigrate into the bloodstream. At the site of infection, monocytes transmigrate into the inflamed tissue and can differentiate into TNF- and iNOS-producing (TIP) DC or classically activated macrophages. This recruitment of inflammatory monocytes is essential for efficient clearance of pathogens. Interestingly enough, the liver and the spleen, which represent the two organs to which $CD33^+$ cells were trafficking in the infected humanized mice, are also the sites where inflammatory monocyte recruitment is necessary to control the early stages of infection with *Listeria monocytogenes,* also a gram-positive bacterium. (Rosen et al. 1989; Serbina et al. 2003; Swirski et al. 2009; Shi et al. 2010; Shi & Pamer 2011).

Granulocytes

Granulocytes, mostly comprised of neutrophils, are also referred to as the first line of defense, since they are the first leukocytes recruited to the site of infection to kill bacteria (Yoshio et al. 2004). Chemotaxis, movement speed and bactericidal activity are decreased in neonatal neutrophils (Anderson et al. 1991; Wolnach et al. 1998). Studies in rats and circumstantial evidence from human neonates suggest that the neutrophil storage pool in the BM of neonates is not only smaller, but also that granulopoiesis during infection is reduced, leading to a rapid exhaustion of the storage pool compared to adult individuals (Christensen et al. 1982; Christensen 1989; Carr & Modi 1997).

The $CD66^+$ granulocyte count in uninfected humanized mice was rather low ($6x10^5$/femur) compared to neonatal rats (>$1x10^7$/femur) or human adults (estimated total of $6x10^{11}$). Also in the pb the population is quite small with <1% in humanized mice compared to 50-70% in humans (Mestas & Hughes 2004). In contrast to $CD33^+$ cells, the duration of infection had a marked effect on the granulocyte populations in humanized mice. During the infection, the granulocyte population increased up to 255% (compared to uninfected animals) on day 3 (Fig. 11), which was most likely caused by increased granulopoiesis due to the GBS infection. A similar effect can also be observed in human adults where granulocyte production is increased by more than 300% during sepsis (Carr & Modi 1997). It is known from animal models of GBS infection that the number of granulocytes significantly increases in the BM as well as the pb (Christensen et al. 1982; Furze & Rankin 2008). While granulocyte numbers increased in the BM of infected humanized mice, a marked increase in the pb or in other organs was not detected on day 1, 3 and 7. On one hand, this could mean that the increase in the pb occurred at a time-point which was not analyzed since there is only a certain timeframe where granulocytes are elevated in the pb in the animal model. The other option is that the cytokines and chemokines needed for the neutrophil release from the BM were not present in the necessary concentrations or that the neutrophils themselves feature deficiencies which keep them from exiting the BM. These defects, in combination with the low numbers of granulocytes in the BM also explain the low amount of circulating granulocytes in the pb.

Cytokine profile in infected animals

Cytokines are small immunomodulatory proteins and peptides, produced by a variety of cells. They play essential roles in host defense, wound healing and have several other functions. While cytokines are important for homeostasis, excessive production and systemic release result in systemic inflammation and organ dysfunction, causing sepsis. In high dose infected humanized mice, high levels of the cytokines TNF, IFNγ, IL-1β, IL-6, IL-8 and IL-10 were detected after 1 day, which matched or even exceeded the maximum concentration in the serum of adult humans with severe sepsis. Compared to septic neonates, the cytokine levels of TNF, IL-1β, IL-6 and IL-8 in high dose infected animals exceeded mean or maximum human levels by far (Kurt et al. 2007; Lvovschi et al. 2011). This indicates that the high dose infected humanized mice indeed developed GBS sepsis on day 1. While the moderate dose infected animals did not display excessive cytokine production, the serum levels of IL-1β, IL-10 and IL-8 were still within range of septic adults (Lvovschi et al. 2011). The connection between the cytokines TNF, IL-1β, IL-6 and IL-8 and sepsis is very pronounced. TNF can cause organ dysfunction and induce systemic inflammatory response syndrome (SIRS) when injected into human subjects (Chapman et al. 1987). Injection of IL-1β also induces SIRS symptoms (Blackwell & Christman 1996). IL-6 has been indicated as a good prognostic marker for organ dysfunction and death in septic humans, although the exact role in sepsis is still unclear due to varying results in animal studies. High levels of IL-8 can lead to tissue injury by activated neutrophils and therefore indicate increased mortality in sepsis. IL-10 is an anti-inflammatory cytokine which is elevated in patients with septic shock (Creasey et al. 1991; Blackwell & Chrisman 1996; Remick et al. 2005).

The second part of my thesis shows that human neonatal immune cells and their counterparts in humanized mice share various deficiencies, which indicates that their immune system, as well as the responses of their immune system, are most likely comparable. Based on serum cytokine levels, the high dose infection model is a well suited GBS sepsis model, reflecting the situation in septic human adults and neonates. While the moderate dose infection model only partially resembles the situation in humans suffering from severe sepsis, this model allows the analysis of longer term effects of GBS infection on the human immune system. These findings indicate that the humanized mouse is a useful tool for investigating new therapies,

test the effect of new therapeutic agents as well as optimizing already existing therapies for human neonatal GBS infections.

4.3 EFFECTS OF TREATMENT ON AN ONGOING GBS INFECTION IN HUMANIZED MICE

In the third part of my thesis this new animal model was used to determine the effect of the two drugs Betamethasone and Indomethacin on a naïve human (neonatal) immune system during an ongoing GBS infection.

4.3.1 EFFECTS OF BETAMETHASONE TREATMENT

Corticosteroids are divided in glucocorticoids and mineralocorticoids which bind to glucocorticoid receptors and mineralocorticoid receptors to exert their effects in cells (Rickard & Young 2009). Glucocorticoids are among the most prescribed drugs worldwide, and known for their pronounced anti-inflammatory effects, which are caused by increasing the expression of anti-inflammatory proteins, inhibition of proinflammatory gene activation and induction of apoptosis in thymocytes, lymphocytes and also monocytes (Necela & Cidlowski 2004; Busillo et al. 2011).

However, after 1 day of infection Betamethasone treatment reduced the systemic bacterial burden and also the CFU count in the peritoneum (Fig. 17). This effect might be explained by increased clearance due to the slightly higher number of granulocytes, (Fig. 20). While glucocorticoids exert immunosuppressive effects especially on cellular immune responses, these drugs also have the ability to boost the innate immune system. Glucocorticoids have been shown to increase granulopoiesis and inhibit neutrophil apoptosis, leading to increased numbers of circulating granulocytes. They also can enhance phagocytic and bactericidal activity in macrophages, which might have been a contributing factor here. (Inada et al. 1988; Meagher et al. 1996; van der Goes et al. 2000; Schleimer 2004).

After 1 day of high dose infection Betamethasone treatment did only induce slight reductions in TNF, IFNγ and IL-6 levels of the analyzed cytokines (Fig. 27). Based on the literature, glucocorticoid treatment should have reduced the serum

concentrations of all analyzed cytokines (IFNγ, TNF, IL-1β, IL-6, IL-8 and IL-10) (Brattsand & Linden 1996; Wiegers & Reul 1998). However, what most studies do not take into account is the fact that there are several pitfalls concerning the effect of glucocorticoids on immune responses. First of all, a variety of *in vitro* studies used corticosteroid concentrations that are unobtainable *in vivo*, at least not for a significant amount of time. Furthermore, most *in vivo* studies were conducted using mice, rats and rabbits, which are all corticosteroid-sensitive species where the effects of treatment are more pronounced than in corticosteroid-resistant species which include humans (Parrillo & Fauci 1979). This example illustrates the usefulness of the humanized mouse as an *in vivo* model, since here the effect of treatment varies between conventional animal models and humans. Two and also 3 days after moderate dose infection, administration of Betamethasone had no pronounced effect on cytokine production. It is interesting though, that in both Betamethasone and Indomethacin treated animals IL-6 levels were elevated (not significantly) probably due to the presence of higher amounts of GBS. As described above, (4.2.3) IL-6 is the only cytokine considered a reliable prognostic marker for sepsis since its serum level correlates well not only with severity of bacterial infection but also with mortality in human patients (Damas et al. 1992). This effect, coupled with the significantly increased systemic CFU count in glucocorticoid treated animals indicates that administration of Betamethasone increases the severity of GBS infection and should therefore be combined with antibiotic treatment in the clinic to reduce the bacterial burden in the infant.

Glucocorticoids are known for their inhibition of lymphocyte proliferation and induction of apoptosis. The major mechanism is inhibition of the production of IL-2, which stimulates the proliferation of T and B cells (Mingari et al. 1984; Horst & Flad 1987; Auphan et al. 1995). The inhibition of IL-2 production by Betamethasone could play a role in the significant reduction of B and T cells in the spleen of humanized mice, after 3 days of infection (Fig. 21). This explanation accounts for the changes in the B cell population, since infection induced a significant increase of this cell type in the spleen after 3 days (Fig. 11). However, T cells were not elevated due to infection, implicating a lack of proliferation. The reduction in T cells in the spleen after Betamethasone treatment might be due to apoptosis, since glucocorticoids are also known for inducing cell death in immature T cell precursors and mature T cells (Sapolsky et al. 2000). The increase in B cells in the BM of Betamethasone-treated animals cannot be explained by a direct effect of glucocorticoids. A possible explanation is the migration of B cells from the spleen into the BM, however it is more

likely that this effect was cause by increased B cell hematopoiesis in the BM induced by higher amounts of bacterial products due to the increased GBS titers in Betamethasone-treated animals (Fig. 17). Monocytes significantly decreased in the BM due to Betamethasone treatment, 3 days post infection (Fig. 21). An explanation could be the apoptosis inducing effect of glucocorticoids on monocytes (Necela & Cidlowski 2004). The reduction in monocytes is probably one of the main reasons why treatment with Betamethasone resulted in systemically elevated GBS counts 3 days post infection (Fig. 17). Another interesting finding after glucocorticoid treatment was the presence of GBS in the brain after 3 days in 3/10 animals, which was absent in untreated controls (Fig. 18). While this effect is not significant, it indicates that glucocorticoid administration increases the likelihood of GBS entering the brain which in turn increases the risk of brain damage.

The Betamethasone-induced changes in leukocyte subpopulations were far less pronounced after 7 days compared to 3 days of infection. The reason was most probably the absence of considerable glucocorticoid levels in the circulation. Betamethasone has a plasma half-life of 6.5 – 9 h and a biological half live (duration of measurable biological activity) of 36 – 54 h (Tegethoff et al. 2009). Therefore, both after day 1 and 3 of infection, relevant glucocorticoid levels should have been present systemically leading to the above mentioned effects. With declining serum levels and waning biological activity of Betamethasone, the immune system of infected humanized mice was most likely able to cope with the infection, resulting in similar CFU counts and immune cell populations after 7 days in treated and untreated animals.

4.3.2 Effects of Indomethacin treatment

Indomethacin is a nonsteroidal anti-inflammatory drug (NSAID) and often used to reduce fever, pain, stiffness and swelling. It is called a "short-acting" NSAID because of the relatively short plasma half-life (5-10h) in adult humans, which is prolonged in neonates (11–36h) (Brash et al. 1981; Helleberg 1981). By inhibiting PG (especially PGE_2) production, Indomethacin affects both cellular and humoral immune responses and inflammation. Similar to glucocorticoid treatment, Indomethacin had no pronounced effects on cytokine production after 1 day of high dose GBS infection. However, not only did it induce a slight increase in IL-6 (not significant), it also led to an increase in IL-8 both after day 2 and 3 in the moderate dose infection model. This

specific chemokine not only attracts neutrophils, it also augments their bactericidal activity by inducing respiratory burst and ROS production among other functions. Neutrophils can cause oxidative tissue damage when eliminating pathogens and several studies have shown that the number of neutrophils correlates with vascular damage and tissue damage leading to decreased organ function and even organ failure (Partrick et al. 1996; Mukaida et al. 1998; Brown et al. 2006). Although Indomethacin increased IL-8 levels in infected humanized mice, this effect did not lead to an increase of neutrophils in the pb or other organs (Fig. 21). As discussed above (4.2.3), this most likely stems from a lack of species specific factors, needed for the emigration from the BM, and/or deficient granulocytes in the humanized mouse model. However, this finding indicates that in GBS infected neonates, where emigration of neutrophils from the BM is unimpaired, an increase in IL-8 induced by Indomethacin could lead to elevated numbers of neutrophils in the pb and organs which in turn might cause, or increase organ damage.

Indomethacin induced a reduction in T as well as B cells in the spleen 3 days after infection (Fig. 21). The decrease in B cells can be explained by the ability of Indomethacin to reduce B cell proliferation (Rojo et al. 1981). Due to the fact that in untreated animals proliferation most likely caused the increase in B cell numbers in the spleen 3 days post infection (Fig. 11), Indomethacin–induced abrogation of proliferation explains the observed reduction in B cell numbers. Since T cells did not increase in the spleen of untreated animals, inhibition of proliferation by Indomethacin does not explain the decrease in treated animals. However studies have shown that Indomethacin does induce the expression of Nur77, which induces T cell apoptosis (Kang et al. 2000; Tao & Hancock 2008), explaining the reduction in splenic T cells.

Other changes in leukocyte subpopulations (B cells and myeloid cells) as well as the increase in systemic CFU count after 3 days of infection were present only by tendency after treatment with Indomethacin but correlate well with the findings in the glucocorticoid treatment group. Similar to Betamethasone, administration of Indomethacin resulted in the presence of live GBS in the brain of some (2/10) animals (Fig 18). In regard to these findings, Indomethacin treatment should also be combined with antibiotics to reduce the bacterial burden in the infants and also reduce the risk of brain damage.

After 7 days of moderate dose infection, no major changes due to Indomethacin treatment were detected. This most likely stems from the short half-live of

Indomethacin, which in turn led to low circulating concentrations, and therefore no major effect of this drug 5 days after the last injection.

In summary, both drugs affect the human immune system and disease progression in GBS infected humanized mice. While administration of Betamethasone initially decreases the systemic CFU count, glucocorticoid treatment causes adverse effects during prolonged GBS infection. After 3 days, Betamethasone leads to a reduction in lymphocytes and myeloid cells, which is accompanied by a systemic increase in CFU. At this time point, Indomethacin also causes a decrease in lymphocytes, which is also combined with an increased bacterial burden. Due to relatively short plasma half-lives, both drugs do not exert major long term effects on human immune cell populations and leukocyte function (7 days post infection). Based on the fact that both Betamethasone and Indomethacin treatment increase the bacterial burden and also seem to facilitate the infiltration of GBS into the brain, both drugs should be combined with antibiotics to reduce the amount of bacteria, which in turn should reduce or might even prevent organ damage, especially brain involvement.

4.4 EFFECTS OF TREATMENT ON HUMAN CORD BLOOD DERIVED MNC *IN VITRO*

In the last part of my thesis I performed *in vitro* experiments using neonatal (cord blood derived) MNC and analyzed the effect of Betamethasone and Indomethacin on human leukocytes with and without the presence of live GBS as well as the effect of treatment on GBS alone. In the following paragraph these findings are compared with the results obtained from the *in vivo* studies on infected and treated humanized mice. This is done to determine if leukocytes from neonatal humans (cord blood) and immune cells in humanized mice behave similarly when challenged with GBS and treated with either drug.

None of the findings *in vitro* were significant, and are therefore only discussed briefly. Since both Betamethasone and Indomethacin affected the CFU count in humanized mice, it was important to determine if this was caused by an effect of both drugs on leukocytes which then altered bacterial clearance or if it was a direct effect of treatment on the growth of GBS. Since neither drug showed a marked impact on

bacterial growth (Fig. 28) it is safe to assume that the effect on the CFU count *in vivo* stems from effects that both drugs exert on immune cells.

In vitro Betamethasone and Indomethacin treatment resulted in reduced bacterial clearance by the human MNC after prolonged cultivation (2 days), which was also observed *in vivo* (3 days). Interestingly enough, the positive effect of glucocorticoids on bacterial clearance which was observed *in vivo* after 24 h of infection was not present *in vitro*. This probably stems from the fact that certain glucocorticoid-mediated effects, like the enhancement of granulocyte efflux from the bone marrow, only play a role *in vivo*.

The effects of treatment during infection (presence of GBS) on leukocyte subsets observed *in vivo* were either less pronounced *in vitro* or absent altogether. However, this is not necessarily an indicator that the humanized mouse is a less-than-ideal model for the neonatal immune system. In fact, it much more implies that the complex mechanisms, involved in the immune response and the effects of treatment on those processes, cannot be sufficiently studied *in vitro*. Hematopoiesis, release of leukocytes (mainly granulocytes and monocytes) from storage pools, leukocyte trafficking and proliferation, but also dissemination of bacteria in the body, plasma clearance of drugs, those are all examples why an animal model is vital to study infectious diseases and the effect or efficacy of treatment.

5 SUMMARY & OUTLOOK

In this thesis I generated a novel animal model for GBS infection using humanized mice and investigated the effect of Betamethasone and Indomethacin on their naïve and deficient human immune system, which resembles that of human neonates quite well. The results not only showed that both drugs induced changes in B, T and myeloid cell populations, treatment also led to an increased bacterial burden. This increase in CFU enhances the risk (or the severity) of organ damage, especially in the brain where GBS was only detected after treatment. These findings suggest, that when Betamethasone or Indomethacin are used in perinatal care and a bacterial infection is present, they should be given in combination with antibiotics due to the adverse effects of both drugs on bacterial clearance.

This new GBS infection model allows for the investigation of the effects of other drugs and treatment options on various parameters (e.g. bacterial clearance and immune cell trafficking) in a naïve and neonatal-like human immune system. To further improve the animal model, the use of a more aggressive, clinically relevant GBS strain should be taken into consideration. This should enable the investigation of treatment on organ damage which was not present in my infection model, most likely due to the use of a less aggressive GBS reference strain.

REFERENCES

Abbas AK; Lichtman AH; Pillai S. 2007. Cellular and molecular immunology 6th edition. 3-537.

Aderem A, Ulevitch RJ. 2000. Toll-like receptors in the induction of the innate immune response. Nature **406**:782-7.

Aderem A. 2003. Phagocytosis and the inflammatory response. J Infect Dis **187**:S340-S345.

Adinstruments. Accessed 29. Aug 2012. www.adinstruments.com/solutions/research/Mouse-Applications/

Adkins B, Bu Y, Vincek V, Guevara P. 2003. The primary responses of murine neonatal lymph node CD4+ cells are Th2-skewed and are sufficient for the development of Th2-biased memory. Clin Dev Immunol **10**:43-51.

Adkins B, Leclerc C, Marshall-Clarke S. 2004. Neonatal adaptive immunity comes of age. Nature Reviews Immunology **4**:553-564.

Adkins B. 1999. T-cell function in newborn mice and humans. Immunol Today **20**:330-5.

Agliano A, Martin-Padura I, Mancuso P, Marighetti P, Rabascio C, et al. 2008. Human acute leukemia cells injected in NOD/LtSz-scid/IL-2Rgamma null mice generate a faster and more efficient disease compared to other NOD/scid-related strains. Int J Cancer **123**:2222-7.

Akima S, Kent A, Graham JR, Gallagher M, Falk MC. 2004. Indomethacin and renal impairment in neonates. Pediatr Nephrol **19**:490-493.

Akkina RK, Rosenblatt JD, Campbell AG, Chen IS, Zack JA. 1994. Modeling human lymphoid precursor cell gene therapy in the SCID-hu mouse. Blood **84**:1393-1398.

Alexander JJ, Quigg RJ. 2007. The simple design of complement factor H: Looks can be deceiving. Mol Immunol **44**:123-32.

Al-Tahan A, Sarkis O, Harajly M, Baghdadi OK, Zibara K, et al. 2012. Retinoic acid fails to induce cell cycle arrest with myogenic differentiation in rhabdomyosarcoma. Pediatr Blood Cancer **58**:877-84.

Anderson DC, Abbassi O, Kishimoto TK, Koenig JM, McIntire LV, Smith CW. 1991. Diminished lectin-, epidermal growth factor-, complement binding domain-cell adhesion molecule-1 on neonatal neutrophils underlies their impaired CD18-independent adhesion to endothelial cells in vitro. J Immunol **146**:3372-3379.

Anderson DC, Hughes BJ, Smith CW. 1981. Abnormal mobility of neonatal polymorphonuclear leukocytes. Relationship to impaired redistribution of surface adhesion sites by chemotactic factor or colchicine. J. Clin. Investig **68**:863-874.

Andre MC, Erbacher A, Gille C, Schmauke V, Goecke B, et al. 2010. Long-term human CD34+ stem cell-engrafted nonobese diabetic/SCID/IL-2R gamma(null) mice show impaired CD8+ T cell maintenance and a functional arrest of immature NK cells. J Immunol **185**:2710-20.

Anthony BF, Okada DM. 1977. The emergence of group B streptococci in infections of the newborn infant. Annu Rev Med **28**:355-69.

Appelbaum FR, Rowe JM, Radich J, Dick JE. 2001. Acute myeloid leukemia. Hematology Am Soc Hematol Educ Program **2001**:62-86.

Areschoug T, Stalhammar-Carlemalm M, Karlsson I, Lindahl G. 2002. Streptococcal beta protein has separate binding sites for human factor H and IgA-Fc. J Biol Chem **277**:12642-12648.

Arulanandam BP, Van Cleave VH, Metzger DW. 1999. IL-12 is a potent neonatal vaccine adjuvant. Eur J Immunol **29**:256–64.

Auphan N, DiDonato JA, Rosette C, Helmberg A, Karin M. 1995. Immunosuppression by glucocorticoids: inhibition of NF-kappa B activity through induction of I kappa B synthesis. Science **270**:286-90.

Baker CJ, Kasper DL. 1976. Correlation of maternal antibody deficiency with susceptibility to neonatal group B streptococcal infection. N Engl J Med **294**:753-756.

Ballen KK, Valinski H, Greiner D, Shultz LD, Becker PS, et al. 2001. Variables to predict engraftment of umbilical cord blood into immunodeficient mice: usefulness of the non-obese diabetic--severe combined immunodeficient assay. Br J Haematol **114**:211-8.

Banchereau J, Steinman RM. 1998. Dendritic cells and the control of immunity. Nature **392**:245-52.

Bankert RB, Balu-Iyer SV, Odunsi K, Shultz LD, Kelleher RJ Jr, et al. 2011. Humanized mouse model of ovarian cancer recapitulates patient solid tumor progression, ascites formation, and metastasis. PLoS One **6**:e24420.

Baron MJ, Bolduc GR, Goldberg MB, Aupérin TC, Madoff LC. 2004. Alpha C protein of group B Streptococcus binds host cell surface glycosaminoglycan and enters cells by an actin-dependent mechanism. J Biol Chem **279**:24714–24723.

Battaglia A, Ferrandina G, Buzzonetti A, Malinconico P, Legge F, et al. 2003. Lymphocyte populations in human lymph nodes. Alterations in CD4+ CD25+ T regulatory cell phenotype and T-cell receptor Vbeta repertoire. Immunology **110**:304-12.

Baud O, Foix-L'Helias L, Kaminski M, Audibert F, Jarreau PH, et al. 1999. Antenatal glucocorticoid treatment and cystic periventricular leukomalacia in very premature infants. N Engl J Med **341**:1190-6.

Bauer K, Zemlin M, Hummel M, Pfeiffer S, Karstaedt J, et al. 2002. Diversification of Ig heavy chain genes in human preterm neonates prematurely exposed to environmental antigens. J Immunol **169**:1349-1356.

Baxter AG, Cooke A. 1993. Complement lytic activity has no role in the pathogenesis of autoimmune diabetes in NOD mice. Diabetes **42**:1574-8.

Beagley KW, Eldridge JH, Kiyono H, Everson MP, Koopman WJ, et al. 1988. Recombinant murine IL-5 induces high rate IgA synthesis in cycling IgA-positive Peyer's patch B cells. J Immunol **141**:2035-42.

Bente DA, Melkus MW, Garcia JV, Rico-Hesse R. 2005. Dengue fever in humanized NOD/SCID mice. J Virol **79**:13797-9.

Berman PH, Banker BQ. 1966. Neonatal meningitis. A clinical and pathological study of 29 cases. Pediatrics **38**:6–24.

Berner R, Niemeyer CM, Leititis JU, Funke A, Schwab C, et al. 1998. Plasma levels and gene expression of granulocyte colony-stimulating factor, tumor necrosis factor-alpha, interleukin (IL)-1beta, IL-6, IL-8, and soluble intercellular adhesion molecule-1 in neonatal early onset sepsis. Pediatr Res **44**:469-477.

Berner R. 2005. Molekulare Mechanismen der neonatalen Abwehr von bakteriellen Infektionen. Molekulare Medizin **5**:477-505

Biolegend. Accessed 29. Aug 2012. http://www.biolegend.com/stemcell

Blackwell TS, Christman JW. 1996. Sepsis and cytokines: current status. Br J Anaesth **77**:110-7.

Bock TA, Orlic D, Dunbar CE, Broxmeyer HE, Bodine DM. 1995. Improved engraftment of human hematopoietic cells in severe combined immunodeficient (SCID) mice carrying human cytokine transgenes. J Exp Med **182**:2037-2043.

Bockstal V, Guirnalda P, Caljon G, Goenka R, Telfer JC, et al. 2011. T. brucei infection reduces B lymphopoiesis in bone marrow and truncates compensatory splenic lymphopoiesis through transitional B-cell apoptosis. PLoS Pathog **7**:e1002089. Epub.

Bolduc GR, Madoff LC. 2007. The Group B Streptococcal α C protein binds α1β1-integrin through a novel KTD motif that promotes internalization of GBS within human epithelial cells. Microbiology **153**:4039–4049.

Bosma GC, Fried M, Custer RP, Carroll A, Gibson DM, Bosma MJ. 1988. Evidence of functional lymphocytes in some (leaky) scid mice. J Exp Med **167**:1016-1033.

Brash AR, Hickey DE, Graham TP, Stahlman MT, Oates JA, Cotton RB. 1981. Pharmacokinetics of indomethacin in the neonate. Relation of plasma indomethacin levels to response of the ductus arteriosus. N Engl J Med **305**:67-72.

Brattsand R, Linden M. 1996. Cytokine modulation by glucocorticoids: mechanisms and actions in cellular studies. Aliment Pharmacol Ther **10**:81-90.

Brown CK, Gu ZY, Matsuka YV, Purushothaman SS, Winter LA, et al. 2005. Structure of the streptococcal cell wall C5a peptidase. Proc Natl Acad Sci USA **102**:18391–18396.

Brown KA, Brain SD, Pearson JD, Edgeworth JD, Lewis SM, Treacher DF. 2006. Neutrophils in development of multiple organ failure in sepsis. Lancet **368**:157-69.

Bryan JD, Shelver DW. 2009. Streptococcus agalactiae CspA is a serine protease that inactivates chemokines. J Bacteriol **191**:1847-54.

Busillo JM, Azzam KM, Cidlowski JA. 2011. Glucocorticoids sensitize the innate immune system through regulation of the NLRP3 inflammasome. J Biol Chem **286**:38703-13.

Cain D, Kondo M, Chen H, Kelsoe G. 2009. Effects of acute and chronic inflammation on B-cell development and differentiation. J Invest Dermatol **129**:266-77.

Cairo MS. 1989. Neonatal Neutrophil Host Defense: Prospects for Immunologic Enhancement During Neonatal Sepsis. Am J Dis Child **143**:40-46.

Caliot E, Dramsi S, Chapot-Chartier MP, Courtin P, Kulakauskas S, et al. 2012. Role of the Group B Antigen of Streptococcus agalactiae: A Peptidoglycan-Anchored Polysaccharide Involved in Cell Wall Biogenesis. PLoS Pathog **8**:e1002756. Epub.

Campell JR; Hillier SL; Krohn MA; Ferrieri P; Zaleznik DF; Baker CJ. 2000. Group B Streptococcal colonization and serotype-specific immunity in pregnant women at delivery. Obstet Gynecol **96**:498-503

Caretto P, Forni M, d'Orazi G, Scarpa S, Feraiorni P, et al. 1989. Xenotransplantation in immunosuppressed nude mice of human solid tumors and acute leukemias directly from patients or in vitro cell lines. Ric Clin Lab **19**:231-43.

Carr R, Huizinga TW. 2000. Low soluble FcRIII receptor demonstrates reduced neutrophil reserves in preterm neonates. Arch Dis Child **83**:F160.

Carr R, Modi N. 1997. Haemopoietic colony stimulating factors for preterm neonates. Arch Dis Child Fetal Neonatal Ed **76**:F128–F133.

Carr R, Pumford D, Davies JM. 1992. Neutrophil chemotaxis and adhesion in preterm babies. Arch Dis Child **67**:813-817.

Carr, R. 2000. Neutrophil production and function in newborn infants. Br J Haematol **110**:18-28.

Carreno BM, Garbow JR, Kolar GR, Jackson EN, Engelbach JA, et al. 2009. Immunodeficient mouse strains display marked variability in growth of human melanoma lung metastases. Clin Cancer Res **15**:3277-3286.

Cha S, Peck AB, Humphreys-Beher MG. 2002. Progress in understanding autoimmune exocrinopathy using the non-obese diabetic mouse: an update. Crit Rev Oral Biol Med **13**:5-16.

Chalmers IM, Janossy G, Contreras M, Navarrete C. 1998. Intracellular cytokine profile of cord and adult blood lymphocytes. Blood **92**: 11–18.

Chapman PB, Lester TJ, Casper ES, Gabrilove JL, Wong GY, et al. 1987. Clinical pharmacology of recombinant human tumor necrosis factor in patients with advanced cancer. J Clin Oncol **5**:1942-51.

Charland N, Kobisch M, Martineau-Doizé B, Jacques M, Gottschalk M. 1996. Role of capsular sialic acid in virulence and resistance to phagocytosis of Streptococcus suis capsular type 2. FEMS Immunol Med Microbiol **14**:195-203.

Charles River. Accessed 29. Aug 2012.
www.criver.com/SiteCollectionDocuments/NMRI%20nude24.04.07.pdf

Chelvarajan RL, Collins SM, Doubinskaia IE, Goes S, Van Willigen J, et al. 2004. Defective macrophage function in neonates and its impact on unresponsiveness of neonates to polysaccharide antigens. J Leukoc Biol **75**:982-94.

Chelvarajan RL, Gilbert NL, Bondada S. 1998. Neonatal murine B lymphocytes respond to polysaccharide antigens in the presence of interleukins-1 and -6. J Immunol **161**:3315–3324.

Cheng Q, Stafslien D, Purushothaman SS, Cleary P. 2002. The group B streptococcal C5a peptidase is both a specific protease and an invasin. Infect Immun **70**:2408–2413.

Chirico G. 2005. Development of the Immune System in Neonates. J Arab Neonatal Forum **2**: 5–11.

Christensen RD, Harper TE, Rothstein G. 1986. Granulocyte-macrophage progenitor cells in term and preterm neonates. J Pediatr **109**:1047-51.

Christensen RD, MacFarlane JL, Taylor NL, Hill HR, Rothstein G. 1982. Blood and marrow neutrophils during experimental group B streptococcal infection: quantification of the stem cell, proliferative, storage and circulating pools. Pediatr Res **16**:549-53.

Christensen RD. Neutrophil kinetics in the fetus and neonate. 1989. Am J Pediatr Hematol Oncol **11**:215-23.

Christianson SW, Greiner DL, Hesselton RA, Leif JH, Wagar EJ, et al. 1997. Enhanced human CD4+ T cell engraftment in beta2-microtubulin-deficient NOD-*scid* mice. J Immunol **158**:3578-3586.

Cornacchione P, Scaringi L, Fettucciari K, Rosati E, Sabatini R, et al. 1998. Group B streptococci persist inside macrophages. Immunology **93**:86-95.

Covassin L, Laning J, Abdi R, Langevin DL, Phillips NE, et al. 2011. Human peripheral blood CD4 T cell-engrafted non-obese diabetic-scid IL2rγ(null) H2-Ab1 (tm1Gru) Tg (human leucocyte antigen D-related 4) mice: a mouse model of human allogeneic graft-versus-host disease. Clin Exp Immunol **166**:269-80.

Cowgill K, Taylor TH Jr, Schuchat A, Schrag S. 2003. Report from the CDC. Awareness of perinatal group B streptococcal infection among women of childbearing age in the United States, 1999 and 2002. J Womens Health **12**:527-32.

Creasey AA, Stevens P, Kenney J, Allison AC, Warren K, et al. 1991. Endotoxin and cytokine profile in plasma of baboons challenged with lethal and sublethal Escherichia coli. Circ Shock **33**:84-91.

Crowley P. 2000. Prophylactic corticosteroids for preterm birth. Cochrane Database Syst Rev CD000065.

Cuzzola M, Mancuso G, Beninati C, Biondo C, Genovese F, et al. 2000. Beta 2 integrins are involved in cytokine responses to whole gram-positive bacteria. J. Immunol. **164**:5871-5876.

Damas P, Ledoux D, Nys M, Vrindts Y, De Groote D, et al. 1992. Cytokine serum level during severe sepsis in human IL-6 as a marker of severity. Ann Surg **215**:356-62.

D'Arena G, Musto P, Cascavilla N, Minervini MM, Di Giorgio G, et al. 1999. Inability of activated cord blood T lymphocytes to perform Th1-like and Th2-like responses: implications for transplantation. J Hematother Stem Cell **8**:381-385.

DeHeus R. 2008. Maternal and Fetal effects of Tocolytic Drugs. Dissertation. ISBN 978-90-3934833-8.

DiGiusto DL, Lee R, Moon J, Moss K, O'Toole T, et al. 1996. Hematopoietic potential of cryopreserved and ex vivo manipulated umbilical cord blood progenitor cells evaluated in vitro and in vivo. Blood **87**:1261-1271.

Dittel BN, LeBien TW. 1995. The growth response to IL-7 during normal human B cell ontogeny is restricted to B-lineage cells expressing CD34. J. Immunol. **154**: 58–67.

Doran KS, Chang JC, Benoit VM, Eckmann L, Nizet V. 2002. Group B streptococcal β-hemolysin/cytolysin promotes invasion of human lung epithelial cells and the release of interleukin-8. J Infect Dis **185**:196–203.

Dramsi S, Caliot E, Bonne I, Guadagnini S, Prévost MC, et al. 2006. Assembly and role of pili in group B streptococci. Mol Microbiol **60**:1401–1413.

Dubrovsky L, Duyne RV, Senina S, Guendel I, Pushkarsky T, et al. 2012. Liver X receptor agonist inhibits HIV-1 replication and prevents HIV-induced reduction of plasma HDL in humanized mouse model of HIV infection. Biochem Biophys Res Commun **419**:95-8.

Dziarski R. 1982. Studies on the mechanism of peptidoglycan- and lipopolysaccharide-induced polyclonal activation. Infect Immun **35**:507-14.

Edwards MS, Kasper DL, Jennings HJ, Baker CJ, Nicholson-Weller A. 1982. Capsular sialic acid prevents activation of the alternative complement pathway by type III, group B streptococci. J Immunol **128**:1278-83.

El Kassar N, Lucas PJ, Klug DB, Zamisch M, Merchant M, et al. 2004. A dose effect of IL-7 on thymocyte development. Blood **104**: 1419–1427.

Elkon KB, Ashany D. 1993. The SCID mouse as a vehicle to study autoimmunity. Br J Rheumatol **32**:4-12.

Environmental Health Services. Accessed 29. Aug 2012. http://ehspest.com/_blog/RI,_MA_EHS_Pest_Control_Blog/post/Baby_Mice_in_a_Bag_of_Potato_CChip_Surprise_Customer/

Erkeller-Yuksel FM, Deneys V, Yuksel B, Hannet I, Hulstaert F, et al. 1992. Age-related changes in human blood lymphocyte subpopulations. J Pediatr **120**:216-22.

Fettucciari K, Quotadamo F, Noce R, Palumbo C, Modesti A, et al. 2011. Group B Streptococcus (GBS) disrupts by calpain activation the actin and microtubule cytoskeleton of macrophages. Cell Microbiol **13**:859-84.

Fogh J, Giovanella BC. 1978. The Nude Mouse in Experimental and Clinical Research. Academic Press 502.

Fraser CC, Kaneshima H, Hansteen G, Kilpatrick M, Hoffman R, Chen BP. 1995. Human allogeneic stem cell maintenance and differentiation in a longterm multilineage SCID-hu graft. Blood **86**:1680-1693.

Fry RM. 1938. Fatal infections by haemolytic streptococcus group B. Lancet i:199-201.

Furze RC, Rankin SM. 2008. Neutrophil mobilization and clearance in the bone marrow. Immunology **125**:281-8.

Galask RP; Varner MW; Petzold CR; Wilbur SL. 1984. Bacterial attachment to the chorioamnionic membranes. Am J Obstet Gynecol **148**:915-28.

Gallo RL, Nizet V. 2003. Endogenous production of antimicrobial peptides in innate immunity and human disease. Curr Allergy Asthma Rep **3**:402–409.

Gan OI, Murdoch B, Larochelle A, Dick JE. 1997. Differential maintenance of primitive human SCID-repopulating cells, clonogenic progenitors, and long-term culture-initiating cells after incubation on human bone marrow stromal cells. Blood **90**:641-650.

Garnick DJ, Sarnwick RD, Shahidi NT, Manning DD. 1980. Inability of intravenously injected mononuclear suspensions of human bone marrow to establish in the nude mouse. Int Arch Allergy Appl Immunol **62**:330-333.

Gasparoni A, Ciardelli L, Avanzini A, Castellazzi AM, Carini R, et al. 2003. Age-related changes in intracellular TH1/TH2 cytokine production, immunoproliferative T lymphocyte response and natural killer cell activity in newborns, children and adults. Biol Neonate **84**:297-303.

Gibson RL, Nizet V, Rubens CE. 1999. Group B streptococcal β-hemolysin promotes injury of lung microvascular endothelial cells. Pediatr Res **45**:626–634.

Giles W, Bisits A. 2007. Preterm labour. The present and future of tocolysis. Best Pract Res Clin Obstet Gynaecol **21**:857-68.

Gille C, Orlikowsky TW, Spring B, Hartwig UF, Wilhelm A, et al. 2012. Monocytes derived from humanized neonatal NOD/SCID/IL2Rγ^{null} mice are phenotypically immature and exhibit functional impairments. J Hum Imm **73**:346-54.

Gladstone IM, Ehrenkranz RA, Edberg SC, Baltimore RS. 1990. A ten-year review of neonatal sepsis and comparison with the previous fifty-year experience. Pediatr Infect Dis J **9**:819-25.

Goldenberg RL. 2002. The management of preterm labor. Obstet Gynecol **100**:1020-37.

Goodwin JS, Ceuppens J. 1983. Regulation of the immune response by prostaglandins. J Clin Immunol **3**:295-315.

Goodwin JS, Selinger DS, Messner RP, Reed WP. 1978. Effect of indomethacin in vivo on humoral and cellular immunity in humans. Infect Immun **19**: 430–433.

Goriely S, Vincart B, Stordeur P, Vekemans J, Willems F, et al. 2001. Deficient IL-12(p35) gene expression by dendritic cells derived from neonatal monocytes. J Immunol **166**:2141-6.

Greer JP, Foerster J, Rodgers GM, Paraskevas F, Glader B, et al. 2009. Wintrobe's clinical hematology. Lippincott Wiliams&Wilkins Volume 1.

Greiner DL, Hesselton RA, Shultz LD. 1998. SCID mouse models of human stem cell engraftment. Stem Cells **16**:166-77.

Hamilton A, Popham DL, Carl DJ, Lauth X, Nizet V, Jones AL. 2006. Penicillin-binding protein 1a promotes resistance of group B streptococcus to antimicrobial peptides. Infect Immun **74**:6179–6187.

Hancock RE, Diamond G. 2000. The role of cationic antimicrobial peptides in innate host defences. Trends Microbiol **8**:402–410.

Harbeck RJ. 1998. Immunophenotyping of Bronchoalveolar Lavage Lymphocytes Clin Diagn Lab Immunol **5**:271–277.

Harris MC, Shalit M, Southwick FS. 1993. Diminished actin polymerization by neutrophils from newborn infants. Pediatr Res **33**:27-31.

Harris TO, Shelver DW, Bohnsack JF, Rubens CE. 2003. A novel streptococcal surface protease promotes virulence, resistance to opsonophagocytosis, and cleavage of human fibrinogen. J Clin Invest **111**:61–70.

Hassan J, Reen DJ. 1997. Cord blood CD4+ CD45RA+ T cells achieve a lower magnitude of activation when compared with their adult counterparts. Immunology **90**:397-401.

Heath PT, Balfour G, Weisner AM, Efstratiou A, Lamagni TL, et al. 2004. Group B streptococcal disease in UK and Irish infants younger than 90 days. Lancet **363**:292-294.

Heike Y, Ohira T, Takahashi M, Saijo N. 1995. Long-term human hematopoiesis in SCID-hu mice bearing transplanted fragments of adult bone and bone marrow cells. Blood **86**:524-530.

Helleberg L. 1981. Clinical Pharmacokinetics of indomethacin. Clin Pharmacokinet. **6**:245-58.

Henneke P, Berner R. 2006. Interaction of neonatal phagocytes with group B streptococcus: recognition and response. Infect Immun **74**: 3085-95.

Henneke P, Morath S, Uematsu S, Weichert S, Pfitzenmaier M, et al. 2005. Role of lipotechoic acid in the phagocyte response to group B streptococcus. J Immunol **174**:6449-6455.

Henneke P, Takeuchi O, van Strijp JA, Guttormsen HK, Smith JA, et al. 2001. Novel engagement of CD14 and multiple Toll-like receptors by group B streptococci. J Immunol **167**:7069-7076.

Henneke P, Takeuchi O, Malley R, Lien E, Ingalls RR, et al. 2002. Cellular activation, phagocytosis, and bactericidal activity against group B streptococcus involve parallel myeloid differentiation factor 88-dependent and independent signaling pathways. J Immunol **169**:3970-3977.

Hesselton RM, Greiner DL, Mordes JP, Rajan TV, Sullivan JL, Shultz LD. 1995. High levels of human peripheral blood mononuclear cell engraftment and enhanced susceptibility to human immunodeficiency virus type 1 infection in NOD/LtSz-scid/scid mice. J Inf Dis **172**:974-982.

Hickey MJ, Kubes P. 2009. Intravascular immunity: the host–pathogen encounter in blood vessels. Nature Reviews Immunology **9**:364-375.

Hogan CJ, Shpall EJ, McNulty O, McNiece I, Dick JE, et al. 1997. Engraftment and development of human CD34+-enriched cells from umbilical cord blood in NOD/LtSz-scid/scid mice. Blood **90**:85-96.

Holub M. 1992. Immunodeficient Rodents - The Nude Mouse. ILAR Journal 34

Hood M; Janney A; Damergon G. 1961. Beta hemolytic Streptococcus group A associated with problems of the perinatal period. Am J Obstet Gynecol **82**:809-18.

Horst HJ, Flad HD. 1987. Corticosteroid-interleukin 2 interactions: inhibition of binding of interleukin 2 to interleukin 2 receptors. Clin Exp Immunol **68**:156-61.

Hyde TB, Hilger TM, Reingold A, Farley MM, O'Brien KL, et al. 2002. Trends in incidence and antimicrobial resistance of early-onset sepsis: population-based surveillance in San Francisco and Atlanta. Pediatrics **110**:690-695.

Ikincioğullari A, Kendirli T, Doğu F, Eğin Y, Reisli I, et al. 2004. Peripheral blood lymphocyte subsets in healthy Turkish children. Turk J Pediatr. **46**:125-30.

Inada K, Ogasawara M, Suzuki M, Kirikae T, Mori KJ, Yoshida M. 1988. Enhancement of in-vitro granulopoiesis and induction of differentiation of M1 cells by a glucocorticoid-dependent factor produced from P388D1 cells. Leuk Res **12**:305-14.

Instituto de Bioquímica Clínical. Accessed 29. Aug 2012.
http://www.ibcrosario.com.ar/articulos/StreptococcusAgalactiaeEnEmbarazo.html

Ishikawa F, Yasukawa M, Lyons B, Yoshida S, Miyamoto T, et al. 2005. Development of functional human blood and immune systems in NOD/SCID/IL2 receptor {gamma} chain(null) mice. Blood **106**:1565-73.

Ito A, Ishida T, Utsunomiya A, Sato F, Mori F, et al. 2009. Defucosylated anti-CCR4 monoclonal antibody exerts potent ADCC against primary ATLL Cells mediated by autologous human immune cells in NOD/Shi-scid, IL-2Rgamma(null) mice in vivo. J Immunol **183**:4782-4791.

Ito A, Nakaya K, Sako Y, Nakao M, Ito M. 2001. NOD-scid mouse as an experimental animal model for cysticercosis. Southeast Asian J Trop Med Public Health **32**:85-9.

Ito M, Hiramatsu H, Kobayashi K, Suzue K, Kawahata M, et al. 2002. NOD/SCID/gamma(c)(null) mouse: an excellent recipient mouse model for engraftment of human cells. Blood **100**:3175-82.

Jackson Laboratories. Accessed 29. Aug 2012.
http://jaxmice.jax.org/strain/003303.html

Jamieson BD, Aldrovandi GM, Zack JA. 1996. The SCID-hu mouse: an in vivo model for HIV-1 pathogenesis and stem cell gene therapy for AIDS. Semin Immunol **8**:215-221.

Jarva H, Hellwage J, Jokiranta TS, Lehtinen MJ, Zipfel PF, Meri S. 2004. The group B streptococcal beta and pneumococcal Hic proteins are structurally related immune evasion molecules that bind the complement inhibitor factor H in an analogous fashion. J Immunol **172**:3111-8.

Jimenez-Diaz MB, Mulet T, Viera S, Gomez V, Garuti H, et al. 2009. Improved murine model of malaria using Plasmodium falciparum competent strains and non-myelodepleted NOD-scid IL2Rgammanull mice engrafted with human erythrocytes. Antimicrob Agents Chemother **53**:4533-4536.

Kamel-Reid S, Dick JE. 1988. Engraftment of immune-deficient mice with human hematopoietic stem cells. Science **242**:1706-9.

Kamel-Reid S, Letarte M, Sirard C, Doedens M, Grunberger T, et al. 1989. A model of human acute lymphoblastic leukemia in immune-deficient SCID mice. Science **246**:1597-1600.

Kang HJ, Song MJ, Choung SY, Kim SJ, Le MO. 2000. Transcriptional induction of Nur77 by indomethacin that results in apoptosis of colon cancer cells. Biol Pharm Bull **23**:815-9.

Kasper DL, Baker CJ, Baltimore RS, Crabb JH, Schiffman G, Jennings HJ. 1979. Immunodeterminant specificity of human immunity to type III group B streptococcus. J Exp Med **149**:327-339.

Kataoka S, Satoh J, Fujiya H, Toyota T, Suzuki R, et al. 1983. Immunologic aspects of the nonobese diabetic (NOD) mouse. Abnormalities of cellular immunity. Diabetes **32**:247-53.

Katsares V, Paparidis Z, ,Nikolaidou E, Karvounidou I, Ardelean KA, et al. 2009. Reference Ranges for Umbilical Cord Blood Hematological Values. LabMedicine **40**:437-439.

Kim CH. 2010. Homeostatic and pathogenic extramedullary hematopoiesis. J Blood Med **1**:13–19.

Kinnby B, Booth NA, Svensäter G. 2008. Plasminogen binding by oral streptococci from dental plaque and inflammatory lesions. Microbiology **154**:924-31.

Klein RB, Fischer TJ, Gard SE, Biberstein M, Rich KC, Stiehm ER. 1977. Decreased mononuclear and polymorphonuclear chemotaxis in human newborns, infants, and young children. Pediatrics **60**:467-472.

Kollmann TR, Kim A, Zhuang X, Hachamovitch M, Goldstein H. 1994. Reconstitution of SCID mice with human lymphoid and myeloid cells after transplantation with human fetal bone marrow without the requirement for exogenous human cytokines. Proc Natl Acad Sci USA **91**:8032-8036.

Krueger M, Nauck MS, Sang S, Hentschel R, Wieland H, Berner R. 2001. Cord blood levels of interleukin-6 and interleukin-8 for the immediate diagnosis of early-onset infection in premature infants. Biol Neonate **80**:118-123.

Kurt AN, Aygun AD, Godekmerdan A, Kurt A, Dogan Y, Yilmaz E. 2007. Serum IL-1beta, IL-6, IL-8, and TNF-alpha levels in early diagnosis and management of neonatal sepsis. Mediators Inflamm **2007**:31397.

Lancefield RC, Hare R. 1935. The serological difference of pathogenic and non-pathogenic strains of hemolytic streptococci from parturient women. J Exp Med **61**:335-49.

Landers CD, Chelvarajan RL, Bondada S. 2005. The role of B cells and accessory cells in the neonatal response to TI-2 antigens. Immunol Res **31**:25-36.

Lang S, Palmer M. 2003 Characterization of Streptococcus agalactiae CAMP factor as a pore-forming toxin. J Biol Chem **278**:38167–38173.

Langrish CL, Buddle JC, Thrasher AJ, Goldblatt D. 2002. Neonatal dendritic cells are intrinsically biased against Th-1 immune responses. Clin Exp Immunol **128**:118–123.

Lapidot T, Pflumio F, Doedens M, Murdoch B, Williams DE, Dick JE. 1992. Cytokine stimulation of multilineage hematopoiesis from immature human cells engrafted in SCID mice. Science **255**:1137-41.

Larochelle A, Vormoor J, Hanenberg H, Wang JC, Bhatia M, Lapidot T, et al. 1996. Identification of primitive human hematopoietic cells capable of repopulating NOD/SCID mouse bone marrow: implications for gene therapy. Nat Med **2**:1329-1337.

Larochelle A, Vormoor J, Lapidot T, Sher G, Furukawa T, et al. 1995. Engraftment of immune-deficient mice with primitive hematopoietic cells from beta-thalassemia and sickle cell anemia patients: implications for evaluating human gene therapy protocols. Hum Mol Genet **4**:163-172.

Larsen JW, Sever JL. 2008. Group B Streptococcus and pregnancy: a review. Am J Obstet Gynecol **198**:440-8.

Laughlin MJ. 2001. Umbilical cord blood for allogeneic transplantation in children and adults. Bone Marrow Transplant **27**:1-6.

Legrand N, Ploss A, Balling R, Becker PD, Borsotti C, et al. 2009. Humanized mice for modeling human infectious disease: challenges, progress, and outlook. Cell Host Microbe **6**:5-9.

Lepus CM, Gibson TF, Gerber SA, Kawikova I, Szczepanik M, et al. 2009. Comparison of human fetal liver, umbilical cord blood, and adult blood hematopoietic stem cell engraftment in NOD-scid/gammac-/-, Balb/c-Rag1-/-gammac-/-, and C.B-17-scid/bg immunodeficient mice. Hum Immunol **70**:790-802.

Lewis AL, Cao H, Patel SK, Diaz S, Ryan W, et al. 2007. NeuA sialic acid O-acetylesterase activity modulates O-acetylation of capsular polysaccharide in group B Streptococcus. J Biol Chem **282**:27562-71.

Liggins GC, Howie RN. 1972. A controlled trial of antepartum glucocorticoid treatment for prevention of the respiratory distress syndrome in premature infants. Pediatrics **50**:515-25.

Liu E, Tu W, Law HK, Lau YL. 2001. Decreased yield, phenotypic expression and function of immature monocyte-derived dendritic cells in cord blood. Br J Haematol **113**:240-6.

Liu GY, Doran KS, Lawrence T, Turkson N, Puliti M, et al. 2004. Sword and shield: linked group B streptococcal beta-hemolysin/cytolysin and carotenoid pigment function to subvert host phagocyte defense. Proc Natl Acad Sci USA **101**:14491-6.

Loe SM, Sanchez-Ramos L & Kaunitz AM. 2005. Assessing the neonatal safety of indomethacin tocolysis. A systematic review with meta-analysis. Obstet Gynecol **106**:173–179.

Long BR, Stoddart CA. 2012. Alpha interferon and HIV infection cause activation of human T cells in NSG-BLT mice. J Virol **86**:3327-36.

Longo ML, Bisagno AM, Zasadzinski JA, Bruni R, Waring AJ. 1993. A function of lung surfactant protein SP-B. Science **261**:453-6.

Luster AD, Alon R, von Andrian UH. 2005. Immune cell migration in inflammation: present and future therapeutic targets. Nat Immunol **6**:1182-90.

Lvovschi V, Arnaud L, Parizot C, Freund Y, Juillien G, et al. 2011. Cytokine profiles in sepsis have limited relevance for stratifying patients in the emergency department: a prospective observational study. PLoS One **6**:e28870. Epub.

Macchiarini F, Manz MG, Palucka AK, Shultz LD. 2005. Humanized mice: are we there yet? J Exp Med **202**:1307-11.

Maisey HC, Doran KS, Nizet V. 2009. Recent advances in understanding the molecular basis of group B Streptococcus virulence. Expert Rev Mol Med **10**:e27

Maisey HC, Quach D, Hensler ME, Liu GY, Gallo RL, et al. 2008. A group B streptococcal pilus protein promotes phagocyte resistance and systemic virulence. FASEB J **22**:1715–1724.

Mancuso G, Midiri A, Beninati C, Biondo C, Galbo R, et al. 2004. Dual role of TLR2 and myeloid differentiation factor 88 in a mouse model of invasive group B streptococcal disease. J Immunol **172**:6324-6329.

Mandler R, Finkelman FD, Levine AD, Snapper CM. 1993. IL-4 induction of IgE class switching by lipopolysaccharide-activated murine B cells occurs predominantly through sequential switching. J Immunol **150**:407-18.

Mariscalco MM, Tcharmtchi MH, Smith VW. 1998. P-selectin support of neonatal neutrophil adherence under flow: contribution of L-selectin, LFA-1, and ligand(s) for P-selectin. Blood **91**:4776-4785.

Maródi L. 2006. Neonatal innate immunity to infectious agents. Infect Immun **74**:1999-2006.

Marshall-Clarke S, Tasker L, Parkhouse RM. 2000. Immature B lymphocytes from adult bone marrow exhibit a selective defect in induced hyperexpression of major histocompatibility complex class II and fail to show B7.2 induction. Immunology **100**:141–151.

Martin F, Oliver AM, Kearney JF. 2001. Marginal zone and B1 B cells unite in the early response against T-independent blood-borne particulate antigens. Immunity **14**:617–629.

Mazzucchelli RI, Warming S, Lawrence SM, Ishii M, Abshari M, et al. 2009. Visualization and identification of IL-7 producing cells in reporter mice. PLoS One **4**:e7637.

McCune JM, Namikawa R, Kaneshima H, Shultz LD, Lieberman M, Weissman IL. 1996. The SCID-hu mouse: murine model for the analysis of human hematolymphoid differentiation and function. Science **241**:1632-9.

McCune JM. 1996. Development and applications of the SCID-hu mouse model. Semin Immunol **8**:187-196.

McDermott SP, Eppert K, Lechman ER, Doedens M, Dick JE. 2010. Comparison of human cord blood engraftment between immunocompromised mouse strains. Blood **116**:193-200.

Meagher LC, Cousin JM, Seckl JR, Haslett C. 1996. Opposing effects of glucocorticoids on the rate of apoptosis in neutrophilic and eosinophilic granulocytes. J Immunol **156**: 4422-8.

Mediglyphics. Accessed 29. Aug 2012.
http://www.mediglyphics.com/public/Pharmacology/tocolytics

Meikle AW and Tyler FH. 1977. Potency and duration of action of glucocorticoids. Am J of Med **63**:200.

Melkus MW, Estes JD, Padget-Thomas A, Gatlin J, Denton PW, et al. 2006. Humanized mice mount specific adaptive and innate immune responses to EBV and TSST-1. Nature medicine **12**:1316-22.

Melvan JN, Bagby GJ, Welsh DA, Nelson S, Zhang P. 2010. Neonatal sepsis and neutrophil insufficiencies. Int Rev Immunol **29**:315-48.

Mestas J, Hughes CC. 2004. Of mice and not men: differences between mouse and human immunology. J Immunol **172**:2731-8.

Meyer KC. 2007. Bronchoalveolar lavage in the diagnosis and management of interstitial lung disease. Clin Pulm Med **14**:148-156.

Mingari MC, Gerosa F, Carra G, Accolla RS, Moretta A, et al. 1984. Human interleukin-2 promotes proliferation of activated B cells via surface receptors similar to those of activated T cells. Nature **312**:641-3.

Mombaerts P, Iacomini J, Johnson RS, Herrup K, Tonegawa S, Papaioannou VE. 1992. RAG-1-deficient mice have no mature B and T lymphocytes. Cell **68**:869-77.

Mook-Kanamori B, Geldhoff M, Troost D, van der Poll T, van de Beek D. 2012. Characterization of a pneumococcal meningitis mouse model. BMC Infect Dis **12**:71.

Moore MR, Schrag SJ, Schuchat A. 2003. Effects of intrapartum antimicrobial prophylaxis for prevention of group-B-streptococcal disease on the incidence and ecology of early-onset neonatal sepsis. Lancet Infect Dis **3**:201-213

Mosier DE, Gulizia RJ, Baird SM, Wilson DB. 1988. Transfer of a functional human immune system to mice with severe combined immunodeficiency. Nature **335**:256-9.

Möst J, Spötl L, Mayr G, Gasser A, Sarti A, Dierich MP. 1997. Formation of multinucleated giant cells in vitro is dependent on the stage of monocyte to macrophage maturation. Blood **89**:662-71.

Mota J, Rico-Hesse R. 2009. Humanized mice show clinical signs of dengue fever according to infecting virus genotype. J Virol **83**:8638-45.

Mota J, Rico-Hesse R. 2011. Dengue virus tropism in humanized mice recapitulates human dengue fever. PLoS One **6**:e20762.

Mukaida N, Harada A, Matsushima K. 1998. Interleukin-8 (IL-8) and monocyte chemotactic and activating factor (MCAF/MCP-1), chemokines essentially involved in inflammatory and immune reactions. Cytokine Growth Factor Rev **9**:9-23.

Nagai Y, Garrett KP, Ohta S, Bahrun U, Kouro T, et al. 2006. Toll-like receptors on hematopoietic progenitor cells stimulate innate immune system replenishment. Immunity **24**:801-12.

National Institute of Child Health and Development. Effect of corticosteroids for fetal maturation on perinatal outcomes. NIH Consens Statement 1994 **12**:1-24.

Necela BM, Cidlowski JA. 2004. Mechanisms of glucocorticoid receptor action in noninflammatory and inflammatory cells. Proc Am Thorac Soc **1**:239-46.

Nizet V, Gibson RL, Chi EY, Framson PE, Hulse M, Rubens CE. 1996. Group B streptococcal β-hemolysin expression is associated with injury of lung epithelial cells. Infect Immun **64**:3818–3826.

Norton ME, Merrill J, Cooper AB, Kuller JA, Clyman RI. 1993. Neonatal complications after the administration of indomethacin for pre-term labor. N Engl J Med **329**:1602-7.

Pahwa SG, Pahwa R, Grimes E, Smithwick E. 1977. Cellular and humoral components of monocyte and neutrophil chemotaxis in cord blood. Pediatr Res. **11**:677-680.

Palys EE, Li J, Gaut PL, Hardy WD. 2006. Tricuspid valve endocarditis with Group B Streptococcus after an elective abortion: the need for new data. Infect Dis Obstet Gynecol **2006**:43253.

Parilla BV, Grobman WA, Holtzman RB, Thomas HA, Dooley SL. 2000. Indomethacin Tocolysis and Risk of Necrotizing Enterocolitis Obstetrics & Gynecology **96**:120-123

Parrillo JE, Fauci AS. 1979. Mechanisms of glucocorticoid action on immune processes. Annu Rev Pharmacol Toxicol **19**:179-201.

Partrick DA, Moore FA, Moore EE, Barnett CC Jr, Silliman CC. 1996. Neutrophil priming and activation in the pathogenesis of postinjury multiple organ failure. New Horiz **4**:194-210.

Pasteur L. 1879. Septicemie puerperale. Bulletin de L'Academie de Medecine (Paris) 2me serie-tome **VIII**:8256-60.

Perrone MG, Scilimati A, Simone L, Vitale P. 2010. Selective COX-1 Inhibition: A Therapeutic Target to be Reconsidered. Curr Med Chem **17**:3769-3805.

Pillay V, Savage N, Laburn H. 1994. Circulating cytokine concentrations and cytokine production by monocytes from newborn babies and adults. Pflugers Arch **428**:197-201.**Pitts LR, Simpson SQ.** 2010. From mice to men: Systematic reviews of animal data could make sepsis trials safer and more productive. Crit care med **38**:2420-22.

Polin RA, Fox WW, Abman SH. 2004. Fetal and Neonatal Physiology. Philadelphia: WB Saunders; **3rd ed**. 1490-1511.

Poyart C, Lamy MC, Boumaila C, Fiedler F, Trieu-Cuot P. 2001. Regulation of D-alanyllipoteichoic acid biosynthesis in Streptococcus agalactiae involves a novel two-component regulatory system. J Bacteriol **183**:6324–6334.

Poyart C, Pellegrini E, Gaillot O, Boumaila C, Baptista M, Trieu-Cuot P. 2001. Contribution of Mn-cofactored superoxide dismutase (SodA) to the virulence of Streptococcus agalactiae. Infect Immun **69**:5098–5106.

Prevention of perinatal group B streptococcal disease: revised guideline from CDC. 2002. MMWR Recomm Rep **51**:1-22.

Purandare CN. 2005. Fetal lung maturity. J Obstet Gynecol India **55**:215-217.

Quirante J, Ceballos R, Cassady G. 1974. Group B β-hemolytic streptococcal infection in the newborn. I. Early onset infection. Am J Dis Child **128**:659–665.

Rajagopal L. 2010. Understanding the reguation of Group B Streptococcal virulence factors. Future Microbiol **4**:201-221.

Rajesh D, Zhou Y, Jankowska-Gan E, Ronneburg DA, Dart MM, Torrealba J, Burlingham WJ. 2010. Th1 and Th17 Immunocompetence in Humanized NOD/SCID/γC-KO mice. Hum Immunol **71**:551–559.

Recher M, Berglund LJ, Avery DT, Cowan MJ, Gennery AR, et al. 2011. IL-21 is the primary common γ chain-binding cytokine required for human B-cell differentiation in vivo. Blood **118**:6824-35.

Remick DG, Bolgos G, Copeland S, Siddiqui J. 2005. Role of interleukin-6 in mortality from and physiologic response to sepsis. Infect Immun **73**:2751-7.

Rickard AJ, Young MJ. 2009. Corticosteroid receptors, macrophages and cardiovascular disease. J Mol Endocrinol **42**:449-59.

Riemersma RA, Armstrong R, Kelly RW, Wilson R. 1998. Essential Fatty Acids and Eicosanoids: Invited Papers from the Fourth International Congress. Book page 64-66.

Rijkers GT, Sanders EA, Breukels MA, Zegers BJ. 1998. Infant B cell responses to polysaccharide determinants. Vaccine **16**:1396–1400.

Ring A, Braun JS, Nizet V, Stremmel W, Shenep JL. 2000. Group B streptococcal beta-hemolysin induces nitric oxide production in murine macrophages. J Infect Dis **182**:150-157.

Royal Society for the Prevention of Cruelty to Animals. Accessed 29. Aug 2012. http://www.rspca.org.uk/allaboutanimals/laboratory/reducingsuffering

Rojo JM, Barasoain I, Portolés A. 1981. Further studies on the immunosuppressive effects of indomethacin. Int J Clin Pharmacol Ther Toxicol **19**:220-2.

Roncarolo MG, Carballido JM, Rouleau M, Namikawa R, de Vries JE. 1996. Human T-and B-cell functions in SCID-hu mice. Semin Immunol **8**:207-213.

Rosen H, Gordon S: North RJ. 1989. Exacerbation of murine listeriosis by a monoclonal antibody specific for the type 3 complement receptor of myelomonocytic cells. Absence of monocytes at infective foci allows Listeria to multiply in nonphagocytic cells. J Exp Med **170**:27–37.

Rowen JL, Smith CW, Edwards MS. 1995. Group B streptococci elicit leukotriene B4 and interleukin-8 from human monocytes: neonates exhibit a diminished response. J Infect Dis **172**:420-426.

Rubens CE, Raff HV, Jackson JC, Chi EY, Bielitzki JT, Hillier SL. 1991. Pathophysiology and histopathology of group B streptococcal sepsis in Macaca nemestrina primates induced after intraamniotic inoculation: evidence for bacterial cellular invasion. J Infect Dis **164**:320-330.

Sacchi F, Augustine NH, Coello MM, Morris EZ, Hill HR. 1987. Abnormality in actin polymerization associated with defective chemotaxis in neutrophils from neonates. Int Arch Allergy Appl Immunol **84**:32-39.

Saito S, Morii T, Umekage H, Makita K, Nishikawa K, et al. 1996. Expression of the interleukin-2 receptor gamma chain on cord blood mononuclear cells. Blood **87**:3344–3350.

Samen U, Eikmanns BJ, Reinscheid DJ, Borges F. 2007. The surface protein Srr-1 of Streptococcus agalactiae binds human keratin 4 and promotes adherence to epithelial HEp-2 cells. Infect Immun **75**:5405–5414.

Sanders LA, Feldman RG, Voorhorst-Ogink MM, de Haas M, Rijkers GT, et al. 1995. Human immunoglobulin G (IgG) Fc receptor IIA (CD32) polymorphism and IgG2-mediated bacterial phagocytosis by neutrophils. Infect Immun **63**:73-81.

Santi I, Scarselli M, Mariani M, Pezzicoli A, Masignani V, et al. 2007. BibA: a novel immunogenic bacterial adhesin contributing to group B Streptococcus survival in human blood. Mol Microbiol **63**:754-67

Sapolsky RM, Romero LM, Munck AU. 2000. How do glucocorticoids influence stress responses? Integrating permissive, suppressive, stimulatory, and preparative actions. Endocr Rev **21**:55-89.

Schelonka RL, Infante AJ. 1998. Neonatal immunology. Semin Perinatol **22**:2-14.

Schleimer RP. 2004. Glucocorticoids suppress inflammation but spare innate immune responses in airway epithelium. Proc Am Thorac Soc **1**:222-30.

Schmitz N, Barrett J. 2002. Optimizing engraftment-source and dose of stem cells. Semin Hematol **39**:3-14.

Schubert A, Zakikhany K, Pietrocola G, Meinke A, Speziale P, et al. 2004. The fibrinogen receptor FbsA promotes adherence of Streptococcus agalactiae to human epithelial cells. Infect Immun **72**:6197–6205.

Schuchat A, Hilger T, Zell E, Farley MM, Reingold A, et al. 2001. Active bacterial core surveillance of the emerging infections program network. Emerg Infect Dis **7**:92-99.

Schuchat A. 2001. Group B streptococcal disease: from trials and tribulations to triumph and trepidation. Clin Infect Dis **33**:751-6.

Schürch S, Lee M, Gehr P. 1992. Pulmonary surfactant: Surface properties and function of alveolar and airway surfactant. Pure & App Chern **64**:1745-1750

Schwab M, Roedel M, Anwar MA, Müller T, Schubert H, et al. 2000. Effects of betamethasone administration to the fetal sheep in late gestation on fetal cerebral blood flow. J Physiol **528**:619-32.

Seepersaud R, Hanniffy SB, Mayne P, Sizer P, Le Page R, Wells JM. 2005. Characterization of a novel leucine-rich repeat protein antigen from group B streptococci that elicits protective immunity. Infect Immun **73**:1671–1683.

Segal AW. 2005. How Neutrophils Kill Microbes. Annu Rev Immunol **23**:197–223.

Sekar KC, Corff KE. 2008. Treatment of patent ductus arteriosus: indomethacin or ibuprofen? J Perinatol **1**:S60-2.

Serbina NV, Salazar-Mather TP, Biron CA, Kuziel WA, Pamer EG. 2003. TNF/iNOS-producing dendritic cells mediate innate immune defense against bacterial infection. Immunity **19**:59-70.

Serreze DV, Gaedeke JW, Leiter EH. 1993. Hematopoietic stem-cell defects underlying abnormal macrophage development and maturation in NOD/Lt mice: defective regulation of cytokine receptors and protein kinase C. Proc Natl Acad Sci USA **90**:9625-9.

Serreze DV, Leiter EH. 1988. Defective activation of T suppressor cell function in nonobese diabetic mice. Potential relation to cytokine deficiencies. J Immunol **140**:3801-7.

Shet A, Ferrieri P. 2004. Neonatal & maternal group B streptococcal infections: A comprehensive review, Indian J Med Res **120**:141-150.

Shi C, Pamer EG. 2011. Monocyte recruitment during infection and inflammation. Nat Rev Immunol **11**:762-74.

Shi C, Velázquez P, Hohl TM, Leiner I, Dustin ML, Pamer EG. 2010. Monocyte trafficking to hepatic sites of bacterial infection is chemokine independent and directed by focal intercellular adhesion molecule-1 expression. J Immunol **184**:6266-74.

Shinkai Y, Rathbun G, Lam KP, Oltz EM, Stewart V, et al. 1992. RAG-2-deficient mice lack mature lymphocytes owing to inability to initiate V(D)J rearrangement. Cell **68**:855-67.

Shultz LD, Brehm MA, Bavari S, Greiner DL. 2011. Humanized mice as a preclinical tool for infectious disease and biomedical research. Ann N Y Acad Sci **1245**:50-4.

Shultz LD, Ishikawa F, Greiner DL. 2007. Humanized mice in translational biomedical research. Nat Rev Immunol **7**:118-30.

Shultz LD, Lyons BL, Burzenski LM, Gott B, Chen X, et al. 2005. Human lymphoid and myeloid cell development in NOD/LtSz-scid IL2R gamma null mice engrafted with mobilized human hemopoietic stem cells. J Immunol **174**:6477-89.

Shultz LD, Schweitzer PA, Christianson SW, Gott B, Schweitzer IB, et al. 1995. Multiple defects in innate and adaptive immunologic function in NOD/LtSz-scid mice. J Immunol **154**:180-91.

Sirard C, Lapidot T, Vormoor J, Cashman JD, Doedens M, et al. 1996. Normal and leukemic SCID-repopulating cells (SRC) coexist in the bone marrow and peripheral blood from CML patients in chronic phase, whereas leukemic SRC are detected in blast crisis. Blood **87**:1539-1548.

Soriani M, Santi I, Taddei A, Rappuoli R, Grandi G, Telford JL. 2006. Group B Streptococcus crosses human epithelial cells by a paracellular route. J Infect Dis **193**:241–250.

Spellerberg B, Rozdzinski E, Martin S, Weber-Heynemann J, Schnitzler N, et al. 1999. Lmb, a protein with similarities to the LraI adhesin family, mediates attachment of Streptococcus agalactiae to human laminin. Infect Immun **67**:871–878.

Spellerberg B. 2000. Pathogenesis of neonatal Streptococcus agalactiae infections. Microbes Infect **2**:1733-42

Splawski JB, Jelinek DF, Lipsky PE. 1991. Delineation of the functional capacity of human neonatal lymphocytes. J Clin Invest **87**: 545–553.

Steele JP, Clutterbuck RD, Powles RL, Mitchell PL, Horton C, et al. 1997. Growth of human T-cell lineage acute leukemia in severe combined immunodeficiency (SCID) mice and non-obese diabetic SCID mice. Blood **90**:2015-2019.

Steinman RM. 1991. The dendritic cell system and its role in immunogenicity. Annu Rev Immunol **9**:271-96.

Stem cell information NIH. Accessed 29. Aug 2012.
http://stemcells.nih.gov/info/scireport/chapter5.asp

Stoll BJ, Hansen NI, Sánchez PJ, Faix RG, Poindexter BB, et al. 2011. Early onset neonatal sepsis: the burden of group B Streptococcal and E. coli disease continues. Pediatrics **127**:817-26.

Suarez RD, Grobman WA, Parilla D. 2001. Indomethacin Tocolysis and Intraventricular Hemorrhage. Obstetrics & Gynecology **97**: 921-925

Suleyman H, Albayrak A, Bilici M, Cadirci E, Halici Z. 2010. Different mechanisms in formation and prevention of indomethacin-induced gastric ulcers. Inflammation **33**:224-34.

Surh CD, Sprent J. 2008. Homeostasis of naive and memory T cells. Immunity **29**:848-62.

Swirski FK, Nahrendorf M, Etzrodt M, Wildgruber M, Cortez-Retamozo V, et al. 2009. Identification of Splenic Reservoir Monocytes and Their Deployment to Inflammatory Sites. Science **325**:612–616.

Tagaya H, Kunisada T, Yamazaki H, Yamane T, Tokuhisa T, et al. 2000. Intramedullary and extramedullary B lymphopoiesis in osteopetrotic mice. Blood **95**:3363-70.

Takagi S, Saito Y, Hijikata A, Tanaka S, Watanabe T, Hasegawa T, et al. 2012. Membrane-bound human SCF/KL promotes in vivo human hematopoietic engraftment and myeloid differentiation. Blood **119**:2768-77.

Takahashi S, Nagano Y, Nagano N, Hayashi O, Taguchi F, Okuwaki Y. 1995. Role of C5a-ase in Group B Streptococcal resistance to opsonophagocytic killing. Infect Immun **63**:4764–4769.

Takenaka K, Prasolava TK, Wang JC, Mortin-Toth SM, Khalouei S, et al. 2007. Polymorphism in Sirpa modulates engraftment of human hematopoietic stem cells. Nat immunol **8**:1313-1323.

Tanaka S, Saito Y, Kunisawa J, Kurashima Y, Wake T, et al. 2012. Development of mature and functional human myeloid subsets in hematopoietic stem cell-engrafted NOD/SCID/IL2rγKO mice. J Immunol. **188**:6145-55.

Tao R, Hancock WW. 2008. Resistance of Foxp3+ regulatory T cells to Nur77-induced apoptosis promotes allograft survival. PLoS One **3**:e2321.

Tasker L, Marshall-Clarke S. 2003. Functional responses of human neonatal B lymphocytes to antigen receptor crosslinking and CpG DNA. Clin Exp Immunol **134**:409–419.

Tazi A, Bellais S, Tardieux I, Dramsi S, Trieu-Cuot P, Poyart C. 2012. Group B Streptococcus surface proteins as major determinants for meningeal tropism. Curr Opin Microbiol. **15**:44-9.

Tegethoff M, Pryce C, Meinlschmidt G. 2009. Effects of intrauterine exposure to synthetic glucocorticoids on fetal, newborn, and infant hypothalamic-pituitary-adrenal axis function in humans: a systematic review. Endocr Rev. **30**:753-89.

Thuresson ED, Lakkides KM, Rieke CJ, Sun Y, Wingerd BA, et al. 2001. Prostaglandin endoperoxide H synthase-1: the functions of cyclooxygenase active site residues in the binding, positioning, and oxygenation of arachidonic acid. J Biol Chem **276**:10347-57.

Timens W, Boes A, Rozeboom-Uiterwijk T, Poppema S. 1989. Immaturity of the human splenic marginal zone in infancy. Possible contribution to the deficient infant immune response. J. Immunol **143**:3200–3206.

Tissi L, Marconi P, Mosci P, Merletti L, Cornacchione P, et al. 1990. Experimental model of type IV Streptococcus agalactiae (group B streptococcus) infection in mice with early development of septic arthritis. Infect Immun **58**:3093-100.

Türeci O, Bian H, Nestle FO, Raddrizzani L, Rosinski JA, et al. 2003. Cascades of transcriptional induction during dendritic cell maturation revealed by genome-wide expression analysis. FASEB J **17**:836-47.

Unsinger J, McDonough JS, Shultz LD, Ferguson TA, Hotchkiss RS. 2009. Sepsis-induced human lymphocyte apoptosis and cytokine production in "humanized" mice. J Leukoc Biol **86**:219-27.

Urashima M, Chen BP, Chen S, Pinkus GS, Bronson RT, et al. 1997. The development of a model for the homing of multiple myeloma cells to human bone marrow. Blood **90**:754-765.

van der Goes A, Hoekstra K, van den Berg TK, Dijkstra CD. 2000. Dexamethasone promotes phagocytosis and bacterial killing by human monocytes/macrophages in vitro. J Leukoc Biol **67**:801-7.

Vane JR, Bakhle YS, Botting RM. 1998. Cyclooxygenases 1 and 2. Annu Rev Pharmacol Toxicol **38**:97-120.

Veronese ML, Veronesi A, Bruni L, Coppola V, D'Andrea E, et al. 1994. Properties of tumors arising in SCID mice injected with PBMC from EBV-positive donors. Leukemia **8**:214-7.

Vets S, Kimpel J, Volk A, De Rijck J, Schrijvers R, et al. 2012. Lens Epithelium-derived Growth Factor/p75 Qualifies as a Target for HIV Gene Therapy in the NSG Mouse Model. Mol Ther **20**:908-17.

Vigano A, Esposito S, Arienti D, Zagliani A, Massironi E, et al. 1999. Differential development of type 1 and type 2 cytokines and beta-chemokines in the ontogeny of healthy newborns. Biol Neonate **75**:1-8.

Vogt TK, Link A, Perrin J, Finke D, Luther SA. 2009. Novel function for interleukin-7 in dendritic cell development. Blood **113**:3961–68.

von Freeden-Jeffry U, Solvason N, Howard M, Murray R. 1997. The earliest T lineage-committed cells depend on IL-7 for Bcl-2 expression and normal cell cycle progression. Immunity **7**:147-54.

Vormoor J, Lapidot T, Pflumio F, Risdon G, Patterson B, et al. 1994. SCID mice as an in vivo model of human cord blood hematopoiesis. Blood Cells **20**:316-320.

Watanabe S, Terashima K, Ohta S, Horibata S, Yajima M, et al. 2007. Hematopoietic stem cell-engrafted NOD/SCID/IL2Rgamma null mice develop human lymphoid systems and induce long-lasting HIV-1 infection with specific humoral immune responses. Blood **109**:212-8.

Watanabe Y, Takahashi T, Okajima A, Shiokawa M, Ishii N, et al. 2009. The analysis of the functions of human B and T cells in humanized NOD/shi-scid/gammac(null) (NOG) mice (hu-HSC NOG mice). Int Immunol **21**:843-58.

Watson W, Oen K, Ramdahin R, Harman C. 1991. Immunoglobulin and cytokine production by neonatal lymphocytes. Clin Exp Immunol **83**:169-74.

Wege AK, Ernst W, Eckl J, Frankenberger B, Vollmann.Zwerenz A, et al. 2011. Humanized tumor mice – A new modelt o study and manipulate the immune response in advanced cancer therapy. Int J Cancer **129**:2194-2206.

Wiegers GJ, Reul JMHM. 1998. Induction of cytokine receptors by glucocorticoids: functional and pathological significance. Trends Pharmacol Sci **19**:317-321

Wikipedia. Accessed 29. Aug 2012. http://de.wikipedia.org/wiki/Betamethason

Wikipedia. Accessed 29. Aug 2012. http://de.wikipedia.org/wiki/Indometacin

Wilson CB, Weaver WM. 1985. Comparative susceptibility of group B streptococci and Staphylococcus aureus to killing by oxygen metabolites. J Infect Dis **152**:323-9.

Wolach B, Sonnenschein D, Gavrieli R, Chomsky O, Pomeranz A, Yuli I. 1998. Neonatal neutrophil inflammatory responses: parallel studies of light scattering, cell polarization, chemotaxis, superoxide release, and bactericidal activity. Am J Hematol **58**:8-15.

Woods KW, McCroskey RW, Michaelides MR, Wada CK, Hulkower KI, Bell RL. 2001. Thiazole analogues of the NSAID indomethacin as selective COX-2 inhibitors. Bioorg Med Chem Lett **11**:1325-8.

Woods NB, Ooka A, Karlsson S. 2002. Development of gene therapy for hematopoietic stem cells using lentiviral vectors. Leukemia **16**:563-9.

Yoshio H, Lagercrantz H, Gudmundsson GH, Agerberth B. 2004. First line of defense in early human life. Semin Perinatol **28**:304-11.

Yost CC, Cody MJ, Harris ES, Thornton NL, McInturff AM, et al. 2009. Impaired neutrophil extracellular trap (NET) formation: a novel innate immune deficiency of human neonates. Blood **113**:6419-27.

Yurasov S, Kollmann TR, Kim A, Raker CA, Hachamovitch M, et al. 1997. Severe combined immunodeficiency mice engrafted with human T cells, B cells, and myeloid cells after transplantation with human fetal bone marrow or liver cells and implanted with human fetal thymus: a model for studying human gene therapy. Blood **89**:1800-10.

Zadura AF, Theander E, Blom AM, Trouw LA. 2009. Complement inhibitor C4b-binding protein in primary Sjögren's syndrome and its association with other disease markers. Scand J Immunol **69**:374-80.

Zemlin M, Bauer K, Hummel M, Pfeiffer S, Devers S, et al. 2001. The diversity of rearranged immunoglobulin heavy chain variable region genes in peripheral blood B cells of preterm infants is restricted by short third complementarity-determining regions but not by limited gene segment usage. Blood **97**:1511-3.

Zola H, Fusco M, Macardle PJ, Flego L, Roberton D.1995. Expression of cytokine receptors by human cord blood lymphocytes: comparison with adult blood lymphocytes. Pediatr Res **38**:397–403.

SUPPLEMENT

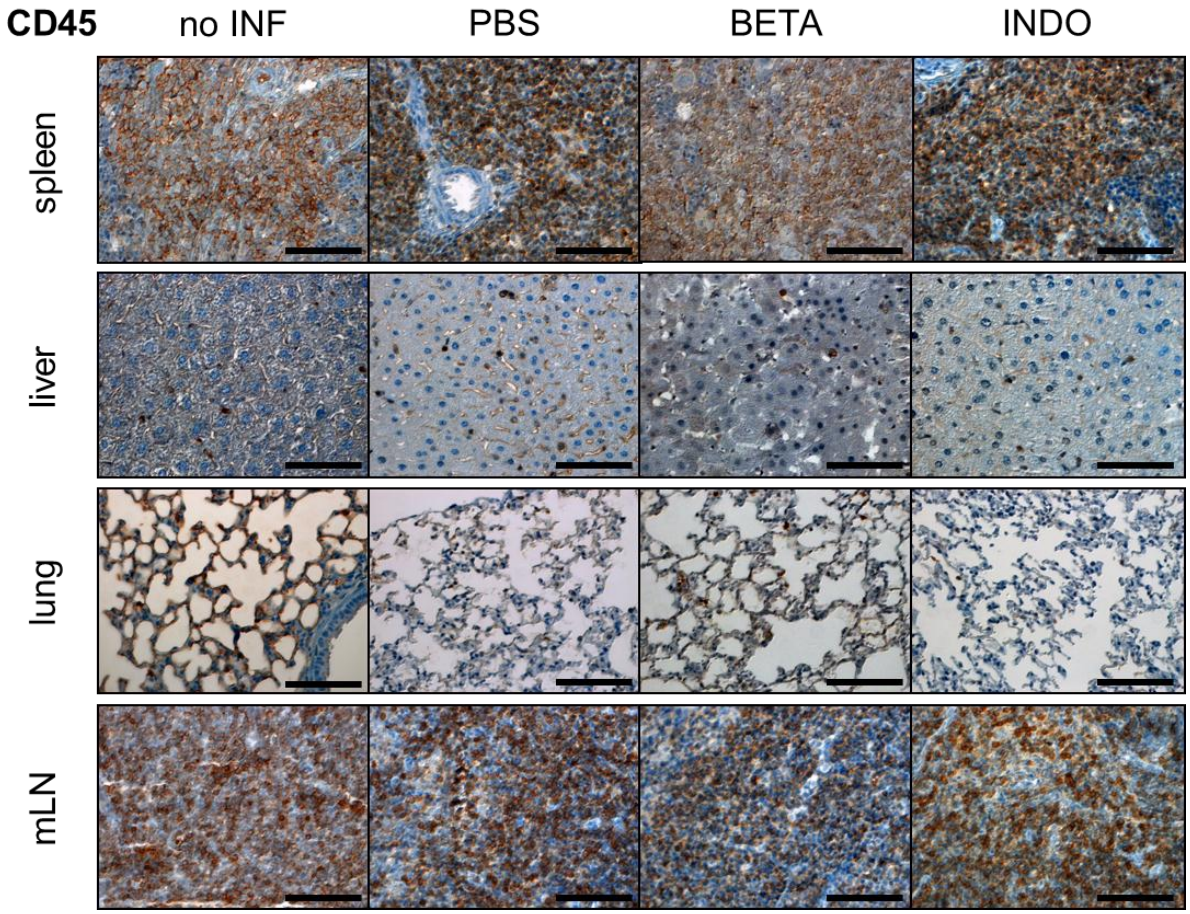

Supplement Fig. 1: *Immunohistochemical staining for CD45^{+} leukocytes in spleen, liver, lung, mLN of uninfected (no INF), vehicle (PBS)-, Betamethasone (BETA)- and Indomethacin (INDO)-treated humanized mice. Animals were infected with moderate doses of GBS (10^{6}) and analyzed at day 3. Black bar = 100µm, objective used 40x.*

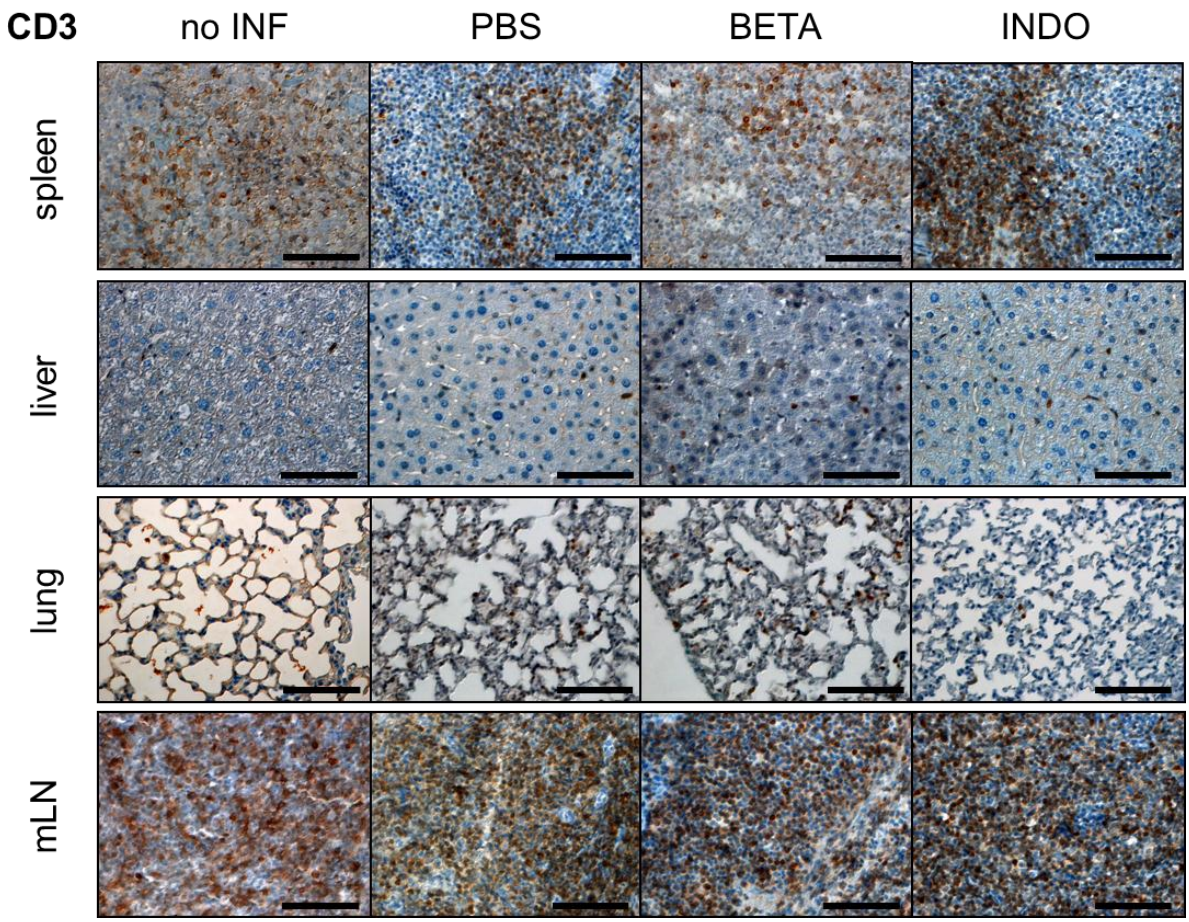

Supplement Fig. 2: *Immunohistochemical staining for $CD3^+$ T cells in spleen, liver, lung, mLN of uninfected (no INF), vehicle (PBS)-, Betamethasone (BETA)- and Indomethacin (INDO)-treated humanized mice. Animals were infected with moderate doses of GBS (10^6) and analyzed at day 3. Black bar = 100µm, objective used 40x.*

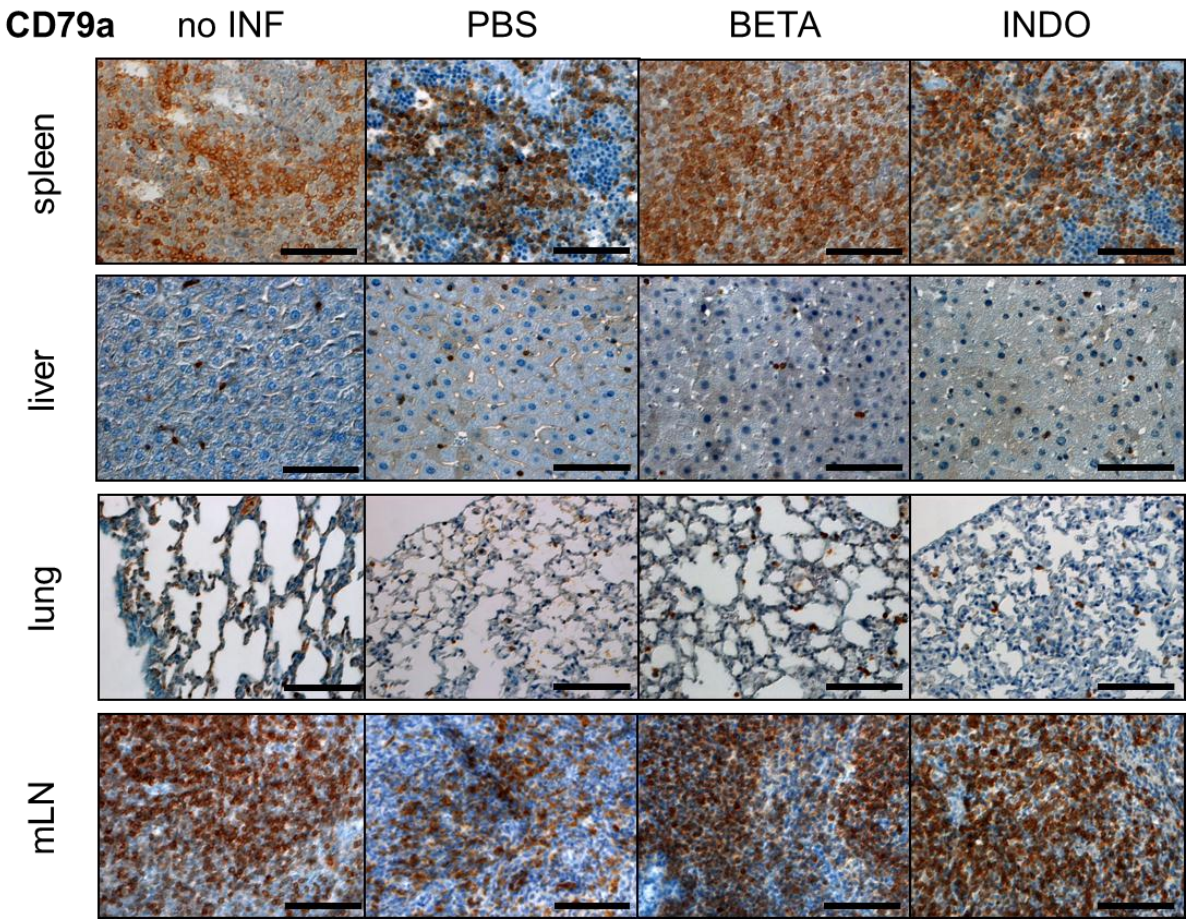

Supplement Fig. 3: *Immunohistochemical staining for CD79a^{+} B cells in spleen, liver, lung, mLN of uninfected (no INF), vehicle (PBS)-, Betamethasone (BETA)- and Indomethacin (INDO)-treated humanized mice. Animals were infected with moderate doses of GBS (10^{6}) and analyzed at day 3. Black bar = 100µm, objective used 40x.*

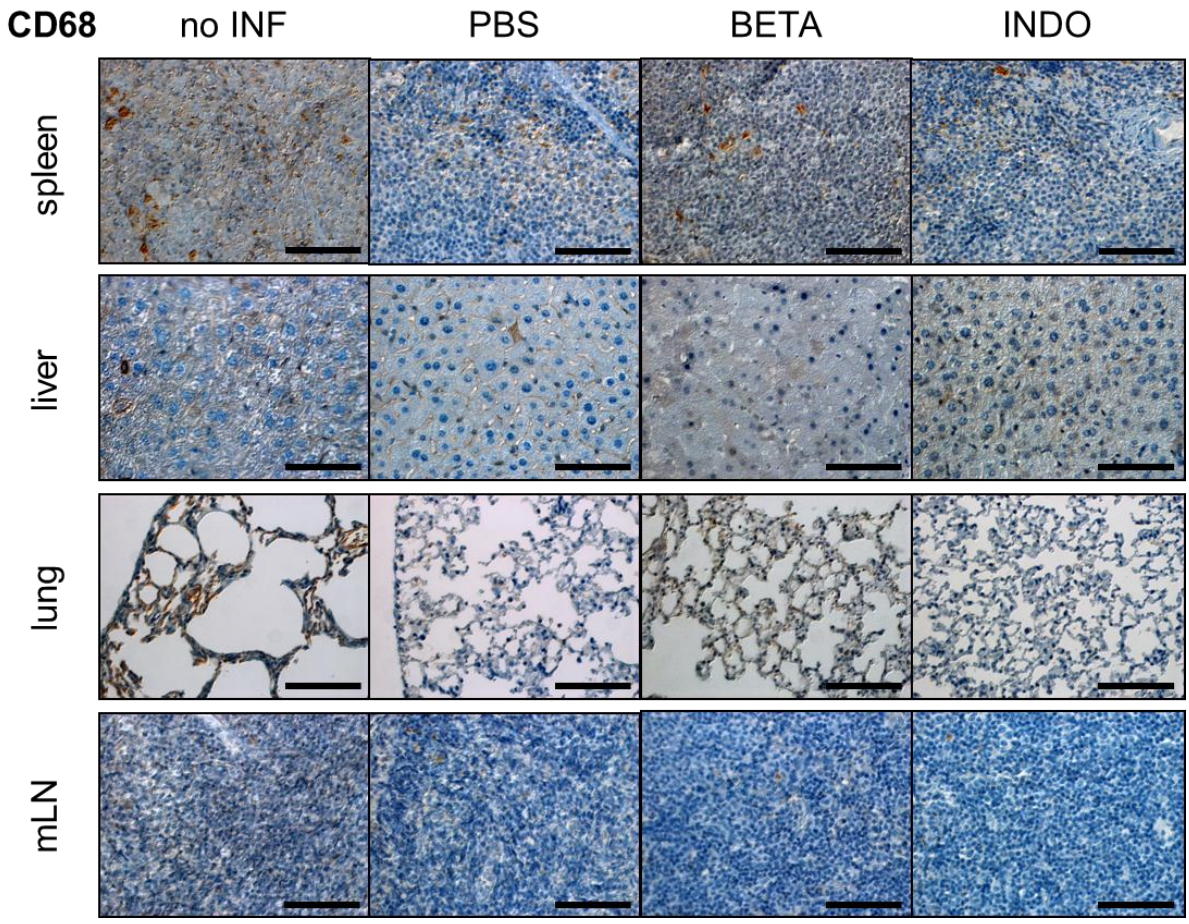

Supplement Fig. 4: *Immunohistochemical staining for CD68$^+$ macrophages in spleen, liver, lung, mLN of uninfected (no INF), vehicle (PBS)-, Betamethasone (BETA)- and Indomethacin (INDO)-treated humanized mice. Animals were infected with moderate doses of GBS (10^6) and analyzed at day 3. Black bar = 100µm, objective used 40x.*

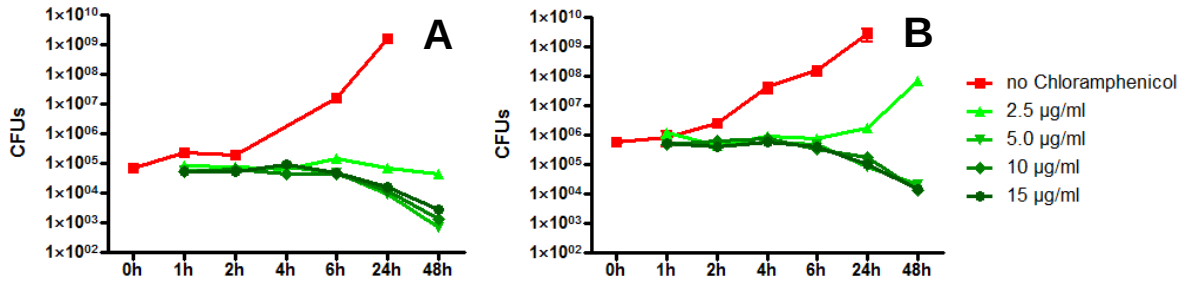

Supplement Fig. 5: *Two concentrations of GBS, 10^5/ml (A) and 10^6/ml (B) were incubated with different concentrations of the bacteriostatic agent Chloramphenicol: no Chloramphenicol (vehicle PBS), 2.5 µg/ml, 5.0 µg/ml, 10 µg/ml and 15 µg/ml.*

Supplement Table 1: CFUs in organs of individual humanized mice infected with GBS

CFUs of individual animals (n=10) after 1 day of high dose infection (10^7 GBS)										
spleen	$1.6x10^6$	0	$1.2x10^8$	$2.2x10^8$	$8.6x10^5$	$4.9x10^7$	0	0	$4.1x10^8$	$7.0x10^7$
kidney	$4.5x10^6$	$4.0x10^3$	$2.8x10^7$	$3.2x10^7$	$2.6x10^6$	$1.9x10^7$	0	$4.3x10^4$	$1.2x10^8$	$3.1x10^7$
liver	$1.2x10^6$	0	$5.7x10^7$	$6.7x10^7$	$6.7x10^5$	$8.6x10^6$	0	0	$1.2x10^8$	$4.3x10^7$
lung	$5.0x10^7$	$1.1x10^3$	$1.4x10^8$	$8.2x10^7$	$6.9x10^6$	$3.8x10^7$	0	0	$7.9x10^7$	$7.7x10^6$
brain	$7.2x10^4$	0	0	$1.6x10^5$	$1.6x10^5$	$2.1x10^5$	0	0	$5.7x10^5$	$1.7x10^5$
BM	$1.8x10^4$	$1.8x10^3$	$8.0x10^5$	$1.9x10^6$	0	$2.8x10^5$	$4.0x10^4$	0	$4.0x10^6$	$1.0x10^5$
peritoneum	$1.1x10^7$	0	$4.4x10^8$	$3.1x10^8$	0	$1.5x10^8$	0	0	$2.3x10^9$	$4.3x10_8$

CFUs of individual animals (n=10) after 3 days of moderate dose infection (10^6 GBS)										
spleen	0	0	0	0	0	0	0	0	$5.0x10^3$	0
kidney	0	0	0	$6.0x10^4$	0	0	0	0	0	0
liver	0	0	0	$1.9x10^2$	$1.8x10^2$	$2.9x10^3$	0	$5.5x10^2$	$2.7x10^5$	0
lung	0	0	0	0	0	0	0	0	$1.2x10^3$	0
brain	0	0	0	0	0	0	0	0	0	0
BM	0	0	0	0	$6.2x10^3$	0	0	0	0	$1.2x10^3$
peritoneum	0	0	0	0	0	$1.0x10^2$	0	0	0	0

CFUs of individual animals (n=6) after 7 days of moderate dose infection (10^6 GBS)						
spleen	0	0	0	0	0	0
kidney	0	0	0	0	0	$2.5x10^7$
liver	0	0	0	0	0	76
lung	0	$1.3x10^3$	0	0	0	0
brain	0	0	0	0	0	0
BM	0	0	0	0	0	$2.0x10^2$
peritoneum	0	$4.3x10^3$	0	0	0	0

Supplement Table 2: Relative amounts (%) of human leukocyte subsets in the pb

	lympho-cytes[#]	B cells[#]	T cells[#]	$CD4^+$ T cells[#]	$CD8^+$ T cells[#]	myeloid cells[§]	granulo-cytes[§]
humanized mouse	33 (27-44)	44 (31-60)	56 (40-70)	62 (57-69)	35 (30-41)	7 (±3)	0.06 (±0.15)
cord blood	41 (35-47)	20 (14-23)	55 (49-62)	35 (28-42)	29 (26-33)	11 (±17)	47 (±25)
adult	32 (28-39)	13 (11-16)	72 (67-76)	42 (38-46)	35 (31-40)	3-9 -	50-72 -

[#]*Values represent the median, ranges from 25th to 75th percentiles in parentheses. Values of cord blood and adult pb (Erkeller-Yuksel et al. 1992).* [§]*Values represent the mean ± standard deviation in parentheses. Values of cord blood and adult pb (Katsares et al. 2009).*

Supplement Table 3: Relative amounts (%) of human leukocyte subsets in the BM

	lymphocytes	granulocytes
humanized mouse	30 (19-41)	4.3 (-1-10)
neonate	14 (3-25)	63 (43-83)
adult	17 (10-24)	60 (40-84)

Values represent the mean, with 95% confidence interval in parentheses. Values of neonate and adult BM (Greer et al. 2009)

Supplement Table 4: Relative amounts (%) of human leukocyte subsets in the lung

	B cells[#]	T cells[#]	myeloid cells (macrophages)	granulocytes
humanized mouse	11	30	13	0.05
adult	<1	7-11	>80	<1-4

Values of adult bronchoalveolar fluid (Harbeck 1998; Meyer 2007)

Supplement Table 5: Relative amounts (%) of human leukocyte subsets in the peritoneum

	B cells[#]	T cells[#]	myeloid cells (macrophages)
humanized mouse	2	6	4
adult	2	8	45

Values of adult peritoneal lavage (Harbeck 1998; Meyer 2007)

Supplement Table 6: Relative amounts (%) of human leukocyte subsets in the LN

	B cells[#]	T cells[#]
humanized mouse	32 (±7)	50 (±12)
adult	41 (±15)	56 (±13)

Values represent the mean ± standard deviation in parentheses. Values of adult LNs (Battaglia et al. 2003).

ABBREVIATIONS

°C	degree Celsius
µ	micro
µl	microliter
ACD	Acid-Citrate-Dextrose
ACK	Ammonium-Chloride-Potassium
ACP	alpha C protein
ADCC	antibody dependent cellular cytotoxicity
AIDS	acquired immune deficiency syndrome
AMP	antimicrobial peptide
ANOVA	analysis of variance
APC	antigen presenting cell
APC	allophycocyanin
APC-Cy7	allophycocyanin- cyanine 7
ATCC	American Type Culture Collection
B2m	β2 microglobulin
BBB	blood brain barrier
BD	Becton, Dickinson and Company
BETA	Betamethasone
bg	beige
BibA	GBS immunogenic bacterial adhesin
BM	bone marrow
BMDC	bone marrow derived cell
BMDM	bone marrow derived macrophage
BSA	bovine serum albumin
C4BP	C4b binding protein
CAMP-factor	Cristie-Atkins-Munch-Petersen-factor
CCR	chemokine receptor
CD	cluster of differentiation

CD40L	CD40 ligand
CDC	Center of Disease Control
CDC42	cell division control protein 42
CFH	complement factor H
CFU	colony forming unit
COX	cyclo-oxygenase
CpG	deoxycytidylate-phosphate-deoxyguanylate
CPS	capsular polysaccharide
d	day
DC	dendritic cells
ddH_2O	double-distilled water
dil.	dilution
DMSO	dimethyl sulfoxide
DPPC	dipalmitoylphosphatidylcholine
DTH	delayed-type hypersensitivity
E. coli	Escherichia coli
e.g.	exempli gratia (for example)
EBV	Epstein Barr virus
ECM	extracellular matrix
EDTA	ethylenediaminetetraacetic acid
ELISA	enzyme-linked immunosorbent assay
EOD	early onset disease
et al.	et aliae (and others)
EtOH	ethanol
FACS	fluorescence activated cell sorting
FAK	focal adhesion kinase
FBS	fetal bovine serum
FbsA	GBS fibrinogen binding protein
Fc	fragment crystallizable
FcαRI	Fc-alpha receptor I
FcγRIIA/C	Fc-gamma receptor II A/C

Fig.	Figure
FITC	fluorescein isothiocyanate
FOXN1	forkhead-box N1
g	gram
GAPDH	glyceraldehyde-3-phosphate dehydrogenase
GBS	group B streptococcus
G-CSF	granulocyte colony stimulating factor
GE	General Electric
GM-CSF	granulocyte/monocyte colony stimulating factor
GVHD	graft versus host disease
Gy	gray
h	hour
H&E	Hematoxilin & Eosin
HBV	hepatitis B virus
HCV	hepatitis C virus
HIV	human immunodeficiency virus
HLA	human leukocyte antigen
HSC	hematopoietic stem cell
IDDM	insulin-dependent diabetis mellitus
IFN	interferon
Ig	immunoglobulin
IL	interleukin
IL-2R	interleukin-2-receptor
IL2rg	interleukin-2-receptor γ-chain locus
IL-2RG	IL-2 receptor γ chain
INDO	Indomethacin
INF	infected
ip	intraperitoneally
IP-10	interferon-inducible protein-10
IVH	intraventricular hemorrhage
k	kilo

l	liter
LAK	lymphokine activated killer
LCA	leukocyte common antigen
LD50	lethal dose, 50%
Lmb	GBS laminin binding adhesin
LN	lymph node
LOD	late onset disease
LPS	lipopolysaccharide
LrrG	leucine-rich repeat protein G
LTA	lipoteichoic acid
m	mili
M	molar
m	meter
Mac-1	Macrophage 1 antigen
MACS	magnetic cell separation
M-CSF	macrophage colony-stimulating factor
mg	milligram
MHC	major histocompatibility complex
min	minute
MIP	macrophage inflammatory protein
ml	milliliter
mLN	mesenteric lymph node
MNCs	mononuclear cells
mRNA	messenger ribonucleic acid
n	number
ND	not determined
NET	neutrophil extracellular trap
NIH	National Institutes of Health
NK	natural killer
NOD	non-obese diabetic
NOG	NOD/LtSz-scid IL2rg$^{-/-}$

NSAID	non-steroidal anti-inflammatory drug
NSG	NOD/Shi-scid IL2rg$^{-/-}$
nu	nude
OD	optical density
OVA	ovalbumin
pb	peripheral blood
PBMC	peripheral blood mononuclear cells
PBS	phosphate buffered saline
PE	phycoerythrin
PEC	peritoneal exudate cell
Pe-Cy7	phycoerythrin-cyanine 7
PEL	peritoneal lavage
PerCP	peridinin-chlorophyll-protein complex
PFA	paraformaldehyde
PG	prostaglandin
pg	picogram
PI3K	phosphoinosiotide-3 kinase
Pil	GBS pilus protein
poly I:C	polyinosinic:polycytidylic acid
Prf	prolactin-releasing factor
Prkdc	protein kinase, DNA activated, catalytic polypeptide
R&D	Research & Diagnostics
Rac1	Ras-related C3 botulinum toxin substrate 1
RAG	recombination activation gene
Ras	Rat sarcoma
rcf	relative centrifugal force
RDS	respiratory distress syndrome
RhoA	Ras homolog gene family, member A
ROS	reactive oxygen species
rpm	rounds per minute
RPMI	Roswell Park Memorial Institute

RT	room temperature
SCF	stem cell factor
scid	severe combined immunodeficiency
ScpB	Streptococcal C5a peptidase
SIRPA	Signal-regulatory protein alpha
SIRS	systemic inflammatory response syndrome
SodA	superoxide dismutase A
SP	surfactant protein
SR-A	scavenger receptor A
SRC	scid-repopulating cell
Srr1	serine-rich repeat 1
TCR	T cell receptor
TD	T cell-dependent
Th	T helper
TI	T cell-independent
TIP	TNF- and iNOS-producing
TLR	Toll-like receptor
TNF	tumor necrosis factor
T_{reg}	regulatory T cells
USA	United States of America
v/v	volume/volume
W	watt
w/v	weight/volume
β-H/C	β-haemolysin/cytolysin
γc	common γ-chain

LIST OF TABLES

LIST OF FIGURES

APPENDIX

PRESENTATIONS

Wege AK, Florian C, Ernst W, Holz K, Seelbach-Göbel B, Männel DN, Ritter U. (2010)
Humanized mice – a new mouse model to study Leishmania infection in context with human hematopoietic immune cells.
14. Symposium “Infektion und Immunabwehr”, Rothenfels.

Ernst W, Wege AK & Männel DN (2010).
Generation of a neonatal sepsis model in humanized mice.
Summer school of the Regensburg International Graduate School of Life Sciences, Regen.

Ernst W, Männel DN, Wege AK, Seelbach-Göbel B (2011).
Streptococcus agalactiae Infektion in humanisierten Mäusen – ein fetales/neonatales Septikämie-Modell.
XXII. Akademische Tagung deutschsprechender Hochschullehrer in der Gynäkologie und Geburtshilfe, Halle.

Ernst W, Seelbach-Göbel B, Männel DN, Wege AK (2011).
Strept. agal. infection in humanized mice - a novel model to improve neonatal sepsis treatment in clinic?
2011 Joint Annual meeting of the Italian Society for Immunology (SIICA) and German Society of Immunology (DGFI); Riccione, Italy.

Ernst W, Seelbach-Göbel B, Männel DN, Wege AK (2011).
Strept. agal. infection in humanized mice - a novel model to improve neonatal sepsis treatment in clinic?
Summer school of the Regensburg International Graduate School of Life Sciences, Regen.

PUBLICATIONS

Wege AK, Ernst W, Eckl J, Frankenberger B, Vollmann-Zwerenz A, Männel DN, Ortmann O, Kroemer A, Brockhoff G. (2011) Humanized tumor mice-A new model to study and manipulate the immune response in advanced cancer therapy. Int J Cancer **129**:2194-206.

Wege AK, Florian F, Ernst W, Zimara N, Schleicher U, Hanses F, Schmid M, Ritter U. (2012) Leishmania major infection in humanized mice induces systemic infection and provokes a nonprotective human immune response. PLoS Negl Trop Dis **6**:e1741.

AWARDS AND SCHOLARSHIPS

Award for the second best talk
14. Symposium “Infektion und Immunabwehr”, Rothenfels, 10.03. – 12.03.2010

DAAD scholarship to work as a visiting researcher at the Special Pathogens Program, Canadian Science Centre for Human & Animal Health, Winnipeg/Canada 05/2010 – 08/2010

Award for best poster
XXII. Akademische Tagung deutschsprechender Hochschullehrer in der Gynäkologie und Geburtshilfe, Halle (Saale), 25.09 – 27.09.2011

ACKNOWLEDGMENTS

I would like to thank all the people who helped and supported me during my thesis.

First I would like to thank Prof. Dr. Daniela N. Männel for being my thesis supervisor, for enabling me to do this interesting thesis project at her institute and for her input, her help and support during the past 3 years.

I also would like to thank Prof. Dr. Richard Warth for being my first thesis mentor, for his constructive input during my progress reports and his friendly support.

I am grateful to Prof. Dr. Birgit Seelbach-Göbel for being my second thesis mentor, for her valuable input, for providing the cord blood samples, for her help and support and all the other significant contributions to this thesis.

Special thanks to Dr. Anja K. Wege for introducing me to the humanized mouse model, for teaching me how to use the flow cytometer, for her help in and supervision of countless experiments and for her friendly manner, encouragement and optimism during the past 3 years.

I would like to thank all my colleagues, especially Dorothea Weber-Steffens, Christian Florian, Judith Proske and Nicole Zimara at the Institute of Immunology for their help and a pleasant working atmosphere. Special thanks to Dr. Sven Mostböck for all his help with my thesis and for his advice and vast knowledge of Immunology. I am also grateful to Mareile Siebörger and Ellen Wiesler for their practical help in my experiments.

Furthermore I am grateful for having the opportunity to work as a visiting researcher at the Special Pathogens Program, Canadian Science Centre for Human & Animal Health, Winnipeg/Canada. Therefore I would like to thank Dr. Anja K. Wege, Dr. Dennis A. Bente, Prof. Dr. Birgit Seelbach-Göbel and all the people at the Special Pathogens Program for their support, their help and for making this wonderful experience possible.

My biggest gratitude goes to Nicole, my parents and my brother for their unfailing support at all times, for their encouragement and for always being there for me.